OULU 2021
C 813

ACTA UNIVERSITATIS OULUENSIS

Matias Hultgren

CONTROL DESIGN FOR CFB BOILERS INTEGRATED WITH PROCESS DESIGN

UNIVERSITY OF OULU GRADUATE SCHOOL;
UNIVERSITY OF OULU,
FACULTY OF TECHNOLOGY

ACTA UNIVERSITATIS OULUENSIS
C Technica 813

MATIAS HULTGREN

CONTROL DESIGN FOR CFB BOILERS INTEGRATED WITH PROCESS DESIGN

Academic dissertation to be presented with the assent of the Doctoral Training Committee of Technology and Natural Sciences of the University of Oulu for public defence in the OP-Pohjola auditorium (L6), Linnanmaa, on 3 December 2021, at 1 p.m.

UNIVERSITY OF OULU, OULU 2021

Copyright © 2021
Acta Univ. Oul. C 813, 2021

Supervised by
Professor Enso Ikonen
Docent Jenő Kovács

Reviewed by
Professor Sigurd Skogestad
Associate Professor Pál Szentannai

Opponents
Associate Professor Pál Szentannai
Doctor Peter Singstad

ISBN 978-952-62-3136-5 (Paperback)
ISBN 978-952-62-3137-2 (PDF)

ISSN 0355-3213 (Printed)
ISSN 1796-2226 (Online)

Cover Design
Raimo Ahonen

PUNAMUSTA
TAMPERE 2021

Hultgren, Matias, Control design for CFB boilers integrated with process design.
University of Oulu Graduate School; University of Oulu, Faculty of Technology
Acta Univ. Oul. C 813, 2021
University of Oulu, P.O. Box 8000, FI-90014 University of Oulu, Finland

Abstract

Integrated control and process design (ICPD) was implemented for circulating fluidized bed power plants (CFB) in this thesis to obtain fast electrical power load changes. The need to reduce global emissions has resulted in new design requirements for CFB boilers: Combustion power plants are needed for fast load changes due to renewable power variations, and process modifications like oxy-combustion have to be implemented for CFB boilers. This thesis addressed the new requirements by integrating control design with process design for CFB boilers, which was done now for the first time.

The work defined an ICPD procedure for closed-loop CFB processes that focuses on load change performance. This was done by reviewing and classifying ICPD literature to select suitable design and analysis methods. The new ICPD procedure consisted of process analysis based on dynamic simulation and state estimation, control structure selection based on relative gain methods, and simultaneous dynamic optimization of process and controller parameters.

The design stages were validated through industrial case studies. In the process analysis stage, CFB combustion and flue gas dynamics were studied to define how the boiler should be modified for oxy-combustion. In the control design stage, the relative gain methods were used to identify feasible control structures and performance-limiting interactions in a once-through CFB boiler. In the ICPD optimization stage, the CFB steam path mass storage parameters and controllers were optimized for simulated load change ramps. The goal was to achieve tight output electrical power control and satisfy selected secondary control objectives.

The results show how faster load changes and a better flexibility for process modifications are obtained through ICPD compared to sequential process and control design. The design guidelines presented in this thesis thus enable more sustainable power generation in the grid.

Keywords: circulating fluidized bed boiler, integrated control and process design, oxy-combustion, process control, process optimization, relative gain array, state estimation

Hultgren, Matias, Säätösuunnittelu CFB-kattiloille yhdistettynä prosessisuunnitteluun.
Oulun yliopiston tutkijakoulu; Oulun yliopisto, Teknillinen tiedekunta
Acta Univ. Oul. C 813, 2021
Oulun yliopisto, PL 8000, 90014 Oulun yliopisto

Tiivistelmä

Tässä väitöstutkimuksessa sovellettiin integroitua säätö- ja prosessisuunnittelua (ICPD) kiertoleijupetivoimalaitoksiin (CFB) nopeiden sähkön kuormanmuutosten saavuttamiseksi. Globaalien päästöjen vähentämisen tarve on asettanut uusia suunnitteluvaatimuksia CFB-kattiloille: Uusiutuvan energiantuotannon vaihteluiden vuoksi polttovoimalaitoksia tarvitaan nopeita kuormanmuutoksia varten ja happipolton kaltaisia prosessimuunnoksia on sovellettava CFB-kattiloille. Uusista vaatimuksista johtuviin haasteisiin väitöstutkimus vastasi integroimalla säätö- ja prosessisuunnittelua CFB-kattiloille. Näin tehtiin nyt ensimmäistä kertaa.

Työssä määritettiin suljetun piirin CFB-prosesseille kuormanmuutosten suorituskykyä painottava ICPD-suunnittelumalli. Tämä suoritettiin tarkastelemalla ja luokittelemalla ICPD-kirjallisuutta sopivien suunnittelu- ja analyysimenetelmien valitsemiseksi. ICPD-suunnittelumalli koostui dynaamiseen simulointiin ja tilaestimointiin perustuvasta prosessianalyysista, suhteellisen vahvistuksen menetelmiin (”relative gain”) perustuvasta säätörakenteen valinnasta sekä prosessin ja säädinten parametrien yhtäaikaisesta dynaamisesta optimoinnista.

Suunnitteluvaiheet validoitiin teollisten tutkimusesimerkkien kautta. CFB:n poltto- ja savukaasudynamiikkaa tutkittiin prosessianalyysivaiheessa, tarkoituksena määrittää, kuinka kattilaa tulisi muuntaa happipolttoa varten. Säätörakenteen valintavaiheessa suhteellisen vahvistuksen menetelmiä käytettiin läpivirtaus-CFB-kattilalle soveltuvien säätörakenteiden ja suorituskykyä rajoittavien vuorovaikutusten määrittämiseen. CFB:n höyrypuolen massavarantoparametrit ja säätimet optimoitiin simuloiduille kuormarampeille ICPD-optimointivaiheessa. Tavoitteena oli saavuttaa tarkka tuotettavan sähkön säätö sekä valitut toissijaiset säätötavoitteet.

Tulokset osoittavat, miten ICPD:n kautta saavutetaan nopeampia kuormanmuutoksia ja parempi joustavuus prosessimuutosten osalta vaiheittaiseen prosessi- ja säätösuunnitteluun verrattuna. Työssä esitetyt CFB-kattiloiden suunnittelukäytännöt mahdollistavat täten ympäristöystävällisemmän voimantuotannon verkossa.

Asiasanat: happipoltto, integroitu prosessi- ja säätösuunnittelu, kiertoleijupetikattila, prosessin optimointi, prosessin säätö, relative gain array, tilaestimointi

Et veritas liberabit vos

Acknowledgements

Research for this thesis was carried out for the Systems Engineering research group (part of the Intelligent Machines and Systems research unit, since 2019), University of Oulu, between 2012 and 2021. The work was largely performed in a regular industrial-academic cooperation with the Sumitomo SHI FW Energia Oy company (previously Foster Wheeler Energia Oy, later Amec Foster Wheeler). The main funding was provided by the Graduate School in Chemical Engineering national-level doctoral program (GSCE) between 2013 and 2016, with additional funding from Sumitomo SHI FW Energia Oy. The work has also been supported financially by the University of Oulu Faculty of Technology, the Systems Engineering group CFBCON project, and travel grants by the Finnish Society for Automation (Automaatiosäätiö). Lastly, the grant awarded by the Finnish Cultural Foundation in 2017 is gratefully acknowledged.

I would like to express my gratitude to my supervisors, Professor Enso Ikonen and Docent Jenő Kovács, for their guidance throughout my doctoral studies. Thank you for the doctoral work opportunity and for introducing me to the exciting world of power plant control. My warm thanks go to Professor Sigurd Skogestad and Associate Professor Pál Szentannai for their efforts and valuable comments during the pre-examination of my thesis. I also wish to thank my follow-up group for doctoral training: Professor Juha Tanskanen and Dr. István Selek from the University of Oulu, and Dr. Jouni Ritvanen from LUT University.

From the Systems Engineering group, I wish to acknowledge all the colleagues that I had the pleasure to work with during my doctoral training. These include Jukka Hiltunen, Lic. Tech., for the numerous inspiring discussions and helpful assistance, Dr. Laura Niva for the scientific-academic collaboration and peer support, as well as Dr. Seppo Honkanen, Antti Yli-Korpela, M.Sc., and Harri Aaltonen, Lic. Tech., for shared ideas, projects, and discussions. In general, I wish to acknowledge the numerous colleagues and friends that I have made over the years from the other research groups of Process and Environmental Engineering at the University of Oulu, as well as the national GSCE community.

From industry, I would like to thank Sumitomo SHI FW Energia Oy in Varkaus for providing me with the resources and expertise to study the most cutting-edge developments in fluidized bed power generation. In addition to my supervisor, Principal Research Engineer Jenő Kovács, I would like to express my sincere gratitude to Dr. Edgardo Coda Zabetta, Ari Kettunen, and Mikko Salo for their support. For my participation in the oxy-fired pilot boiler experimental testing at

the VTT Technical Research Centre of Finland in Jyväskylä in 2011, special thanks go to Dr. Antti Tourunen, Hannu Mikkonen, and Mikko Jegoroff for the test work and the valuable discussions about the results.

For the last years of my doctoral training, I would like to express my gratitude to my line managers at Metso Outotec (Outotec, until 2020): vice president Jussi Järvinen and Dr. Antti Roine, especially to Dr. Roine for his continuous encouragement and for giving me the spark to pursue a doctoral degree in the first place. Since 2017, I have had the great pleasure to work in the Modeling and Simulation team at the Metso Outotec Research Center located in Pori, which has enabled me to further develop my skills in process modeling and control. I extend my thanks to all members of the team, as well as my other past and present close colleagues in the company.

I am very grateful to my close relatives and friends for their role in my life. For the doctoral training period, I especially wish to thank the three original process engineering musketeers, as well as the more recent fourth musketeer, for the numerous entertaining adventures. Hopefully there will be many more!

Lastly, the most important thanks go to my mother Marjatta and father Gösta. I can’t begin to express the amount of gratitude I have to you for your unending support, wisdom, and advice during these years. Without you, none of this would be possible.

Pori, 17 June 2021 Matias Hultgren

List of abbreviations and symbols

Abbreviations

ASU	air separation unit
CCS	carbon capture and storage
CCU	carbon compression unit
CDOF	control degrees of freedom
CFB	circulating fluidized bed
CHP	combined heat and power plant
CLDG	closed-loop disturbance gain
CPU	carbon purification unit
CV	controlled variable
DOF	degrees of freedom
DRGA	dynamic relative gain array
DSH	desuperheater water spray
ECO	economizer preheater
EVAP	evaporator
FG	flue gas
FW	feedwater
G	generator
HE	heat exchanger
HP	high-pressure turbine section
ICI	integral controllability with integrity
ICI PRG	ICI analysis with the PRG for all partially controlled subsystems
ICPD	integrated control and process design
ISE	integral square error
kW_{th}	kilowatts, thermal
LP	low-pressure turbine section
LTI	linear time-invariant
MIDO	mixed-integer dynamic optimization
MIMO	multiple-input-multiple-output
MILP	mixed-integer linear programming
MINLP	mixed-integer nonlinear programming
MPC	model predictive control
MV	manipulated variable

MW_e	megawatts, electrical
MW_{th}	megawatts, thermal
nDRGA	dynamic relative gain number
NI	Niederlinski index
norm.	normalized
NO_X	nitrogen oxides, generic expression
nRGA	relative gain number
OTU	once-through steam path
OTU-CFB	once-through circulating fluidized bed boiler
oxy-CFB	oxy-fired circulating fluidized bed boiler
PID	proportional-integral-derivative controller
PRG	partial relative gain
PRG_{mn}	PRG matrix for partially controlled subsystem, loops *m*–*n* closed
PRGA	performance relative gain array
PSE	process systems engineering
prim.	primary
RFG	recirculated flue gas
RGA	relative gain array
RH	reheater heat exchanger
RHvalve	reheater bypass valve
sec.	secondary
SH	superheater heat exchanger
SO_X	sulfur oxides, generic expression
SP	setpoint
TPM	throughput manipulator
tot.	total
T.valve	turbine valve
UKF	unscented Kalman filter
vol%	volume percentage

Latin symbols

a_{yu}	real term of the DRGA element between output *y* and input *u* ($a_{\lambda yu}$ in Publication IV)
A	process state matrix in the state-space model state equation
b_{yu}	complex term of the DRGA element between output *y* and input *u* ($b_{\lambda yu}$ in Publication IV)

B	thermodynamic irreversibility rate [W]
$\mathbf{B}$	process input matrix in the state-space model state equation
$c(s)$	controller transfer function
c_{ss}	state noise vector (v in Publication II)
C	covariance (P in Publication II)
$\mathbf{C}$	process state matrix in the state-space model measurement equation
d	process disturbance variable
d_{ss}	measurement noise vector (w in Publication II)
D_i	PID controller derivative gain for controlled variable i
$\mathbf{D}$	process input matrix in the state-space model measurement equation
E	output electrical power [MW]
f_{des}	process and control performance equations
f_{proc}	process, control, and measurement physical equations; "0" subscript denotes initial conditions
f_{ss}	state equation in the state-space model (f in Publication II)
g_{yu}	static gain between process output y and input u
$\mathbf{G}$	process static gain matrix between CV and MV variables
$\hat{\mathbf{G}}$	diagonal $\mathbf{G}$ that only contains control connection MV–CV gains
$\bar{\mathbf{G}}_{mn}$	gain matrix for partially controlled subsystem of $\mathbf{G}$, loops m–n closed
$\mathbf{G}(s)$	process transfer function matrix between CV and MV variables
$\hat{\mathbf{G}}(s)$	diagonal scaled $\mathbf{G}(s)$ that only contains control connection MV–CV transfer functions
$\bar{\mathbf{G}}(s)$	scaled $\mathbf{G}(s)$ matrix
$\mathbf{G}_d(s)$	disturbance transfer function matrix between CVs and disturbances
$\hat{\mathbf{G}}_d(s)$	process CLDG matrix
$\bar{\mathbf{G}}_d(s)$	scaled $\mathbf{G}_d(s)$ matrix
h_w	specific enthalpy of a stream [J/kg]
$h_{yu}(s)$	transfer function between process output y and input u
$\mathbf{H}(j\omega)$	frequency response matrix of $\mathbf{G}(s)$ at frequencies ω
I_i	PID controller integral gain for controlled variable i
$\mathbf{I}$	identity matrix
J	ICPD optimization objective function
j_i	individual ICPD design objective i
j_{ni}	value of objective i with nominal process/control parameters
k	sampling instance
K	UKF Kalman gain

L	firing power [kg/s]
m	amount of matrix rows
n	amount of matrix columns
n_i	amount of variable, stream, or component i (N_i in Publication IV)
N_i	PID controller derivative filter for controlled variable i
p	pressure [bar]
P_i	PID controller proportional gain for controlled variable i
$p(i\|j)$	probability density function for event i, given j
Q	heat transfer rate [W]
q_{E}	parameter for evaporator storage percentage of total storage [%]
q_{S1}	parameter for SH storage percentage before DSH cooling [%]
s	Laplace s-plane operator [rad/s]
s_{w}	specific entropy of a stream [J/(kg·K)]
T	temperature [°C]
T_{K}	temperature [K]
t	time, "0" subscript denotes initial time [s]
t_{I}	thermal inertia delay [s]
u	process input variable or input variable vector
U	vector of controller design parameters
u_{c}	closed-loop input variable in partial control
u_{ci}	input variable that is used to control output variable i
u_{o}	open-loop input variable in partial control
$\tilde{u}_i$	scaled process input variable i (u_i in Publication V)
v	turbine valve position
$\overline{v}$	nominal turbine valve position
$v_{\max}$	maximum bound of the turbine valve signal
$v_{\min}$	minimum bound of the turbine valve signal
w	mass flow (m in Publications III, V) [kg/s]
w_{des}	process and control performance inequality constraints
w_{proc}	process and control physical inequality constraints
w_{ss}	measurement equation in the state-space model (h in Publication II)
W	output work [W]
x	process state variable or state variable vector
$\overline{x}$	process state vector mean
$x(t; x_0)$	differential equation system solution with initial condition x_0
X	vector of process design parameters
y	process output variable or output variable vector

$\bar{y}$	process output vector mean
y_c	closed-loop output variable in partial control
y_o	open-loop output variable in partial control
$\tilde{y}_i$	scaled process output variable i (y_i in Publication V)
$\mathbf{Y}_k$	matrix with measurements up to instance k ($\tilde{Y}_k$ in Publication II)
z_i	reference signal for controlled variable i (i_{SP} in Publication V)

Greek and Cyrillic symbols

α	scaling parameter in the scaled unscented transform
$\mathbf{\Gamma}(s)$	process PRGA matrix
δ	process inequality constraints in CFB steam path ICPD (n in Publication V)
ε	flow exergy [W]
$\varepsilon_{ch,w}$	specific chemical exergy of a stream [J/kg]
η_{ex}	exergy efficiency
η_{th}	energy efficiency
Θ	simulated time range upper limit (T in Publication V) [s]
κ	scaling parameter in the scaled unscented transform
λ	parameter equation in the scaled unscented transform
λ_{yu}	relative gain between output y and input u
μ	measurement equations in CFB steam path ICPD
ξ	process open-loop equations in CFB steam path ICPD (m in Publication V), "0" subscript denotes initial conditions
σ	controllability equations in CFB steam path ICPD
τ_{TOT}	total steam path storage coefficient [$m \cdot s^2$]
Υ	UKF transformed measurement (**Y** in Publication II)
υ	solution distance in Lyapunov stability definition
φ	controller equations in CFB steam path ICPD
ψ	initial condition distance in Lyapunov stability definition
Ω	analyzed frequency range upper limit [rad/s] (F in Publication V)
ω	radial frequency [rad/s]
χ	UKF sigma point (**X** in Publication II)

List of original publications

This thesis is based on the following publications, which are referred throughout the text by their Roman numerals:

I Hultgren, M., Ikonen, E., & Kovács, J. (2014). Oxidant control and air-oxy switching concepts for CFB furnace operation. *Computers & Chemical Engineering, 61*, 203–219. https://doi.org/10.1016/j.compchemeng.2013.10.018

II Hultgren, M., Ikonen, E., & Kovács, J. (2014). Circulating fluidized bed boiler state estimation with an unscented Kalman filter tool. In *2014 IEEE Conference on Control Applications (CCA)* (pp. 310–315). Antibes: Institute of Electrical and Electronics Engineers (IEEE). https://doi.org/10.1109/CCA.2014.6981364

III Hultgren, M., Ikonen, E., & Kovács, J. (2017). Integrated control and process design in CFB boiler design and control – Application possibilities. *IFAC-PapersOnLine, 50*(1), 1997–2004. https://doi.org/10.1016/j.ifacol.2017.08.180

IV Hultgren, M., Ikonen, E., & Kovács, J. (2017). Once-through circulating fluidized bed boiler control design with the dynamic relative gain array and partial relative gain. *Industrial & Engineering Chemistry Research, 56*(48), 14290–14303. https://doi.org/10.1021/acs.iecr.7b03259

V Hultgren, M., Ikonen, E., & Kovács, J. (2019). Integrated control and process design for improved load changes in fluidized bed boiler steam path. *Chemical Engineering Science, 199*, 164–178. https://doi.org/10.1016/j.ces.2019.01.025

All of the publications listed above were written by the author of the thesis. The main responsibilities of the author were research design, modeling for control design, implementation of design and control tools, conduction of simulations, data analysis, and reporting of the results. Experimental data and industrial power plant simulators were obtained from the industrial research partners of this work, and the author participated in experimental testing related to Publications I and II.

Other related publications by the author:

Hultgren, M., Kovács, J., & Ikonen, E. (2015). Combustion control in oxy-fired circulating fluidized bed combustion. In D. Bankiewicz, M. Mäkinen, & P. Yrjas (Eds.), *Proceedings of the 22nd International Conference on Fluidized Bed Conversion: Vol. 2* (pp. 1195–1205). Turku: Åbo Akademi.

Contents

1 Introduction

The thesis investigates the integration of control and process design in circulating fluidized bed (CFB) boilers. In integrated control and process design (ICPD), the process and its control system are designed simultaneously to obtain improved dynamics and control performance. ICPD thus differs from conventional sequential design, where the process is synthesized first based on steady-state specifications, and the control design is performed for the resulting flowsheet to satisfy dynamic performance and stability criteria. The thesis claims that ICPD tools based on first-principles simulation, relative gain analysis, and closed-loop process optimization provide a means for enhanced load change performance in a CFB power plant.

Systematic ICPD design has rarely been applied in scientific literature to large-scale conventional power plants. Dynamic optimization of process and controller parameters has been discussed in a series of works on a residential-scale combined heat and power (CHP) system (Burnak, Diangelakis, Katz, & Pistikopoulos, 2019; Diangelakis, Burnak, & Pistikopoulos, 2017; Diangelakis & Pistikopoulos, 2017a, 2017b; Pistikopoulos & Diangelakis, 2016; Pistikopoulos et al., 2015), where the latest papers also encompassed operational scheduling. Cao, Fuentes-Cortes, Chen, and Zavala (2017) applied multi-objective stochastic programming for minimizing the cost, emissions, and water consumption of a residential-scale CHP system. Teichgraeber, Brodrick, and Brandt (2017) optimized process parameters together with time-variant setpoints for an oxy-fired combined cycle, but with no explicit closed-loop ICPD considerations. Chen and Bollas (2017) applied simultaneous optimization to a combined cycle power plant and Capra and Martelli (2015) to an organic Rankine cycle plant. Powell, Hedengren, and Edgar (2014) investigated the operational flexibility of a hybrid solar-fossil fuel power plant through dynamic optimization. Interestingly, ICPD design has been employed more frequently for improving the load flexibility of the post-combustion capture process for carbon capture and storage (CCS), which is used to separate CO_2 from boiler flue gases (e.g., Sharifzadeh, Bumb, & Shah, 2016; Sharifzadeh & Shah, 2019).

ICPD design has been applied to the fluidized bed boiler for the first time in this thesis and its related publications. ICPD has also never been considered as a solution for improving the performance of industrial load-following boilers prior to the thesis, as this problem has previously only been addressed in a sequential manner through improved control design or new boiler operational modes (Kovács, Kettunen, Ikonen, Hultgren, & Niva, 2015; Zhao, Liu, et al., 2018; Zhao, Wang, Liu, Chong, & Yan, 2018). Improving load changes in combustion power plants is

an essential prerequisite for quickly building a more sustainable energy market with a high percentage of renewables, as flexible generation is a more promising short- to medium-term option for this purpose than demand response or energy storage technologies (Gonzalez-Salazar, Kirsten, & Prchlik, 2018). At the same time, boiler design continuously needs to contribute to the lowering of emissions and increased profitability. These challenges make this thesis a significant contribution to the power generation field and a platform for continued fluidized bed boiler research.

1.1 Research context

Combustion power plants are facing significant challenges in modern power generation, where reducing greenhouse gas emissions has become a priority. Most importantly, boilers are required to perform fast, frequent, and large transitions between load levels (International Energy Agency [IEA], 2011; Kovács et al., 2015). As the portion of renewable energy sources with output power variations increases in the grid (e.g., wind and solar), conventional power plants increasingly need to adjust their own power output to maintain the network balance. The resulting load ramp size and speed requirements can be very challenging for a large industrial power plant (e.g., a 60% to 100% load ramp with a 5%/min speed), which greatly increases the importance of dynamics and control in boiler design.

The new focus on load transitions has had a significant effect on boiler design goals and constraints. Solid fuel power plants were previously mainly operated at full load with the focus on maximum efficiency. Control design centered on fast disturbance rejection, and processes were designed to decrease the effects of disturbances on the power output. In load transition-oriented operation, setpoint tracking is emphasized instead, as the boiler should be able to follow the output electrical power (MW_e) demand trajectory accurately. Boilers are also required to operate at partial loads for long time periods and recover from load changes quickly. Process solutions that contribute to increased MW_e control reserves are essentially favorable for both operational modes, but units with a large thermal storage can also reduce the ability of the process to move rapidly between operating points in load-following mode. Control reserves also typically result in increased capital costs for the power plant due to increased equipment size.

In addition to the load change performance, adequate power generation efficiency should also preferably be maintained in load-following boilers to maximize profits. As higher efficiencies are typically achieved through extreme operating conditions, disturbances caused by large load changes require tight state

variable control due to material safety constraints. Moreover, higher efficiencies have been achieved through large greenfield CFB boiler sizes and interconnected flowsheets, which has resulted in novel and challenging process dynamics.

The second major effect of sustainable power generation on combustion power plants is that the plants themselves should contribute to the lowering of emissions, with the main emission components being CO_2, especially for fossil fuels, as well as SO_X and NO_X. This emphasizes active combustion control, which is complicated further by the current focus on biofuels and waste combustion, mainly because of fuel quality variations and high fuel moisture content. Emission reduction technologies may require extensive changes to the boiler flowsheet and its control system. One prominent example is the oxy-combustion configuration for CCS, where fuel is combusted with a mixture of pure oxygen and recirculated flue gas instead of air in order to concentrate and capture CO_2 emissions.

The new sustainability requirements for solid fuel boilers call for advanced control methods and a plant-wide focus for control design. However, as the open-loop dynamics are fully determined by the process design, the consequent control design has limited possibilities for improving the overall dynamic performance. Clearly, the decision-making domains of process and control design overlap, yet they are usually treated as separate steps. By combining the process and control design stages through ICPD, dynamic aspects and control requirements can affect the process flowsheet design, and process specific dynamics can become more effectively incorporated into the control solution (Fig. 1).

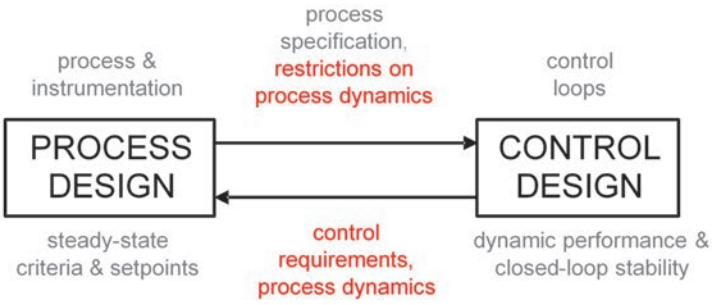

Fig. 1. The ICPD design principle. The red markings illustrate the interaction between the design stages (Reprinted, with permission, from Publication III © 2017 International Federation of Automatic Control [IFAC]).

The design stage interaction has the potential to improve closed-loop responses, and design decisions with a negative influence on control performance can be

avoided. This is the motivation for introducing an integrated design approach for combustion power plants, as described in this thesis. Improving CFB load changes through ICPD allows an increased use of renewable energy, while maintaining network balance. An improved disturbance rejection in boiler state variables enables the use of more extreme operating conditions through control squeeze and shift, leading to increased efficiency and reduced emissions. Lastly, a flexible design approach facilitates the adaptation of existing closed-loop CFB designs to new technologies that offer the potential for emission reduction or improved efficiency, such as oxy-combustion or large supercritical boiler units.

The choice of the CFB as the target boiler for ICPD research was motivated by the current state of solid fuel power generation. CFB technology contributes to reduced SO_X and NO_X emissions and enables the effective combustion of difficult fuels; however, it is also a complex process with turbulent flow conditions, solid material recycle dynamics, and tight furnace temperature constraints. For the water-steam cycle, the thesis focuses on once-through (OTU) boiler control. The OTU setup enables high efficiencies, but is also challenging to control. Together, these aspects create a challenging load-following boiler design problem that would benefit from process and control design integration. Moreover, while the CFB and OTU technologies are well-known separately, the first full-scale supercritical OTU-CFB was only constructed in 2009 (Kovács, Kettunen, & Ojala, 2012).

1.2 Objectives and contributions

ICPD was applied to the industrial-scale CFB boiler process in the work described in this thesis. The main objective was to obtain closed-loop CFB designs with improved load change performance. The secondary objective was to form guidelines for modifying existing CFB designs for process configurations that aim at reduced emissions. Therefore, the goal was ultimately to enable a more sustainable electrical power generation in a grid of both conventional and renewable power plants.

Both objectives were addressed successfully in the thesis and its publications. Faster and more accurate load changes were obtained through an ICPD approach compared to sequential design, and the air-fired CFB boiler was successfully modified for oxy mode. The results showed for the first time that CFB power plant design practices can be improved by forming a link between process and control design. Overall, the contributions of the thesis can be summarized as follows:

1. Control-oriented process analysis based on dynamic simulation was applied to the CFB combustion side. The approach resulted in a detailed comparison of air- and oxy-combustion for the CFB, as well as the novel application of advanced state estimation for CFB model analysis (Publications I and II).
2. A novel characterization of the ICPD research field was formed through an extensive literature review. ICPD design implementation was evaluated for the CFB boiler problem for the first time (Publication III).
3. A relative gain procedure was defined for CFB control design, combining multiple relative gain methods and stepwise variable analysis. It was used to define a zero-level control structure for the OTU-CFB boiler, which is the first extensive plant-wide relative gain application for the CFB boiler (Publication IV).
4. A novel hierarchical ICPD design procedure was formed from established process and control design methods (Publications III, IV, and V).
5. Integrated control and process design was applied to the fluidized bed boiler for the first time through the defined ICPD approach (Publication V).
6. The work showed that improved overall load changes can be obtained for the CFB boiler through ICPD (Publication V).
7. The work established design guidelines for improved load-following performance and effective operation in CFB boilers (Publications I and V).

Publication I showed how control design aspects can be included in CFB process design through first-principles parameter analysis and dynamic simulation. The work resulted in guidelines for modifying the CFB hotloop (furnace, gas-solid separator, solids return leg) for oxy-combustion, including schemes for performing transitions between air and oxy mode. The design integration was promoted for the oxy-CFB by connecting the chemical, physical, operational, and structural properties of the boiler to its control performance, verified through simulations with an industrial hotloop simulator. Publication I differed from much of the prior oxy-CFB process design research through this control-oriented focus. The control design outcomes were further tested through closed-loop simulations by Hultgren, Kovács, and Ikonen (2015).

Publication II demonstrated how unscented Kalman filter (UKF) estimation can be used in ICPD as an offline model analysis tool. This application area differs from the conventional role of state estimation in monitoring and filtering. This publication extended the research described in Publication I by applying a UKF tool to the oxy-CFB hotloop simulator. The tool was used for obtaining accurate

estimates of time-variant process states, inputs, and parameters based on experimental data. The UKF was successfully validated as a suitable tool for CFB process timeseries analysis. This outcome is important, as the performance of the UKF compared to linearized methods is known to be application specific (Daum, 2005). The estimated states can be used to improve process model accuracy and to enable more informed process design decisions.

Publication III formulated a novel characterization of the ICPD research field, where the focus was on reoccurring properties of ICPD methodologies that can be used to select suitable design methods for new process applications. An extensive ICPD literature review was conducted for this purpose, and ICPD was reviewed for power plants for the first time. Two ICPD design examples were also presented for a simple CFB steam path model, constituting the first CFB boiler ICPD case studies. The first example illustrated the effect of steam storage parameters on the dynamic relative gain array (DRGA) and how DRGA changes were reflected in the electrical power control. In the second example, the superheater mass storage was optimized together with the main steam pressure controller for simulated load ramps.

In Publication IV, an extensive controllability and interaction analysis procedure was formulated for the CFB boiler, based on the steady-state partial relative gain (PRG) and the DRGA. While these methods are established in the literature, their combination into a detailed procedure that examines control loop sets of increasing complexity is a novel contribution. The procedure was applied to an industrial OTU-CFB simulator, resulting in a zero-level control structure that supports fast load changes. This work was supported by Hultgren et al. (2015), who used the PRG for the oxy-CFB hotloop. Publication IV also validated the feasibility of using relative gain methods as controllability measures, as the defined procedure was able to highlight the main performance-limiting variable interactions in the OTU-CFB. Control interactions had not been analyzed for the CFB power plant to this extent in earlier literature.

The work carried out in Publications III and IV was expanded in Publication V by defining a novel ICPD procedure for the CFB boiler, with a focus on fast load changes. This was also the first systematic application of ICPD design to a CFB power plant. The publication forms the basis for the ICPD approach of this thesis, by combining closed-loop dynamic process/controller parameter optimization with control structure analysis based on the performance relative gain array (PRGA), and closed-loop disturbance gain (CLDG). Publication V showed how using the procedure for an industrial CFB steam path resulted in improved load changes compared to sequential process design and controller tuning. It was also stated in

this publication that CFB load change performance can be quantified in terms of electrical power tracking, steam pressure control, disturbance rejection capacity, first-principles efficiency, and controllability based on the PRGA and the CLDG.

The research publications and their contributions to the overall research aim are summarized in Table 1. The thesis outline is structured as follows. Chapter 2 describes the CFB power plant and its main control tasks. Chapter 3 presents the ICPD review, and performance evaluation is discussed separately in Chapter 4. Chapter 5 describes the analysis and design methods that are used in the ICPD procedure, and the chapter also summarizes the industrial CFB boiler case studies that were used in Publications I–V to validate the individual methods. Chapter 6 discusses the design results of the case studies and their significance for CFB boiler ICPD development. Finally, Chapter 7 presents the conclusions of the thesis.

Table 1. Introduction of the research papers and their contribution to the research aim.

Original publication	Contribution
Publication I	
Oxidant control and air-oxy switching concepts for CFB furnace operation	Control aspects were integrated into CFB process design through model analysis and dynamic simulation. Guidelines for modifying the CFB for oxy-combustion and performing air to oxy transitions were provided.
Publication II	
Circulating fluidized bed boiler state estimation with an unscented Kalman filter tool	ICPD model analysis was extended with an unscented Kalman filter tool. Estimation of time-variant parameters and states for control-oriented process design was demonstrated for the oxy-CFB.
Publication III	
Integrated control and process design in CFB boiler design and control – application possibilities	A novel ICPD research characterization was made, and ICPD was reviewed for power plants. Relative gain analysis guided process design and ICPD optimization were implemented for the CFB boiler for the first time.
Publication IV	
Once-through circulating fluidized bed boiler control design with the dynamic relative gain array and partial relative gain	An extensive relative gain procedure was defined for CFB control design and interaction analysis in ICPD. Plant-wide control structure selection guidelines were created for the OTU-CFB boiler based on the procedure.
Publication V	
Integrated control and process design for improved load changes in fluidized bed boiler steam path	A novel ICPD procedure was defined for the CFB boiler, combining dynamic ICPD optimization with relative gain control design. Improved load changes were gained for the CFB steam path based on the procedure.

2 CFB boiler process and control

The work carried out for this thesis examined load changes in the circulating fluidized bed (CFB) boiler, depicted in Fig. 2 with a once-through (OTU) steam path. The CFB and the bubbling fluidized bed boiler are fluidized bed processes, and like other solid fuel boilers they consist of the combustion/flue gas side and the water-steam cycle subsystems. Section 2.1 discusses the CFB combustion side, which was the focus of Publications I and II. Section 2.2 deals with the water-steam cycle, which was the target process in Publications III and V. The control tasks of the boiler are presented in Section 2.3; this topic was investigated in Publication IV.

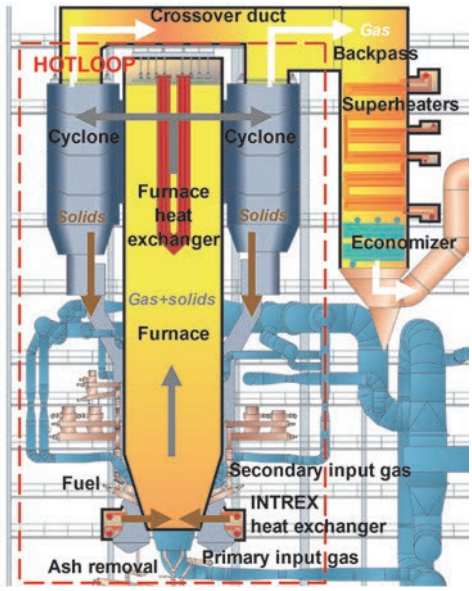

Fig. 2. Operational schematic figure of a CFB boiler (Adapted, with permission, from Publication IV © 2017 American Chemical Society).

2.1 Combustion and flue gas side

In fluidized bed boilers, fuel is combusted in a bed of incombustible material (e.g., sand or ash), which is fluidized in the furnace with the input oxidant gas flows. In the CFB setup, the particles are entrained with the oxidant gas and leave the furnace from the top. The solids are separated from the flue gas in cyclones and the gas is directed to the flue gas duct (Basu, 2006; Sarkar, 2015). The solids are circulated

back to the furnace through the return leg, which often contains solid material heat exchangers (HE) such as Intrex^{TM} fluidized bed units. The furnace temperature is maintained within an 800–900 °C range, and limestone is commonly fed into the bed for SO_X gas capture. The input oxidant gas is heated in LUVO preheaters and fed as the fluidizing primary gas flow (prim.) from the bottom of the furnace, and as secondary gas flows higher up in the riser (sec.).

The input oxidant gas is typically air, and it provides the necessary oxygen for combustion. The oxidant can also be formed in other ways, such as in oxy-combustion carbon capture and storage (CCS). In oxy-combustion (Stanger et al., 2015), fuel is combusted with a mixture of high purity oxygen (typically from an air separation unit, ASU) and recirculated flue gas (RFG), so that the flue gas CO_2 content is elevated to 70–98 vol% (dry). This enables the recovery of CO_2 in carbon compression and purification units (CCU + CPU), see Fig. 3. Aside from greenfield oxy boilers or retrofits to existing power plants, CFB boilers can be constructed as dual-fired units that can operate flexibly in both air and oxy mode. ASU, CCU, and CPU units were considered beyond the scope of this work.

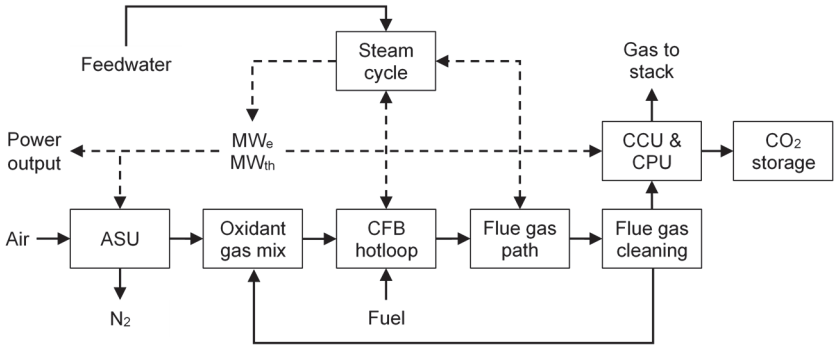

Fig. 3. Oxy-CFB schematic figure, material streams (solid lines), heat (dashed lines).

Oxy-combustion findings from the literature were discussed for both pulverized fuel and fluidized bed boilers in Publication I, and the design aspects explored in Publication I have been discussed in several references since. The fundamentals of fluidized bed oxy-firing were reviewed by Anthony and Hack (2013), Singh and Kumar (2016), and Stanger et al. (2015). The different design requirements for retrofit, dual-fired, and greenfield oxy-CFB boilers were addressed through theory and simulations by Leckner and Gómez-Barea (2014), and Seddighi (2017), similarly to Publication I. Seddighi, Clough, Anthony, Hughes, and Lu (2018) also

examined oxy-CFB scale-up issues. Similarly to the simulations in Publication I, Lappalainen, Tourunen, Mikkonen, Hänninen, and Kovács (2014) performed CFB simulations for transitions between air and oxy mode. Effects of oxy-combustion on solid material heat exchangers (e.g., Intrex units) were omitted from Publication I, and Bolea, Romeo, and Pallarés (2012), and Seddighi, Pallarès, Normann, and Johnsson (2015) concluded that oxy-firing at high O_2 percentages would increase the external heat exchanger material load. With regard to the control design results of Publication I, Niva, Hultgren, Ikonen, and Kovács (2017) carried out plant-wide control synthesis for the oxy-CFB hotloop based on self-optimizing control and relative gain analysis. Liu, Shi, Zhong, and Yu (2019) reviewed the experimental work and the numerical modeling of oxy-CFB coal and biomass co-firing.

Together, the furnace, gas-solid cyclones, and the return leg form the CFB hotloop (Fig. 2). The hotloop and the flue gas path contain heat exchangers, where heat is transferred to the water-steam side to generate steam. The positioning of the heat exchangers on the combustion side is boiler specific, although the evaporator is usually implemented as furnace water-wall tubes, and water and air preheaters are often located as the last heat exchangers of the flue gas path (Joronen, Kovács, & Majanne, 2007). The resulting interconnected process structure and the case-by-case design are the central motivators for studying ICPD for CFB power plants.

2.2 Water-steam cycle

In the water-steam cycle (Joronen et al., 2007; Sarkar, 2015), feedwater (FW) is pumped to a high pressure (pump + valve) and preheated, with the economizer (ECO) as the final preheater before evaporation. Saturated steam is formed in the evaporator (EVAP), and the steam temperature is elevated further in the superheating section, which typically consists of several superheaters (SH) and cooling desuperheater (DSH) water sprays. The pressure and temperature of the resulting superheated main steam (live steam) are the boiler steam parameters.

The main steam expands in the turbine high-pressure (HP) and low-pressure (LP) sections to generate electrical power (MW_e), with possible reheating of the steam between the sections (reheater, RH). The expanded steam is condensed back to water in the condenser. In CHP plants, a portion of the main steam bypasses the turbine and is fed to a CHP heat exchanger to generate heating power. In this work, only condensing plants with electrical power generation are considered.

Based on their evaporator setup, boilers are classified into drum and OTU units (Fig. 4). In drum boilers, water is separated from steam after evaporation and

recirculated back to the evaporator. In OTU boilers, feedwater transforms into main steam in a "once-through" pass without separation, and the boundaries between preheating, evaporation, and superheating may shift depending on the boiler operation. OTU steam generation enables the construction of large CFB boilers with fast changes in the evaporation rate, as well as high efficiencies resulting from the supercritical steam parameters that are enabled by this steam cycle setup. The OTU steam path was investigated in Publication IV.

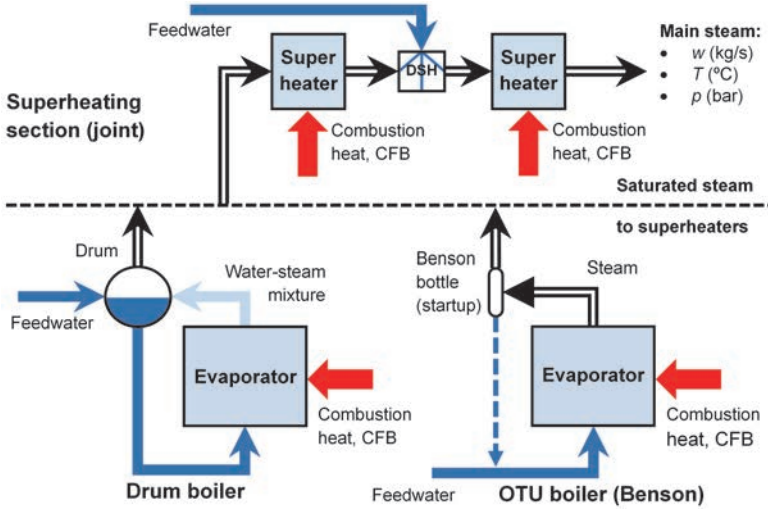

Fig. 4. Basic water-steam paths for generating main steam: the drum boiler and the OTU (Benson) boiler. A two-stage superheating block with one DSH spray is shown.

The steam cycle can either be operated with a constant main steam pressure at all load levels (constant-pressure mode) or with load-dependent main steam pressures (sliding-pressure mode). The steam pressure is maintained with the turbine throttle valve, which enables the use of fast stored steam control reserves. Due to its steam path structure, sliding-pressure operation can more readily be implemented for the OTU boiler than for drum boilers. ICPD design outcomes were compared for constant- and sliding-pressure load changes in Publication V.

The OTU steam path presents challenges for load-following electrical power control. The steam control reserves are limited due to the small evaporator storage capacity, which also causes combustion disturbances to be carried over to the steam quality more easily than in drum boilers. The flow conditions are complex, and the configuration results in a direct connection between the feedwater flow and the

main steam properties (Fig. 5). The resulting interactions have the potential to reduce MW_e control performance, and they were explored in Publication IV.

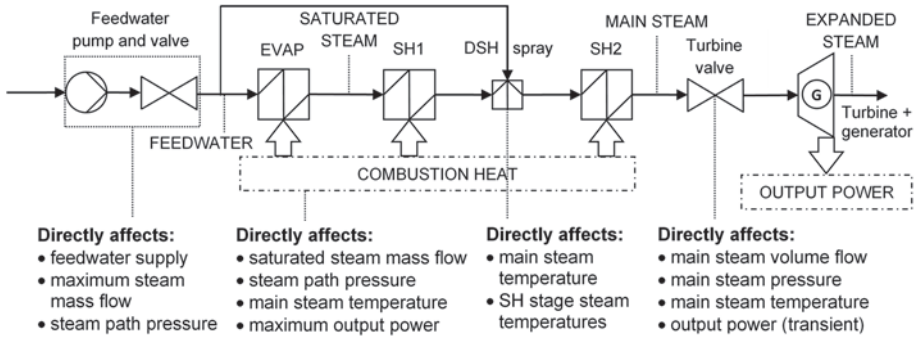

Fig. 5. Effects of manipulated variables on generated power and steam properties.

2.3 Main control tasks

The control objectives of a condensing power plant can be divided between those related to power output and those related to state variables (Doležal & Varcop, 1970; Joronen et al., 2007; Klefenz, 1986). The main control task is to maintain the output electrical power at its setpoint. CHP plants have a separate control target for the generated heat. State variables are controlled to maintain output power quality, high plant efficiency, and operational safety. CFB control tasks and typical control setups from industry were outlined in Publications I and IV:

- *Output MW_e control:* determined by turbine or combustion control.
- *Main steam pressure control:* determined by turbine or combustion control.
- *Turbine-generator unit control:* output MW_e adjusted with the turbine valve; also frequency and voltage for boilers that participate in grid frequency control.
- *Feedwater control:* the feedwater flow should match the generated steam and combustion heat, typically implemented as drum level control (drum boiler) or evaporator output steam enthalpy control (OTU boiler).
- *Steam temperature control:* control of main steam temperature and SH stage intermediate temperatures; most commonly adjusted with DSH sprays.
- *Combustion control:* coordination of fuel and oxidant flows to generate the required heat for steam formation, maintain fluidization, and ensure complete combustion; usually includes separate flue gas O_2 percentage control.

- *Furnace pressure control:* can be adjusted with induced draft flue gas fans.
- *CHP heat control:* can be adjusted using the turbine HP and LP bypass flows.
- *Supporting units:* coordination of boiler with flue gas cleaning, ASU, etc.

The focus of this thesis is on electrical power control during load setpoint changes. This control task is basically a 2 × 2 variable problem between the generated power at the turbine and the generated steam in the boiler. The MW_e output is altered by adjusting the steam flow with the turbine throttle valve or by adjusting the firing power (fuel + oxidant flows). As these actions also affect the main steam pressure, output MW_e control and steam pressure control are coordinated with the upper-level unit master control strategy (Fig. 6). In boiler-following control, the MW_e is controlled with the turbine valve and the main steam pressure with the firing power. In turbine-following control, the opposite control connections are applied. Boiler-following mode enables fast output MW_e changes using the turbine valve, but the new load level can only be maintained permanently by changing the firing power.

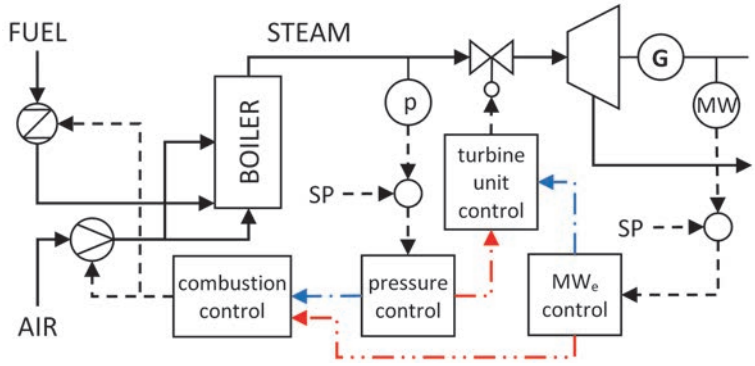

Fig. 6. Boiler-following (blue) and turbine-following (red) control (Reprinted, with permission, from Publication IV © 2017 American Chemical Society).

Multi-loop PID control was used for all CFB control tasks in Publications I–V. This approach was chosen due to the prevalence of PID control even in modern steam power plants, as ICPD control design should preferably be suitable for current industrial practices. Nevertheless, much research has also been conducted for improving MW_e control through advanced control methods. Several references of advanced and model-based load-following control were listed in Publication V, and some recent studies on centralized multiple-input-multiple-output (MIMO) model predictive control (MPC) are mentioned for the CFB boiler in Section 3.2.

3 Integrated control and process design

This chapter describes the integrated control and process design (ICPD) literature review of Publication III. ICPD or "simultaneous design" aims at improving closed-loop performance by increasing the interaction between process and control design. Publication III focused on power plant ICPD applications, and two major outcomes were derived. Firstly, formal ICPD was introduced, which has never been reported for CFB boilers before, and rarely for power plants in general (cf. Chapter 1). Secondly, a novel ICPD classification was formulated, focusing on individual methodology characteristics. The purpose of this chapter is to explain how this characterization influenced the selection of ICPD design methods in the thesis. References were presented for each methodology type in Publication III, and recent reference lists have also been provided by Burnak, Diangelakis, and Pistikopoulos (2019), Rafiei and Ricardez-Sandoval (2020b), Sharifzadeh (2013), Swartz and Kawajiri (2019), and Vega, Lamanna de Rocco, Revollar, and Francisco (2014).

This chapter is structured according to the formulated ICPD characterization, with performance evaluation discussed separately in Chapter 4. Section 3.1 outlines the characterization and compares it with other literature reviews. Section 3.2 deals with the scope and structure of an ICPD methodology. Sections 3.3–3.4 deal with process knowledge oriented ICPD and mathematical programming ICPD. Section 3.5 summarizes the ICPD procedure that was formed based on the literature review.

3.1 ICPD classifications in the literature

The need to integrate control and process design has been recognized for a long time in chemical process engineering. As a result, ICPD is currently a wide research field with numerous approaches for different design needs. Ziegler and Nichols (1943) first stated that control performance depends on both the process and its control system, which summarizes the basic concept of ICPD. Other works that are often cited as pioneering in the field (e.g., Grossmann & Harjunkoski, 2019; Luyben, 2004; Pistikopoulos & Diangelakis, 2016) were provided by Buckley (1964), Lee, Koppel, and Lim (1972), and Sargent (1967).

For systematic ICPD, the first major research direction focused on designing processes that are easy to control, where concepts like controllability and flexibility (cf. Section 4.5) were defined as a bridge between process and control design (Morari, 1992; Perkins, 1989). The second advancement was to formulate process and control design into a simultaneous optimization problem (Perkins & Walsh,

1996). The development of ICPD optimization progressed rapidly (cf. Burnak, Diangelakis, & Pistikopoulos, 2019; Kookos & Perkins, 2004; Sakizlis, Perkins, & Pistikopoulos, 2004) from simpler approaches such as economic back-off evaluation (Narraway, Perkins, & Barton, 1991) to the dynamic optimization of structural and continuous parameters in the closed-loop system (Bahri, Bandoni, & Romagnoli, 1996; Mohideen, Perkins, & Pistikopoulos, 1996; Schweiger & Floudas, 1998). This mathematical programming approach to ICPD has largely dominated contemporary research.

The most recent development in ICPD research is the inclusion of scheduling and operational optimization into the problem (e.g., Burnak, Diangelakis, Katz, & Pistikopoulos, 2019; Koller & Ricardez-Sandoval, 2017). Model-based control is also increasingly used in ICPD (e.g., Gutierrez, Ricardez-Sandoval, Budman, & Prada, 2014; Sakizlis et al., 2004), which coincides with the increased interest in MPC control in industry. Rafiei and Ricardez-Sandoval (2020b) summarized the current challenges for ICPD research: the need for suitable disturbance and uncertainty descriptions, problem size inflation, multi-objective nature of the problem, tendency for local optima, and the added complexity caused by discrete decision variables. On the whole, despite the extensive research history of ICPD, the challenge of fast load changes in large power plants has never been addressed through formal ICPD prior to this thesis.

ICPD approaches were characterized in Publication III according to Table 2, which is a novel contribution of the thesis. The characterization differs from most other reviews, as it highlights individual characteristics that occur in ICPD methodologies rather than defining rigid methodology classes. This thesis posits that the novel characterization facilitates the selection of ICPD methods for a new application area like the CFB. Three main groups were defined in Table 2: “problem definition”, “design decision-making structure”, and “methodology basis”. The first group outlines how the design problem is set up. The second group concerns how process and control design interact. The third group consists of process knowledge and mathematical programming ICPD.

Table 2. Basic ICPD characteristics that were defined in this thesis (Adapted, with permission, from Publication III © 2017 IFAC).

Problem definition	Design structure	Methodology basis
Performance evaluation	Degree of interaction	Process knowledge ICPD
Economic & environmental	Anticipating sequential	Heuristics
Thermodynamic analysis	Partially integrated	Phenomenon based
Dynamic control performance	Fully integrated	System analysis based
System properties for control		
Purpose	Decomposition	Mathematical programming ICPD
Attain achievable performance	Hierarchy of design steps	Controllability optimization
Improve dynamics with design	Decomposition methods	Dynamic optimization, MIDO
Form process + control system	Closed design framework	Embedded control optimization
Scope	Control design	Robust optimization
Continuous/discrete decisions	Adapt default control template	Back-off optimization
Dynamic/static operation	Plant-wide control design	Multi-objective search
Process/control design basis	Model-based control ICPD	Stochastic/probabilistic search

The main connection between Publication III and other reviews comes from the separation between process knowledge and mathematical programming ICPD. Vega et al. (2014) distinguished between dynamic integrated optimization and "projecting methods", where dynamics are incorporated into the design through controllability and multiplicity methods, recycle dynamics, and first-principles analysis. Burnak, Diangelakis, and Pistikopoulos (2019) outlined three ICPD classes: static flexibility analysis, dynamic controllability and resiliency analysis, and the full integration of process and control design in one framework. Similar separations between linear controllability index methods and optimization-based ICPD were described by Engell, Trierweiler, Völker, and Pegel (2004), and Jørgensen, Gani, and Andersen (1999), who also considered passivity-based methods (cf. Subsection 4.5.1) as a separate class. Mencarelli, Chen, Pagot, and Grossmann (2020) grouped process superstructure design methods (cf. Section 3.4) into chemical/physical "targeting techniques", hierarchical decomposition methods, and superstructure optimization.

The characterization in Table 2 differs from most prominent ICPD reviews, as far as process knowledge ICPD is concerned. Firstly, it is considered to be proper ICPD design in the thesis, while many works only label mathematical programming ICPD as "integrated" (e.g., Sharifzadeh, 2013). Secondly, "process knowledge" includes both first-principles and system analysis in Table 2, whereas many authors simply divide ICPD between system analysis approaches and simultaneous

optimization (e.g., Burnak, Diangelakis, & Pistikopoulos, 2019; Sakizlis et al., 2004; Yuan, Chen, Sin, & Gani, 2012). Lastly, the thesis suggests that the difference between heuristics (e.g., Martín & Adams, 2019) and process characterization should be emphasized more in the literature, especially for detailed multi-stage methodologies.

The subclasses of mathematical programming ICPD in Table 2 were inspired by the review of Yuan et al. (2012). The classification focused on solution strategies, while a more property-oriented approach was presented by Vega et al. (2014). Sharifzadeh (2013) outlined a somewhat different classification, containing multi-objective controllability methods, model reduction methods (including robust and embedded control optimization), nonlinearity analysis, geometric operability analysis, flexibility methods, simulator-based dynamic optimization, back-off methods, and the perfect control approach. Gutierrez et al. (2014), Huusom (2015), and Ricardez-Sandoval, Budman, and Douglas (2009) listed classes for controllability index methods, dynamic optimization, and robust optimization. A common general classification (e.g., Sakizlis et al., 2004) considers multi-objective optimization for economically optimal processes with feasible dynamics around nominal operating points, and approaches that use a single economic objective in a dynamic optimization framework with operability constraints.

Here, the ICPD scope was limited to the process (flowsheet, equipment sizing, operating conditions) and its control system (structure, controllers). As such, integrated scheduling and control was considered beyond the scope of this thesis. ICPD was also separated from the broader topic of "process systems engineering" (PSE), which encompasses process simulation, synthesis, control, operations, and optimization (Grossmann & Harjunkoski, 2019), but does not emphasize the interaction between process and control design. Despite this, many design methods are similar in ICPD and PSE, especially for process optimization (e.g., Martín & Adams, 2019; Mitsos et al., 2018). Lastly, ICPD is often connected to process integration and intensification in the literature (Daoutidis, Zachar, & Jogwar, 2016), which are also beyond the scope. For reference, Nikačević, Huesman, Van den Hof, and Stankiewicz (2012) reviewed the effects of process intensification on control and presented a conceptual ICPD approach that focused on intensified processes.

3.2 Problem definition and design structure

The features used for defining the ICPD problem (Table 2, first column) are the purpose, scope, and performance goals of the methodology, as described in

Publication III. Three general purposes can be defined. Firstly, the design can map the achievable dynamic performance, which gives ICPD a benchmarking role. Secondly, the design can suggest modifications for improving control performance and reveal causes for poor open- and closed-loop dynamics. Thirdly, the closed-loop process can be fully generated by the ICPD approach. The ICPD procedure of this thesis considers the latter two approaches in Publications III–V, although the achievable performance was also mapped for oxy-combustion in Publication I.

Regarding scope, ICPD is primarily based on either process or control design, and either static or dynamic operation. Huusom (2015) highlighted how the control problem is always restricted by the process, whereas operational measures from control design must be included separately in the process synthesis problem. The thesis focused on the CFB dynamic operation and relied on control design tools. Available design scopes in ICPD are shown in Fig. 7. Most of the listed continuous variables for process and control design, as well as discrete control connection variables, were considered in Publications I–V. As boiler flowsheets were based on in-house data, discrete variables were not used for the process design.

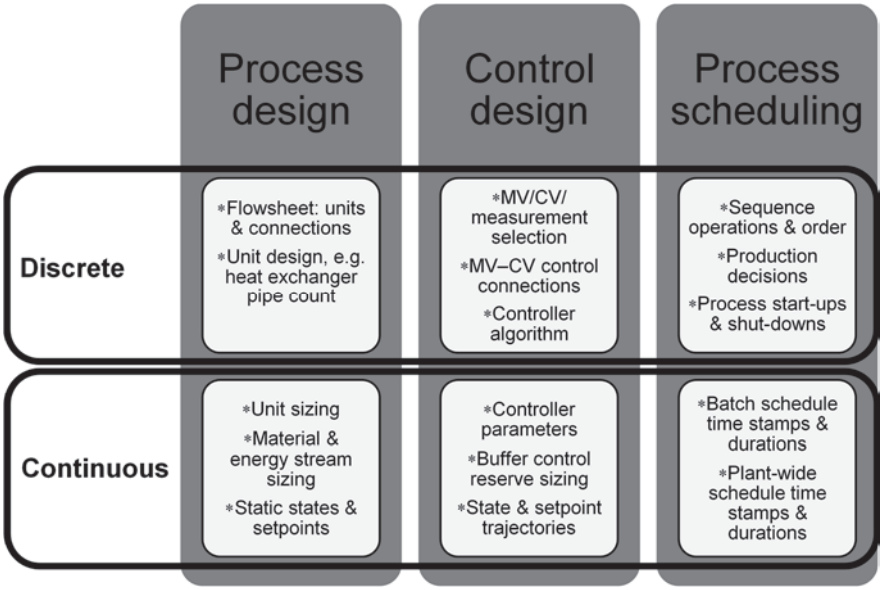

Fig. 7. Decision domains of ICPD, separated into discrete and continuous design.

ICPD is structured (Table 2, second column) based on the degree of process–control interaction, the methodology decomposition, and the control design framework.

The most comprehensive methodologies are fully integrated for all process and control design activities. In partial integration, some design decisions are made outside the main ICPD steps. In anticipating sequential approaches, control aspects are only taken into account during the process design. The ICPD procedure of the thesis is partially integrated, as it consists of two distinct stages: control structure selection (Publications IV and V), and integrated process/controller optimization (Publications III and V). Moreover, Publications I and II represent an anticipating sequential approach, as the goal was to achieve improved CFB dynamic operation in the oxy-fired mode based on knowledge from the air-fired mode.

ICPD methodologies are decomposed as closed frameworks, sets of individual tools, or hierarchies of design steps. Common hierarchical decomposition strategies for control tasks have been discussed by Larsson and Skogestad (2000), Sharifzadeh (2013), Stephanopoulos and Ng (2000), and Vasbinder, Hoo, and Mann (2004). The ICPD procedure of this thesis is a hierarchy of connected design steps, although the ICPD optimization (Publication V) is a fully closed framework.

For the control design framework, Publication III stated how MPC control and especially plant-wide control are important for ICPD. Plant-wide control defines the control strategy for an entire plant, with a particular focus on variable selections and the control system topology. The design is cast as a multi-objective MIMO problem, subject to process dynamics, disturbances, constraints, and control law (Larsson & Skogestad, 2000; Luyben, Tyréus, & Luyben, 1999; Stephanopoulos & Ng, 2000). Many plant-wide control design frameworks contribute to process and control design integration, such as self-optimizing control (Skogestad, 2004) and the eigenvalue-based analytical hierarchical procedure (Vasbinder et al., 2004).

Plant-wide control design tools were used in Publication IV for defining the control structure between pre-selected manipulated variables (MV) and controlled variables (CV) of the CFB boiler. The selection of MVs and CVs was based on design experience (cf. Section 2.3), but formal selection criteria are also available in the literature (Larsson & Skogestad, 2000; Skogestad & Postlethwaite, 2005; van de Wal & de Jager, 2001). Generally speaking, few results are available in the literature regarding plant-wide control in conventional power plants. Aside from the references listed in Publication IV, Niva et al. (2017) and Zotică, Nord, Kovács, and Skogestad (2020) recently applied self-optimizing control to solid fuel boilers.

Several advantages have been presented in the literature for using MPC control in ICPD (Huusom, 2015; Rafiei & Ricardez-Sandoval, 2020b): The controller model can be linked to process parameters, process and controller optimization can be combined, optimal control action is ensured, and effective constraint handling

is possible. Economic-MPC is seen as especially promising for enabling flexible control design during early process design stages (Oyama & Durand, 2020). A centralized MPC can also bypass the need for a separate control structure design step in the ICPD procedure. However, a plant-wide MIMO controller is often challenging to implement in practice (Sharifzadeh, 2013; Skogestad, 2004).

The main question regarding the use of MPC control in CFB boiler ICPD is the availability of suitable controller models for the desired load range. In addition, the models would need to be re-identified for each process structure during the ICPD iteration (Gutierrez et al., 2014; Huusom, 2015). While MPC was not used in the thesis for these reasons, previous CFB boiler MPC applications are available in the literature, with recent papers from Zhang, Gao, Hong, Liu, and Wang (2019) on load-following performance, and Zimmerman, Kyprianidis, and Lindberg (2018) on furnace and steam temperature control, for example. These studies indicate the potential feasibility of MPC-based ICPD for CFB boiler problems in the future.

3.3 Process knowledge oriented ICPD

Process knowledge ICPD relies on modeling and operational knowledge of the process and its control system. The process is examined using first-principles theory, simulation, and system analysis to determine how design decisions affect dynamics and control performance. Closed-loop operation is thus improved through an increased qualitative understanding of the process (Luyben, 2004). Process knowledge ICPD was classified according to Fig. 8 in Publication III.

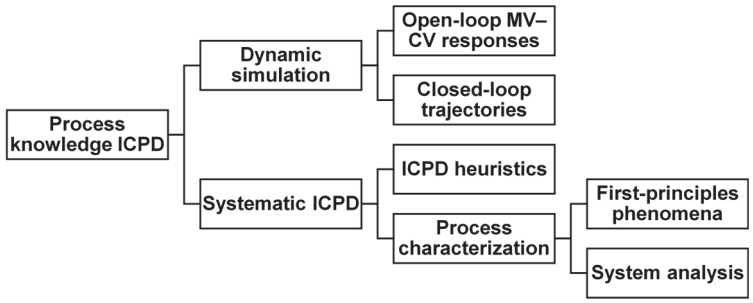

Fig. 8. Classification of process knowledge oriented ICPD methodologies.

The simplest way to implement ICPD is to examine open- or closed-loop dynamics with a simulator during the process design to verify that design decisions do not

lead to dynamic limitations (Lyman & Luyben, 1994). This approach was used for power plants by e.g., Majanne and Maasalo (2009) for analyzing the control system operation, by Mertens, Alobaid, Starkloff, Epple, and Kim (2015) for comparing drum and OTU steam cycle start-up dynamics, by Zhao, Liu, et al. (2018) and Zhao, Wang, et al. (2018) for analyzing different steam extraction modes, as well as by Sharifzadeh and Shah (2019) for post-combustion capture dynamic sensitivity analysis. More systematic ICPD approaches are divided here between heuristics and process characterization, both of which are usually set up as hierarchical procedures or method toolboxes.

Heuristic methods for process and control design (e.g., Larsson & Skogestad, 2000; Luyben, 2004; Luyben et al., 1999) consist of rules and decision charts that determine how specific design questions should be handled to ensure beneficial control properties. Heuristics thus utilize design experience in its most direct form, and most ICPD approaches employ at least some degree of heuristics. Notably, heuristics are used in mathematical programming ICPD for complexity reduction (Perkins & Walsh, 1996) and for ensuring solution optimality and feasibility (Lewin, Seider, & Seader, 2002). The main downside of heuristics is that they can be challenging to employ for new, complex, and unconventional process applications.

Process characterization uses systematic model and response analysis to form a detailed picture about the factors that influence the control of the process. Multiple criteria are usually analyzed to classify the system and characterize its different properties (e.g., Hernjak, Doyle, Ogunnaike, & Pearson, 2004; Huusom, 2015). The resulting qualitative and quantitative information can then be used for more informed closed-loop synthesis. A process can primarily be characterized on a phenomenological or a system analysis basis, cf. Publication III.

Phenomenon-based analysis evaluates how control performance is affected by the chemical and physical properties of the process through first-principles theory and simulations. Some approaches extend first-principles process design procedures (Smith, 2005) with control considerations, such as the methodology proposed by Alvarado-Morales et al. (2010), and Hamid, Sin, and Gani (2010), where the yield and selectivity of reaction and separation processes were connected to the attainable region and the maximum driving force. System analysis focuses on the dynamics of the multi-loop process, with the aim of identifying correlations between design decisions and control-relevant system properties (cf. Section 4.5), such as controllability and resiliency (Engell et al., 2004; Jacobsen & Skogestad, 1991; Weitz & Lewin, 1996). The approach typically relies on low-complexity models and frequency domain methods from classical control theory.

Both phenomenon- and system-oriented process characterization was used in this thesis: chemical and physical analysis for comparing air- and oxy-combustion in Publication I, and relative gain interaction analysis for the OTU-CFB flowsheet in Publication IV. In general, process knowledge ICPD enables the straightforward inclusion of different kinds of control insight into process design, especially qualitative criteria. However, it can be inefficient for managing multiple design objectives, parameter interconnections might be omitted, it is challenging to ensure global optimality, and results may be influenced by designer bias.

3.4 Mathematical programming ICPD

Mathematical programming ICPD formulates the simultaneous process and control design problem as a closed mathematical framework, where solutions are obtained through optimization. Mathematical programming ICPD was classified according to Fig. 9 in Publication III, where the "ICPD methods" group was listed in Table 2 (third column). Methodologies can contain properties from multiple classes.

All of the approaches shown in Fig. 9 can be derived from a generalized problem statement for simultaneous process and control optimization, although the specific formulations for objectives, constraints, and the optimization progression depend on the methodology. General problem formulations have been given by Kookos and Perkins (2004), Sakizlis et. al (2004), Swartz and Kawajiri (2019), and Yuan et al. (2012). A basic formulation based on the literature was also presented in Publication III. This definition is generalized further here to generate

$$\min_{X,U} J(x,u,y,X,U,t,\omega), \tag{1}$$

with conditions

$$\begin{cases} f_{\mathrm{proc}}(x',x,u,y,X,U,t)=0 \\ f_{\mathrm{proc},0}(x,u,y,X,U,t_0)=0 \\ w_{\mathrm{proc}}(u',x,u,X,t)\le 0 \\ f_{\mathrm{des}}(x',u',x,u,y,X,U,t,\omega)=0 \\ w_{\mathrm{des}}(x',u',x,u,y,X,U,t,\omega)\le 0 \end{cases}, \tag{2}$$

where J is a vector of ICPD objective functions, x are state variables, y are output variables, u are input variables, X are process design variables, U are control design variables, t is time, and ω is frequency. f_{proc} contains all the equations of the physical system model, i.e., the process, controllers, and measurements, with initial conditions $f_{\mathrm{proc},0}$ at time t_0. w_{proc} are the physical system inequality constraints. f_{des}

contains all the equations for system performance analysis, including calculated output indicators. w_{des} are performance inequality constraints, including minimum and maximum bounds for X and U, i.e., the ICPD search space.

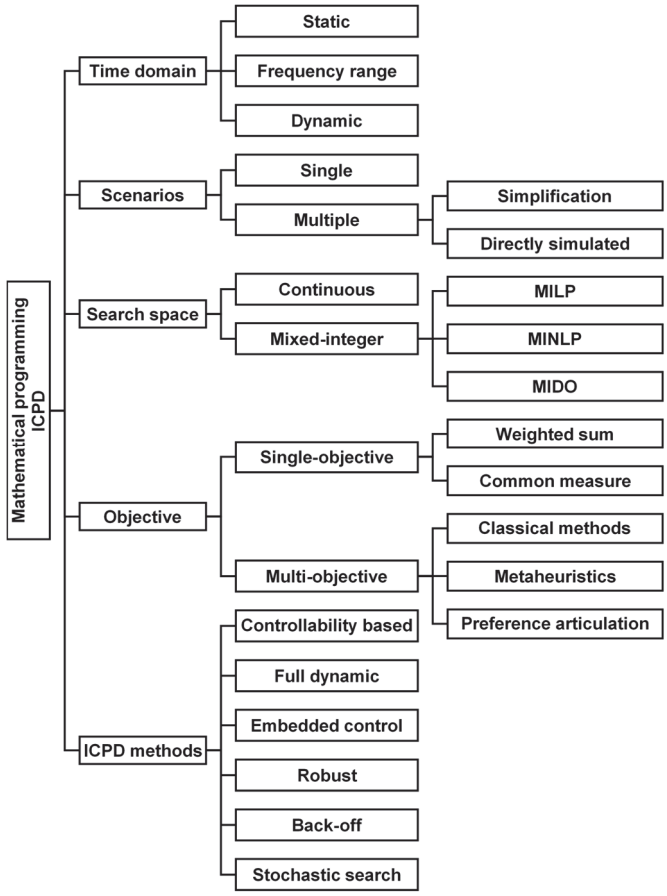

Fig. 9. Classification of mathematical programming oriented ICPD methodologies.

The remainder of this section discusses the classes illustrated in Fig. 9. First, ICPD optimization can be performed for static calculations, multiple frequencies, or full dynamic responses. This selection influences how constraints are formulated and how the process is simulated during the optimization. Similarly, optimization can be performed either for an open-loop or closed-loop system. Closed-loop optimization adds controller model constraints to the problem. In this thesis, the

CFB boiler optimization (Publications III and V) was performed for simulated dynamic closed-loop transients, as well as for open-loop frequency responses.

Dynamic optimization contributes to an increased computational complexity for ICPD. Solution strategies were recently discussed by Biegler (2018), and the ICPD procedure of the thesis employed a simulator-based setup with separate differential equation solver and optimizer layers (Mitsos et al., 2018; Sharifzadeh, 2013). Swartz and Kawajiri (2019) further explored the differences between intentionally dynamic and intrinsically dynamic ICPD problems. The load-following power plant problem can be viewed as intentionally dynamic, although primary regulation already resembles an intrinsically dynamic problem.

Optimization can be performed for one operating point (static) or scenario (dynamic). Alternatively, a range of operating points or scenarios can be evaluated. Many ICPD approaches simplify this multiple scenario setup by considering worst-case disturbances, variability regions, and disturbance rejection capacities. In this thesis, the CFB boiler was optimized for pre-specified scenarios, which were simulated with an internal design model during the optimization iteration.

Depending on the inclusion of structural decisions in the problem (Fig. 7), ICPD optimization is conducted in a continuous framework, or as a mixed-integer linear (MILP) or nonlinear (MINLP) programming setup. This also relates ICPD to flowsheet superstructure optimization (Mencarelli et al., 2020). MINLP is the most comprehensive, but also the most computationally intensive way to synthesize a closed-loop flowsheet. In this thesis, the CFB boiler optimization was continuous, as the flowsheet, control structure, and controller type were determined a priori.

The CFB boiler optimization approach was defined as a weighted sum single-objective problem, where weights were chosen based on objective importance. Alternatively, objectives can be converted into a common measure, e.g., a monetary value. As weighting or normalizing of different types of objectives is often challenging, ICPD can also be performed as proper multi-objective optimization, but in that case additional criteria are necessary for selecting the final solution from the resulting solution plane. Fig. 9 distinguishes between classical multi-objective methods (e.g., ε-constraint, goal programming) and metaheuristics (Alhammadi & Romagnoli, 2004; Liu, Li, Liu, & Guo, 2020), as well as the "preference articulation" between decision and search operations (Chiandussi, Codegone, Ferrero, & Varesio, 2012). Cao et al. (2017) emphasized how the combination of multiple objectives affects the interpretation of process optimization results.

The "ICPD methods" group of Fig. 9 was described in Publication III. The "controllability" approach combines economic optimization with controllability

objectives or constraints. “Dynamic optimization” considers the direct optimization of dynamic economic performance, with the most extensive and challenging approach being mixed-integer dynamic optimization (MIDO). “Embedded control optimization” employs iterative process and control design layers. The “back-off” approach minimizes the dynamic back-off region around an economically optimal operating point. “Robust optimization” is based on robust control methods, and “stochastic search” focuses on the effects of uncertain parameters and disturbances on the design outcome. Recent research has largely centered on robust and stochastic ICPD (Grossmann, Apap, Calfa, García-Herreros, & Zhang, 2016; Rafiei & Ricardez-Sandoval, 2020b). Notably, several works have combined aspects of robust optimization (Ricardez-Sandoval et al., 2009) with back-off optimization (Kookos & Perkins, 2004). The normal vector approach that was used recently by Muñoz, Gerhard, and Marquardt (2012) utilizes the distance to feasible operating regions as a back-off type robustness criterion, while another series of works (e.g., Mehta & Ricardez-Sandoval, 2016; Rafiei & Ricardez-Sandoval, 2020a) presented a robust dynamic approach that used a power series expansion for constraints and variable back-off evaluation through trust-region methods. The need for advanced solution strategies highlights the challenges related to fully simultaneous dynamic optimization, despite the constantly increasing availability of computing power. This applies especially to MIDO, with recent results from e.g., Biegler (2018), Burnak, Diangelakis, Katz, and Pistikopoulos (2019), and Koller and Ricardez-Sandoval (2017).

The main benefit of mathematical programming ICPD is that it can produce a complete solution to a process/control problem with several interacting objectives, also accounting for unconventional solutions. However, the resulting problem is often computationally intensive, especially for plant-wide models. The entire ICPD problem must be expressed in a feasible mathematical format, which can be a limitation for qualitative and non-continuous criteria. The problem definition has a large impact on the optimization outcome, and calculated optima might not be applicable in practice. These factors served as the motivation for the stepwise ICPD procedure of this thesis, where process knowledge and system analysis pre-design are used to reduce the complexity of the ICPD optimization problem.

3.5 Summary of chosen approach for CFB ICPD

The main components of the ICPD procedure that was derived in the thesis are summarized here, with more detailed descriptions given in Chapter 5. The aim of

the procedure is to combine closed-loop load change trajectory design with open-loop system analysis independent of controller type, first-principles modeling, and expert interaction. As such, the procedure consists of dynamic ICPD optimization, systematic control structure selection, and process knowledge pre-design:

- *ICPD optimization:* Continuous process and controller parameters were simultaneously optimized in Publications III and V for simulated closed-loop load change trajectories in a fixed time range. A single weighted optimization objective was used, with the main weight on MW_e setpoint tracking.
- *Control structure selection:* Control connections between MVs and CVs were evaluated in Publications IV and V using different relative gain methods. The analysis provided the preferred control structure and highlighted how process parameters affected controllability and control loop interactions.
- *Process pre-analysis:* The effects of the process and control parameters on dynamic performance were analyzed qualitatively in Publications I and II using the first-principles theory, detailed simulation, and advanced state estimation.

4 Quantifying performance

Publication III emphasized how the performance evaluation framework forms the basis for the ICPD implementation, especially for ICPD optimization. The evaluation methods should accurately quantify the desired system performance, identify the factors that affect it, and provide a suitable ranking of process solutions. The purpose of this chapter is to establish the performance guidelines for the load-following CFB boiler problem, with separate Sections 4.1–4.5 for economic performance, environmental performance, thermodynamic analysis, control performance, and system analysis. Section 4.6 summarizes the chosen guidelines.

4.1 Economic performance

Economic performance evaluation aims at minimizing the capital and operating costs of the process or maximizing product revenue compared to production costs (Smith, 2005). Capital costs are principally derived from the process (equipment sizing, nominal throughput, etc.), whereas operating costs are more influenced by process setpoints, control, and scheduling. Some ICPD approaches define more detailed cost decompositions, such as the "communication costs" for the control structure alternatives described by Gutierrez et al. (2014). Process economics can also be assessed in ICPD through on-specification production amounts or standard metrics like the total annual cost, economic potential, return on investment, discounted cash flow, and net present value (Frumkin & Doherty, 2020; Liu, Georgiadis, & Pistikopoulos, 2011; Luyben, 2004; Smith, 2005). Economic performance is usually evaluated for longer timespans, e.g., on an annualized basis.

Contemporary ICPD increasingly aims at optimizing process economics directly, as this is usually the most important design objective for the plant. The main benefit of economic evaluation for ICPD is that it enables a direct comparison of different objectives by assigning economic values to them. This was exemplified for power plants by Kragelund, Wisniewski, Mølbak, Nielsen, and Edlund (2008), who connected process economics to lower-level efficiency, controllability, and availability objectives. Economic evaluation also creates an inherent trade-off between process and control design, as extra disturbance rejection capacity in the process typically leads to capital cost penalties (Huusom, 2015; Luyben, 2004).

Despite these benefits, many authors have highlighted how closed-loop design based on process economics alone is often not sufficient for dynamic performance and sustainability (Liu et al., 2011; Martín & Adams, 2019; Siirola & Edgar, 2012).

Examining operating costs and allocating capital costs can be challenging for short time periods like a load change scenario, and economic penalties for primary regulation MW_e setpoint violations can be unintuitive to estimate or compare with other costs. In addition, assigning representative economic values for objectives like robustness or stability can be difficult. Lastly, fuel and electricity price variations make the design results market dependent, although this limitation can be addressed to some extent through robust and stochastic methods.

Due to these considerations, a separate economic objective was not considered in Publications I–V, although the process parameter search space was based on acceptable capital costs. As stated in Publication V, economic evaluation should be included in future work to avoid designs with significant economic penalties, and Publication III stated that economic performance should be evaluated as the fuel and annualized investment costs, scaled with the generated power. This evaluation could be performed for the final solution candidates from the ICPD procedure, or the ICPD optimization objective could be expanded with an economic penalty term.

4.2 Environmental performance

Environmental performance evaluation aims at minimizing selected emissions or the environmental footprint of the process. Environmental regulations can usually be specified as averages for pollutant mass flows. In addition, relevant performance indices for power plants like the global warming potential are derived from life cycle analysis, LCA (Klöpffer & Grahl, 2014; Smith, 2005). For example, Liu et al. (2011) used a cradle-to-gate greenhouse gas index for the mixed-integer multi-objective process optimization of a poly-generation energy system. In general, the increased capital and operating costs of emission management often call for multi-objective design (Alhammadi & Romagnoli, 2004; Martín & Adams, 2019).

Environmental analysis can be expanded to the general topic of sustainability (Daoutidis et al., 2016; Rafiei & Ricardez-Sandoval, 2020b), which also includes central power plant design objectives like safety. Sustainability and environmental objectives are often evaluated on a steady-state basis, as they can be challenging to align with dynamics and control. Moreover, they can be difficult to translate into actual process modifications (Daoutidis et al., 2016; Siirola & Edgar, 2012).

For solid fuel boilers like the CFB, the main pollutants to be considered are CO_2, NO_X, and SO_X gases, as well as CO for incomplete combustion scenarios. The specific emission factors of these gases were recently analyzed for subcritical and supercritical pulverized coal power plants by Gonzalez-Salazar et al. (2018). The

flue gas CO_2 percentage was a central performance target in Publications I and II, as it directly reflects the CCU + CPU operating costs in oxy-combustion. Similarly, either the flue gas CO_2 or the global warming potential should be included as a steady-state objective or constraint for generic CFB boiler problems in the ICPD procedure. The low furnace temperatures and in-bed limestone feed in the CFB (cf. Section 2.1) made NO_X and SO_X less relevant concerns for this thesis. Like process economics, environmental goals should be scaled with the generated power.

4.3 First-principles analysis

In first-principles analysis, the chemical and physical properties of the process are direct design objectives, or they are indicative of the desired performance, such as in the approach of Alvarado-Morales et al. (2010) and Hamid et al. (2010). The analysis quantifies how effectively the process transforms raw materials into products by describing the process through first-principles models, which are then linked to the system performance, such as economics in the screening approach of Frumkin and Doherty (2020). First-principles evaluation is prevalent in process knowledge ICPD, such as the analysis outlined in Publication I, where the effects of chemical and physical properties on load change performance were investigated.

Energy and exergy efficiency analysis are notable first-principles performance evaluation fields for power plants (Joronen et al., 2007; Kaushik, Reddy, & Tyagi, 2011). A key design objective for base load power plants has conventionally been energy efficiency of

$$\eta_{\mathrm{th}} = \frac{W}{Q_{\mathrm{in}}} = \left(1 - \frac{Q_{\mathrm{out}}}{Q_{\mathrm{in}}}\right), \tag{3}$$

where η_{th} is energy efficiency, Q is the heat transfer rate (in and out), and W is work. Exergy is the maximum useful work performed by a system that brings it into equilibrium with its surroundings. When excluding kinetic, potential, and nuclear exergy, it can be defined (Szargut, 2005) for a stream as

$$\varepsilon = w \cdot \left(\varepsilon_{\mathrm{ch,w}} + (h_{\mathrm{w}} - h_{\mathrm{w}}^{*}) - T_{\mathrm{K}}^{*} \cdot (s_{\mathrm{w}} - s_{\mathrm{w}}^{*})\right) + Q \cdot \left(1 - \frac{T_{\mathrm{K}}^{*}}{T_{\mathrm{K}}}\right), \tag{4}$$

where ε is flow exergy and T_K is the temperature. The stream has a mass flow w, specific enthalpy h_{w}, specific entropy s_{w}, and specific chemical exergy $\varepsilon_{\mathrm{ch,w}}$, derived from compound Gibbs standard free energies of formation and elemental specific chemical exergies. Superscript * denotes the reference state. Exergy efficiency

accounts for the thermodynamic irreversibility in the process, and it can be used as a convenient environmental performance measure as

$$\eta_{\mathrm{ex}} = \frac{\varepsilon_{\mathrm{out}}}{\varepsilon_{\mathrm{in}}} = \left(1 - \frac{B}{\varepsilon_{\mathrm{in}}}\right), \tag{5}$$

where η_{ex} is exergy efficiency, ε is flow exergy (in and out), and B is the irreversibility rate.

For CFB boiler ICPD, thermodynamic efficiency is useful as an alternative indicator to economic performance, especially as it is independent of assigned costs and market assumptions. Exergy was accounted for in Publication V by minimizing steam throttling: Turbine valve control action contributes to exergy destruction in Eq. 4 due to the increase in specific entropy, but it is also essential for achieving fast load changes. Relevant examples for Publications I and II were provided recently by Jin, Zhao, and Zheng (2016), and Luo, Wang, Guo, Liu, and Zheng (2015), who employed a dynamic exergy analysis framework for comparing control setups and operating modes for the oxy-fired boiler, ASU, and CCU + CPU units.

4.4 Dynamics and control performance

Dynamic performance evaluation focuses on optimizing system responses directly, including CV setpoint tracking, CV disturbance rejection, and MV trajectories. Performance is evaluated by analyzing closed-loop responses during specified setpoint changes and disturbances or by generating a system with beneficial open-loop dynamics. The approach is thus based on data or dynamic simulation, and the focus is typically on regulative control performance rather than optimizing control.

The closed-loop approach relies on norms and time integrals for CV and MV signals (Skogestad & Postlethwaite, 2005). Setpoint tracking is usually evaluated in ICPD through the integral square error (ISE), the integral absolute error (IAE), or time-weighted IAE and ISE formats (Ogata, 2010; Ogunnaike & Ray, 1994). Notably, Ulbig and Andersson (2015) defined custom dynamic response measures for power system operational flexibility, which were applied by Zhao, Liu, et al. (2018) and Zhao, Wang, et al. (2018) to simulated boiler responses. In Publication V, electrical power and main steam pressure setpoint tracking were evaluated with the ISE of

$$\mathrm{ISE} = \int_0^{\Theta} |y(t) - z(t)|^2 dt, \tag{6}$$

where y is the output, z is the reference signal, t is time, and Θ is the time range.

Closed-loop disturbance rejection properties include metrics like the MV and CV variances, the MV change rate, the maximum setpoint deviation, the minimum and maximum MV magnitudes, and the idle index (Hovd, Ma, & Braatz, 2003; Jelali, 2006; Lee et al., 1972). In general, control performance can be evaluated based on MV signals by comparing the closed-loop system either to an ideal MV benchmark or an ideally tuned feedback controller. MV benchmarks can be divided further into variance-based methods (e.g., Harris index modifications) and advanced benchmarks, such as those based on linear quadratic Gaussian control.

Specifying the investigated disturbance scenarios is an essential part of closed-loop evaluation. An example was provided for load-following boilers by Gonzalez-Salazar et al. (2018), who outlined a set of standard disturbance types for variable-load cyclic operation. In this thesis, the setpoint change magnitudes and rates of load transitions were based on boiler design requirements and in-house data.

When ICPD focuses on open-loop responses, the design assumes that fast and simple MV–CV dynamics contribute to good control performance and enable effective controller tuning. Dynamics can be evaluated from step responses by calculating rise times, settling times, time constants, time delays, overshoots, and inverse response magnitudes (Ogunnaike & Ray, 1994). A more quantitative approach is to compare the response to a suitable low-order linear time-invariant (LTI) model (Hernjak et al., 2004). Another open-loop approach is to evaluate the magnitude of disturbances that can be rejected with available control reserves, back-calculated from simulations or first-principles theory. This approach was used in Publication V by monitoring the saturation time of the turbine valve.

Dynamic analysis is the most direct way of quantifying control performance, which makes it a key tool for load-following CFB boiler ICPD design. However, the design also depends heavily on the chosen simulation scenarios. This includes the examined time range (Fig. 10), which should be short enough to focus on the transition, but long enough to ensure that the new setpoint is maintained. The latter issue can be mitigated by monitoring state derivatives at the end of the time range (Bahri et al., 1996) or through closed-loop stability evaluation (cf. Section 4.5). Another limitation for measures like the ISE is that they do not explicitly account for the response shape, as any setpoint deviation adds to the error norm value. This can lead to tightly controlled systems with large overshoots, slow integral action, and oscillation. Different responses can produce the same ISE value (Fig. 10), which contributes to the formation of local optima (Schweiger & Floudas, 1998).

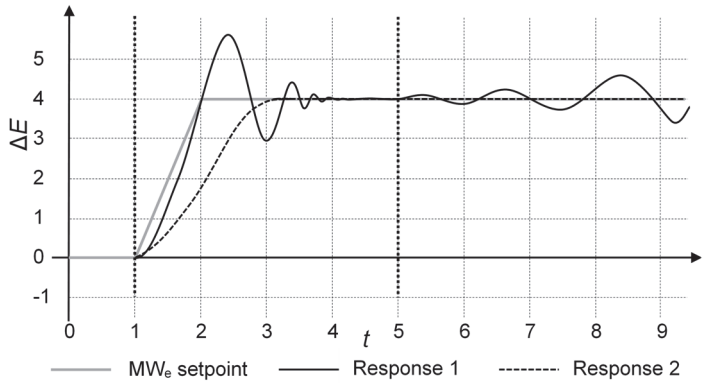

Fig. 10. Conceptual figure of two electrical power (*E*) setpoint ramp responses, where the ISE has been optimized between 1 s and 5 s. The chosen time range results in an unstable system for response 1, and similar ISE values for responses 1 and 2.

4.5 System analysis

System analysis aims at generating processes with inherent properties that are favorable for control, and control systems that contribute to good dynamic performance. Basic approaches rely on concepts from classical control design and are largely based on LTI process descriptions such as transfer function, state-space, frequency response, or impulse response models (Ogunnaike & Ray, 1994; Skogestad & Postlethwaite, 2005). More advanced concepts make use of nonlinear models and dynamic optimization to evaluate performance measures.

System analysis concepts that are common in ICPD are listed in Subsection 4.5.1. The focus is on controllability, which was used as a control structure selection criterion in Publications IV and V, and a design objective in Publications III and V. The relevant system analysis tools for this thesis are discussed in Subsection 4.5.2.

The benefit of system analysis performance evaluation is that it enables the efficient quantification of control-relevant system properties that are difficult to describe through other means. However, methods based on steady-state or linear dynamic analysis may be unsuitable, especially for a wide process operating region, and more advanced nonlinear approaches have elevated computational costs. The connection between performance measure values and the desired system behavior (e.g., economics) is also often not straightforward (Sakizlis et al., 2004; Yuan et al., 2012). Lastly, analysis methods typically only provide a relative ranking of solutions or indicate the existence of control problems (Perkins & Walsh, 1996).

4.5.1 Concepts

Controllability is defined in various ways in the literature (Skogestad & Postlethwaite, 2005). Originally, it was specified as the ability of the process to achieve and maintain a desired equilibrium value (Ziegler & Nichols, 1943). Rosenbrock (1970) later generalized it for all specified control aims, including the evaluation of the degree of controllability. Common controllability definitions are listed below. Integral and input–output controllability were the main forms of controllability considered in this thesis.

- *Input–output controllability:* A system is input–output controllable if it is able to keep outputs $y(t)$ within specified bounds or displacements from their references $z(t)$ despite unknown bounded disturbances and dynamic variations, using available inputs $u(t)$ and measurements (Skogestad, 1994). This has to be verified through multiple criteria (Skogestad & Postlethwaite, 2005).
- *Integral controllability & integrity:* A system is integral controllable if there exists a controller with integral action, $1/s \cdot c(s)$, which will make the system "unconditionally" stable ("internal" stability, detuning of loops is possible). Integrity requires that the closed-loop system remains internally stable when any combination of loops is opened. Together, these concepts form the definitions of ICI and DIC (Campo & Morari, 1994; Chiu & Arkun, 1990). A system is integral controllable with integrity (ICI) if it remains stable when all loops (with integral control action) are detuned by the same factor between 0 and 1. Decentralized integral controllability (DIC) further demands that all loops can be detuned by individual factors.
- *Functional controllability:* A system is functionally controllable if given any suitable output vector $y(t)$, there exists an input vector $u(t)$ ($t > 0$) that generates $y(t)$ from the initial condition $x(0) = 0$ (Rosenbrock, 1970). Controllability can be verified by requiring that the normal rank of the process transfer function matrix (cf. Subsection 4.5.2) must equal the amount of outputs $y(t)$.
- *State controllability:* The system $x'(t) = \mathbf{A}x(t) + \mathbf{B}u(t)$, $y(t) = \mathbf{C}x(t) + \mathbf{D}u(t)$ is state controllable if for any initial state $x(0) = x_0$, any time $t_1 > 0$, and any final state x_1, there exists an input $u(t)$ that produces $x(t_1) = x_1$ (Kalman, 1960). While commonly used in control theory, state controllability has limitations in practice (Perkins, 1989; Skogestad & Postlethwaite, 2005). It is verified by evaluating whether the rank of the controllability matrix $[\mathbf{B}, \mathbf{AB}, \ldots, \mathbf{A}^{n-1}\mathbf{B}]$ equals the length of the state vector, n. State observability is defined

analogously: a system is observable if knowledge of its past inputs $u(t)$ and outputs $y(t)$ between $0 < t < t_1$ fully determines its initial state $x(0) = x_0$. In this case, the rank of the observability matrix $[\mathbf{C}^T , (\mathbf{CA})^T , \dots , (\mathbf{CA}^{n-1})^T]^T$ is n.

– *Structural controllability:* The system $x'(t) = \mathbf{A}x(t) + \mathbf{B}u(t)$ is structurally controllable if there exists a structurally equivalent system (same locations of fixed zero and non-zero matrix entries) to the pair (**A**, **B**) that is controllable (Shields & Pearson, 1976).

Beside controllability, the related concepts of resiliency, flexibility, switchability, and operability have a central role in ICPD performance evaluation (Burnak, Diangelakis, & Pistikopoulos, 2019; Jørgensen et al., 1999). Dynamic resiliency is defined as the dynamic capability of the process to recover from disturbances quickly and smoothly (Grossmann, Calfa, & Garcia-Herreros, 2014; Weitz & Lewin, 1996). Essentially, it determines the upper bound for the achievable closed-loop performance independent of controller type, originally obtained through internal model control. The main properties that limit plant resiliency are non-minimum phase behavior (time delays, right-half plane zeros), MV constraints, and plant-model mismatch.

Flexibility, switchability, and operability are typically evaluated through optimization. Flexibility is the ability of the process to attain feasible operation at different operating points over a range of uncertainties and disturbances (Grossmann et al., 2014; Koller & Ricardez-Sandoval, 2017; Mohideen et al., 1996), and it has been defined for both steady-state and dynamic operation. The analysis consists of a flexibility test and a flexibility index. The flexibility test maximizes the minimum deviation from the process active constraints, whereas the flexibility index maximizes the largest deviation that can be handled by the system.

Switchability is the ability of the process to move feasibly, effectively, and safely between operating points (Perkins, 1989; Vu, Bahri, & Romagnoli, 1997; White, Perkins, & Espie, 1996). It consists of feasibility and optimality evaluation for the dynamic switch trajectory. Typically, the control signal trajectory is optimized, with CV setpoint tracking error measures as objectives, cf. Section 4.4.

Operability is the ability of the closed-loop process to satisfy steady-state and dynamic requirements in the presence of expected disturbances without violating process constraints, using available input MVs (Bahri et al., 1996; Perkins, 1989). It contains aspects of controllability, resiliency, flexibility, and switchability. Operability analysis is usually set up as a dynamic optimization problem. In

addition, approaches based on geometric operational input/output regions are notable in ICPD research (Georgakis, Vinson, Subramanian, & Uztürk, 2004).

Like controllability, process stability is defined in various ways (Åström & Murray, 2008; Ogata, 2010; Ogunnaike & Ray, 1994). A common definition is Lyapunov stability for a solution $x(t; x_0)$ to a differential equation system with initial condition x_0. The solution is stable if, for all distances $\upsilon > 0$ and times $t > 0$, there exists a distance $\psi > 0$ for which $||x(t; x_1) - x(t; x_0)|| < \upsilon$, when $||x_1 - x_0|| < \psi$ (Åström & Murray, 2008). Further conditions are defined for asymptotical stability, stability within a domain, and global stability. Stable LTI components do not contain hidden unstable modes, and the injection of bounded external signals at any point in the system results in bounded outputs in the entire system, designated as "internal" stability (Skogestad & Postlethwaite, 2005). Some ICPD approaches are based on the concept of passivity, which guarantees asymptotically stable flowsheets as combinations of passive systems (Jørgensen et al., 1999; Sharifzadeh, 2013).

Process nonlinearity signifies the degree to which the process dynamics deviate from linear responses. Formally, linearity can be verified through three conditions (Åström & Murray, 2008): output linearity in the initial condition response (input is zero), output linearity in the forced response (initial condition is zero), and input superposition. Control nonlinearity can be inherent (e.g., saturation, dead zone, hysteresis), or it can be introduced intentionally for the control design (Ogata, 2010). Nonlinearity analysis is used in ICPD to assess control limitations, control design challenges, problematic process operating modes, and the applicability of linear system analysis methods (Jelali, 2006; Schweickhardt & Allgöwer, 2004).

Robustness is defined as insensitiveness to model uncertainty and plant-model mismatch (Åström & Murray, 2008; Skogestad & Postlethwaite, 2005). Robustness consists of robust stability and robust performance. Robust stability guarantees that the system remains stable for a defined uncertainty set, and robust performance guarantees that all desired performance criteria are satisfied for the uncertainty set.

4.5.2 Methods and tools

Many classical control methods have been used in ICPD for quantifying the concepts described in Subsection 4.5.1. These include Nyquist and Bode plots, root locus and pole/zero analysis, H_2 and H_∞ norms, stability criteria (e.g., Routh criterion, Hurwitz criterion), Lyapunov functions, and the ν-gap metric. These methods are well-documented in the control literature and are not elaborated on here (e.g., Åström & Murray, 2008; Ogata, 2010; Ogunnaike & Ray, 1994;

Skogestad & Postlethwaite, 2005). Process nonlinearity can be quantified by comparing a response to a corresponding linear operator, e.g., through error norms. Various nonlinearity-centric ICPD approaches have been devised (Sharifzadeh, 2013), where control-relevant nonlinearity (Schweickhardt & Allgöwer, 2004) and nonlinear controllability analysis through bifurcations (Jørgensen et al., 1999; Morari, 1992) can be highlighted.

Of the linear approaches, five connected methods are often employed in ICPD: eigenvalues, singular values, the condition number, sensitivity functions, and the relative gain array. These methods are used to examine input–output controllability, resiliency, high- and low-gain parameter/disturbance directions, stability, robustness, and loop interactions (Engell et al., 2004; Morari, 1992; Perkins, 1989; Skogestad & Postlethwaite, 2005; van de Wal & de Jager, 2001). For their calculation, the MIMO process is described as a matrix of LTI models between system MVs and CVs in the static domain (steady-state gains) by

$$\mathbf{G} = \begin{bmatrix} g_{11} & \cdots & g_{1n} \\ \vdots & \ddots & \vdots \\ g_{m1} & \cdots & g_{mn} \end{bmatrix} = \begin{bmatrix} \frac{y_1(0)}{u_1(0)} & \cdots & \frac{y_1(0)}{u_n(0)} \\ \vdots & \ddots & \vdots \\ \frac{y_m(0)}{u_1(0)} & \cdots & \frac{y_m(0)}{u_n(0)} \end{bmatrix}, \tag{7}$$

or in the dynamic domain for multiple frequencies (transfer functions) by

$$\mathbf{G}(s) = \begin{bmatrix} h_{11}(s) & \cdots & h_{1n}(s) \\ \vdots & \ddots & \vdots \\ h_{m1}(s) & \cdots & h_{mn}(s) \end{bmatrix} = \begin{bmatrix} \frac{y_1(s)}{u_1(s)} & \cdots & \frac{y_1(s)}{u_n(s)} \\ \vdots & \ddots & \vdots \\ \frac{y_m(s)}{u_1(s)} & \cdots & \frac{y_m(s)}{u_n(s)} \end{bmatrix}, \tag{8}$$

where $\mathbf{G}$ is the process gain matrix, $\mathbf{G}(s)$ is the process transfer matrix with Laplace operator s, g_{yu} are the static gains between output y and input u, $h_{yu}(s)$ are the transfer functions between y and u, and m and n are the total amounts of y and u.

State and transfer matrix eigenvalues are used for analyzing dominant process directions, and large eigenvalue variations imply parameter and input sensitivity. The singular value decomposition of $\mathbf{G}(s)$ determines how close the process is to being singular, and it addresses some of the shortcomings of eigenvalue analysis (Skogestad & Postlethwaite, 2005). The process condition number is the ratio between the minimum and maximum singular value. A large condition number can signify that the plant is ill-conditioned, which can manifest itself as correlated CVs or as similar effects of various MVs on the CVs. The sensitivity functions of $\mathbf{G}(s)$ are used for analyzing the changes in input–output sensitivity caused by feedback and interactions. As the relative gain array is a central method in this thesis, it is

discussed next in greater detail. While relative gain methods are most commonly used for selecting control structures between MVs and CVs, authors like Jacobsen and Skogestad (1991) also employed them more directly for guiding process design.

Relative gain methods are derived from the static relative gain array, the RGA (Bristol, 1966). For square systems with an equal number of MVs (columns) and CVs (rows), the basic RGA is defined as

$$\mathrm{RGA}(\mathbf{G}) = \mathbf{G} \times (\mathbf{G}^{-1})^{\mathrm{T}} = \begin{bmatrix} \lambda_{11} & \cdots & \lambda_{1n} \\ \vdots & \ddots & \vdots \\ \lambda_{m1} & \cdots & \lambda_{mn} \end{bmatrix}, \tag{9}$$

where λ_{yu} are relative gains between outputs y and inputs u (total amounts m and n), and "×" signifies an element-by-element multiplication. The RGA can also be generalized for non-square plants (Skogestad & Postlethwaite, 2005).

The RGA is scaling invariant and forms row/column sums of ones. It contains interaction terms λ_{yu} that signify how much MV–CV open-loop gains change due to interactions in the multi-loop system, cf. Publication IV. Each control structure with its MV–CV connections is characterized by its λ_{yu} elements, which can also be combined into one measure with the RGA number by equation

$$\mathrm{nRGA}(\mathbf{G}) = \|\mathrm{RGA}(\mathbf{G}) - \mathbf{I}\|_{\mathrm{N}}, \tag{10}$$

where nRGA is the relative gain number, $\mathbf{I}$ is the identity matrix, and N indicates a chosen norm. The sum of diagonal elements or the absolute sum were used as N in the thesis, cf. Publications IV and V. In the RGA, λ_{yu} values close to 1 are good and signify minimal loop interaction. Negative λ_{yu} are to be avoided due to gain sign change. Small positive λ_{yu} are poor, as there is a gain increase when other loops are closed. For λ_{yu} larger than 1, the open-loop gain is dampened in the closed-loop system. Large λ_{yu} values (above 10) require large controller gains and may indicate ill-conditioning in the system.

Several modifications have been proposed for the static RGA to mitigate some of its shortcomings for practical problems (Sharifzadeh, 2013). The most important is the dynamic RGA (DRGA) for multiple frequencies. Frequency range DRGA examination has also been streamlined by combining static gains with specific frequencies (Xiong, Cai, & He, 2005) or with integrated dynamic response metrics (He, Cai, Ni, & Xie, 2009; Jain & Babu, 2015; Luo, Cao, & Xu, 2016). The block relative gain (BRG) is an RGA generalization for block-decentralized control (Manousiouthakis, Savage, & Arkun, 1986), which is useful in large MV–CV systems. RGA evaluation for uncertain systems has been studied by Kariwala, Skogestad, and Forbes (2006), for example. Exergy-based RGA methods have been

proposed as ecoefficiency tools by Montelongo-Luna, Svrcek, and Young (2011), and Munir, Yu, and Young (2013). The available RGA modifications influenced the selection of relative gain methods in Publications III–V. To account for control-relevant high-frequency interactions and partial control in large systems, the DRGA, the performance relative gain array (PRGA), the closed-loop disturbance gain (CLDG), and the partial relative gain (PRG) were chosen for the ICPD procedure (cf. Section 5.5). In addition, the Niederlinski index (NI) was used to ensure the stability of selected control structures (Chiu & Arkun, 1990; Häggblom, 1997b).

Lastly, system analysis also contains methods for flowsheet structural analysis, most notably degrees of freedom (DOF) evaluation. DOF signify the amount of independent MVs available for managing CVs. As a performance measure, they indicate how the flowsheet structure affects the possibilities to control and optimize the process. Further distinctions have been made for design (DDOF), control (CDOF), and steady-state degrees of freedom (Larsson & Skogestad, 2000; Luyben, 1996; Sharifzadeh, 2013). CDOF were considered in Publications I and IV. They account for disturbances by subtracting the number of external variables from the DOF, which corresponds to the available MVs for control (Skogestad, 2004).

4.6 Summary of chosen approach for CFB ICPD

This section summarizes how the approaches from Sections 4.1–4.5 are used in the ICPD procedure and how they were implemented in Publications I–V. The ICPD procedure employs a combination of simulation-based dynamic performance, controllability, and first-principles qualitative objectives:

- *Electrical power setpoint tracking:* The setpoint tracking for the electrical power is the main objective, measured as the ISE error over simulated load change ramps, as described in Publication V.
- *Main steam quality setpoint tracking:* The secondary objective is to reject main steam quality disturbances that result from MW_e control (Publications III and V), evaluated with the ISE for the main steam pressure in Publication V.
- *Disturbance rejection capacity:* Steam path design aims at improving the rejection of unplanned MW_e disturbances during load changes. In Publication V, this objective was specified through MV signal saturation and the CLDG.
- *Controllability:* The PRG, DRGA, PRGA, and CLDG methods are used in the procedure as measures for interactions and controllability in control structure

selection (Publications IV and V) and ICPD process design (Publications III and V).

- *CDOF analysis:* Control degrees of freedom analysis is used for evaluating the influence of process configurations on control (Publication I) and for plant-wide control design (Publication IV).
- *Exergy efficiency:* The minimization of destroyed exergy is an objective for steam throttling, implemented indirectly for the turbine valve in Publication V.
- *Flue gas CO_2:* The maximization of the flue gas CO_2 concentration is a static or low-frequency environmental goal for oxy-combustion, as described in Publications I and II.

5 ICPD procedure

This chapter presents the simulation-based ICPD procedure that is proposed for CFB boilers. The design tools from Publications I–V are combined into a hierarchy of steps for obtaining the closed-loop boiler flowsheet from design data. The procedure is listed below, and a more detailed decomposition for step 3 is given in Publication V. As summarized in Section 3.5, the hybrid approach employs both process knowledge and mathematical programming ICPD, and each design step focuses on different objectives from Section 4.6. The purpose of Chapter 5 is to form guidelines for applying the chosen tools to general CFB boiler problems.

1. Simulator-based pre-design
   1.1. Control-oriented qualitative process analysis (Publication I)
   – CFB process analysis with detailed industrial simulators: How are dynamics and control affected by parameter and flowsheet changes?
   – First-principles parameter analysis & transition scenario simulations.
   1.2. Model-based state estimation (Publication II)
   – Refinement of simulator-based analysis with experimental data.
   – Unscented Kalman filter (UKF) nonlinear state estimation.
   1.3. Control degrees of freedom (CDOF) analysis (Publications I and IV)
   – Selection of MVs and CVs for decentralized control structure.
   – Evaluation of control possibilities based on process structure.
   – Evaluation of throughput manipulator (TPM) dynamics for MW_e control.
2. Control structure & interaction analysis (Publications III–V)
   – Relative gain analysis with different methods and for multiple frequencies.
   – Selection of control connections between MVs and CVs.
   – Variable interaction analysis for ensuring process controllability.
3. ICPD optimization (Publications III and V)
   – Optimization of process and controller parameters together in the defined closed-loop plant structure from steps 1 and 2.
   – Closed-loop dynamic optimization for timeseries, e.g., load ramp tests.
   – Objective: Minimization of MW_e setpoint tracking error together with secondary objectives (weighted single-objective optimization).
4. Design result validation against relevant reference simulations (Publication V)

This chapter is structured as follows. Firstly, Section 5.1 presents the CFB boiler modeling guidelines and industrial case studies that were used throughout the thesis. The remaining sections follow the outlined ICPD procedure. In the simulator-based

pre-design of step 1, the target process is analyzed based on its structure and its operating conditions. Structural analysis highlights how the flowsheet design affects process dynamics and control. Operating conditions focus on how specific parameters and states influence control performance in a fixed flowsheet. Sections 5.2–5.4 present three interconnected steps for examining these aspects: control-oriented qualitative process analysis in Section 5.2 (step 1.1), UKF state estimation analysis in Section 5.3 (step 1.2), and plant-wide CDOF analysis in Section 5.4 (step 1.3). Section 5.5 deals with the relative gain control structure selection of step 2, and Section 5.6 presents the ICPD optimization setup of step 3.

5.1 CFB boiler systems and models

The selection of suitable modeling approaches for each design step is a crucial prerequisite for the simulation-based ICPD procedure, as also noted by e.g., Mitsos et al. (2018), and Rafiei and Ricardez-Sandoval (2020b). This section presents the CFB process models from Publications I–V to demonstrate what kind of models are needed when applying the procedure to CFB boiler problems. For this purpose, the industrial case studies of Publications I–V are also summarized here (Table 3), with more specific test matrices in Sections 5.2–5.6. In this thesis, the term "case study" thus encompasses the target boiler process, the system models utilized, and all related simulation runs and computations. Two modeling approaches can be defined: industrial simulators for detailed analysis (Subsection 5.1.1), and "design" models that are used directly by the ICPD algorithms (Subsection 5.1.2).

Table 3. Summary of all CFB boiler case study simulations in Publications I–V.

Target system and tests	Plant scale	Model	Publications
Air/oxy-fired CFB combustor	Pilot		
Open-loop dynamic simulation	<100 kW_{th}	First-principles simulator	I
State estimation		First-principles simulator	II
Closed-loop simulation		First-principles simulator	Hultgren et al. (2015)
Relative gain analysis		Black-box identified static	Hultgren et al. (2015)
OTU-CFB power plant	Industrial		
CDOF analysis	>200 MW_e	First-principles simulator	IV
Open-loop step testing		First-principles simulator	IV
Relative gain analysis		Black-box identified dynamic	IV
Drum CFB steam path	Industrial		
ICPD optimization	>100 MW_e	Physical design model	III, V
Relative gain analysis		Physical design model	III, V

5.1.1 CFB power plant simulator

First-principles detailed simulators are used in the pre-analysis stage of the ICPD procedure (step 1) for transition simulations and state estimation, as well as for generating design models in step 2. The aim of the thesis was to utilize existing simulators and data from industry to a maximal extent for these steps. The main limitation for the industrial models is set by the state estimation computational load in step 1.2, as the full simulator is used directly as the UKF internal model in the ICPD procedure. Another requirement is that process parameters of interest must be directly adjustable in the simulator, meaning that even complex black-box models (e.g., MV–CV neural networks) are undesirable.

A dynamic CFB power plant simulator was obtained for the ICPD pre-analysis from the Sumitomo SHI FW Energia Oy company (referred to here as "Sumitomo SHI FW"). The simulator had previously been validated for various CFB project deliveries by the company (Kovács et al., 2012), including the plants studied in this thesis. The simulator was implemented in the commercial APROS 5 software, with a separate hotloop block in Matlab/Simulink. The hotloop block (Fig. 11) was studied in Publications I and II, and the full simulator (Fig. 12) in Publication IV.

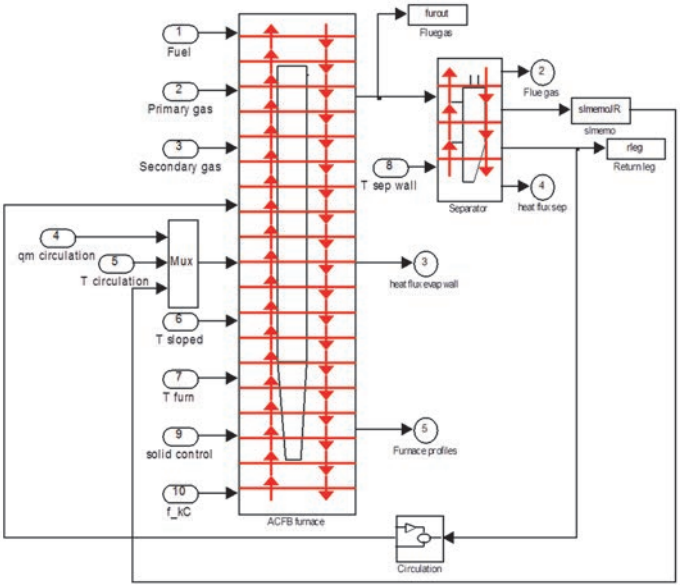

Fig. 11. Hotloop model of the pilot CFB case study. qm and f_kC are the circulation and reactivity parameters (Adapted, with permission, from Publication I © 2013 Elsevier Ltd.).

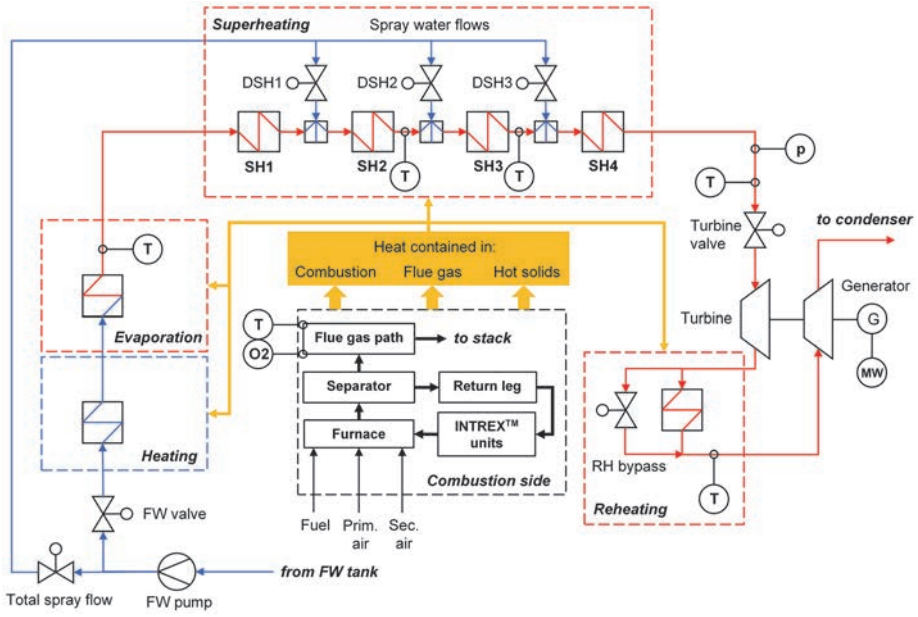

Fig. 12. Schematic figure of the OTU-CFB simulator flowsheet (Reprinted, with permission, from Publication IV © 2017 American Chemical Society).

The hotloop block (Ritvanen et al., 2012) was a 1-D model (Fig. 11), where the furnace (furn), separator (sep), and return leg (rleg) were modeled as ideally mixed connected calculation elements (e.g., 20 elements for the furnace), containing mass and energy differential balance equations. A combined energy equation was defined for element temperatures, and the hydrodynamics, density profile, and heat transfer were evaluated using empirical and semi-empirical correlations. The combustion reactions of carbon, hydrogen, and sulfur were considered in the model.

The main hotloop model case study in Publications I and II was an air-/oxy-fired pilot CFB combustor. The fuel power was 20–50 kW_{th} in air mode and 50–100 kW_{th} in oxy mode, with anthracite (1–2 fractions) and petcoke as fuel. The model inputs consisted of the fuel mass flow, oxidant mass flows (mixture of air, pure O_2, and RFG), and water-wall temperature parameters for the furnace and the separator. The outputs contained the flue gas flow (mass, composition, temperature), furnace profiles (temperature, density, gas velocity), and the hotloop heat fluxes, which were evaluated iteratively with the wall temperatures in the full simulator.

The main power plant simulator contained sub-models for the water-steam path and the flue gas path in APROS. The full simulator was implemented for a condensing OTU-CFB power plant (Benson steam cycle, one coal fuel fraction) in

a range of several hundred megawatts (Fig. 12). Process units beyond the turbine or the flue gas duct were not considered in this work. Unit dimensions and operating conditions for different load levels were obtained from in-house data.

In APROS, thermal hydraulics are simulated based on the dynamic conservation equations of mass, momentum, and energy, which are discretized in time and solved through implicit or semi-implicit integration (Hänninen & Ylijoki, 2008). Process units are divided into control volumes, where mass and energy equations are solved in the middle of the volume, and momentum equations at the border. The OTU-CFB simulator consisted of standard APROS process units (heat exchangers, valves, turbines, etc.), with various correlations for heat transfer and wall friction (cf. Publication IV). Fluid compositions were calculated in a separate elementary layer.

5.1.2 CFB design models

The CFB design model approach proposed in this thesis was illustrated in the case studies of Publications III–V. Simplified internal models are needed in the ICPD procedure especially for the ICPD optimization in step 3, but also for frequency response evaluation in control design step 2. Design models should provide a good computational performance for a large number of simulations, but also have a generic modeling approach that is applicable to different CFB boiler case studies.

Design models are generated in two ways in the ICPD procedure. In the main approach, the process is described as a series of low-order dynamic elements, which are directly derived from first-principles process parameters and describe the relevant dynamics of the ICPD problem. The secondary approach is more conventional, where black-box MV–CV transfer functions are identified from responses that are simulated with the first-principles models described in Subsection 5.1.1. Both approaches enable a significant increase in computational performance, at the cost of modeling accuracy and a more restricted validity region.

The main design model approach of connected elements was demonstrated in Publications III and V for the steam path of an industrial drum CFB boiler in the range of >100 MW_e. Evaporator and superheater units were modeled as lumped storages of steam, consisting of a storage coefficient equation and a pressure drop equation (Doležal & Varcop, 1970; Smith, 2005). The boiler thermal inertia was modeled as a first-order + delay block, and the turbine sections as first-order steam storage blocks. As detailed drum water-steam dynamics were not modeled, this storage model approach can also be applied to OTU boiler case studies.

The overall steam path model, shown in Fig. 13, was formed by combining the low-order unit elements. The model was calibrated for a feasible region around the 80% load level based on design data from Sumitomo SHI FW. Transfer function matrices could then be formed analytically from Fig. 13 for the main unit master control variables as

$$\begin{bmatrix} \frac{p(s)}{L(s)} & \frac{p(s)}{v(s)} \\ \frac{E(s)}{L(s)} & \frac{E(s)}{v(s)} \end{bmatrix} = \begin{bmatrix} e^{-t_{\mathrm{I}}s}\frac{\alpha_{11}}{s^4+\beta_{11}s^3+\gamma_{11}s^2+\delta_{11}s+\varepsilon_{11}} & \frac{-\alpha_{12}s^2-\beta_{12}s-\gamma_{12}}{s^3+\delta_{12}s^2+\varepsilon_{12}s+\zeta_{12}} \\ e^{-t_{\mathrm{I}}s}\frac{\alpha_{21}s+\beta_{21}}{s^6+\gamma_{21}s^5+\delta_{21}s^4+\varepsilon_{21}s^3+\zeta_{21}s^2+\eta_{21}s+\theta_{21}} & \frac{\alpha_{22}s^4+\beta_{22}s^3+\gamma_{22}s^2+\delta_{22}s}{s^5+\varepsilon_{22}s^4+\zeta_{22}s^3+\eta_{22}s^2+\theta_{22}s+\kappa_{22}} \end{bmatrix} \tag{11}$$

and for DSH mass flow disturbances as

$$\begin{bmatrix} \frac{p(s)}{d(s)} \\ \frac{E(s)}{d(s)} \end{bmatrix} = \begin{bmatrix} \frac{\alpha_{\mathrm{d}1}s^2+\beta_{\mathrm{d}1}s+\gamma_{\mathrm{d}1}}{s^3+\delta_{\mathrm{d}1}s^2+\varepsilon_{\mathrm{d}1}s+\zeta_{\mathrm{d}1}} \\ \frac{\alpha_{\mathrm{d}2}s^3+\beta_{\mathrm{d}2}s^2+\gamma_{\mathrm{d}2}s+\delta_{\mathrm{d}2}}{s^5+\varepsilon_{\mathrm{d}2}s^4+\zeta_{\mathrm{d}2}s^3+\eta_{\mathrm{d}2}s^2+\theta_{\mathrm{d}2}s+\kappa_{\mathrm{d}2}} \end{bmatrix}, \tag{12}$$

where p is the main steam pressure, E is the electrical power, L is the firing power, v is the turbine valve position, d is the DSH mass flow, and t_{I} is the thermal inertia time delay. The coefficients α_{mn}, β_{mn}, γ_{mn}, δ_{mn}, ε_{mn}, ζ_{mn}, η_{mn}, θ_{mn}, and κ_{mn} in Eqs. 11 and 12, as well as the notation to Fig. 13, are provided in Publication V and are not repeated here.

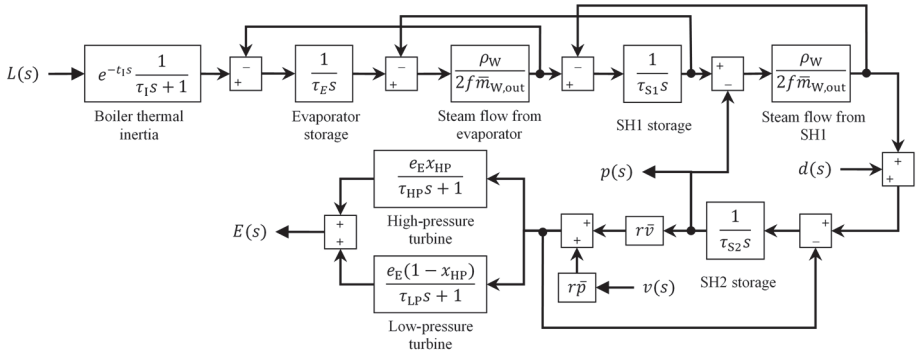

Fig. 13. CFB steam path design model schematic chart (Reprinted, with permission, from Publication V © 2019 Elsevier Ltd.).

The black-box modeling approach was used in Publication IV, where a transfer function matrix $\mathbf{G}(s)$, Eq. 8, was identified between selected MVs and CVs (cf. Section 5.4) of the full OTU-CFB simulator. The MVs were altered one at a time with ±5–10% steps from the 95% load operating point, while keeping other MVs constant. All responses could be modeled adequately with first- or second-order LTI models: fit percentages were mostly above 90%, and even for moderate fits the general response shape could be replicated well. The process static gain matrix in Eq. 7 was obtained from $\mathbf{G}(s)$ at zero frequency, $\mathbf{G}(0)$.

5.2 First-principles process analysis and simulation

In the pre-analysis stage of the ICPD procedure (step 1), the CFB boiler is examined through simulations and model analysis on a first-principles basis. The purpose is to integrate the boiler dynamics into the early process design, generate data for the control design and parameter optimization steps 2 and 3, and answer qualitative design questions that would be challenging to address later in the ICPD procedure. The analysis focuses on open-loop dynamics, MV effects, and control connections, and it enables more informed process design decisions for fast load changes.

The purpose of the control-oriented qualitative process analysis in ICPD step 1.1 is to discover how a proposed boiler design affects control and load changes in the CFB, with the aim of defining the first-principles reasons for the observed dynamic behavior. Firstly, the chemical/physical properties of the industrial simulator are analyzed based on the theory to connect them to the process dynamics. Secondly, extensive dynamic simulation is carried out to examine how changes in these properties affect specified performance goals. The analysis approach is inherently comparative, where the investigated process is compared to a similar "default" open-loop process.

The described simulator-based pre-analysis was performed for the CFB boiler hotloop in Publication I in order to compare air- and oxy-combustion. This case study presented a clear design task for load-following boilers: How should the process and control design of an air-fired CFB be modified to maintain or improve load change performance in oxy mode? Regarding the scope of the thesis, the oxy-combustion process thus primarily served as a suitable application area for ICPD rather than the focus of the work: It formed a comparative design problem that could be quantified for similar CFB flowsheets, while also supporting the overall goal of flexible and sustainable power generation.

The focus of the simulations in ICPD step 1.1 was on the operating conditions in the oxy-CFB. Flowsheet structural modifications were mainly addressed by the CDOF analysis in ICPD step 1.3 (cf. Section 5.4), but this step was also supported by suitable simulation results from step 1.1 (cf. Subsection 6.3.1). Based on the first-principles theory, it was discovered that most of the changes related to operating conditions resulted from the modified combustion atmosphere: CO_2 replaced N_2 as the main gas flow component, and minor components became concentrated due to flue gas recirculation. Another aspect is the possibility to use varying oxidant O_2 percentages in the gas feed (oxidant O_2 enrichment). Based on these findings, the following questions could be formulated for the pre-analysis:

- Are heat exchanger (static) loads affected by the atmosphere?
- Are hotloop open-loop dynamics affected by the atmosphere?
- Is the fluidization in the furnace bed affected by the atmosphere?
- How does oxidant O_2 enrichment influence hotloop design and control?
- How does the flue gas recirculation modify the open-loop dynamics?

To answer these questions, the open-loop simulation campaign shown in Table 4 was conducted for the pilot combustor hotloop model shown in Subsection 5.1.1, with setpoints and operating conditions from the real plant. The air to oxy mode switching schemes are illustrated separately in Figs. 14 and 15.

Table 4. Test matrix for the air/oxy-fired pilot CFB simulations with an elevated oxidant O_2 content in oxy mode (Publication I).

Simulation scenario	Modified flows (others constant)	Modification
Load step tests		
Air mode steps	Fuel, air	Multiple +/– step changes
Oxy mode steps	Fuel, pure O_2, RFG	Multiple +/– step changes
Oxy mode load ramp tests		
Slow ramps	Fuel, pure O_2, RFG	One +/– ramp change from full load
Fast ramps	Fuel, pure O_2, RFG	One +/– ramp change from full load, 3X faster ramp rate
Transitions from air to oxy mode		
“Direct” switch	Fuel, air, pure O_2, RFG	Air –; fuel/pure O_2/RFG + (Fig. 14)
“Sequenced” switch	Fuel, air, pure O_2, RFG	Air –; fuel/pure O_2/RFG + (Fig. 15)
RFG rate tests in oxy mode		
RFG steps	RFG	RFG step changes, approx. +12% – 24% + 12% to total oxidant
Fuel step, constant RFG levels	Fuel, three RFG levels	Fuel –10%; RFG flow at 80%/100%/120% of nominal

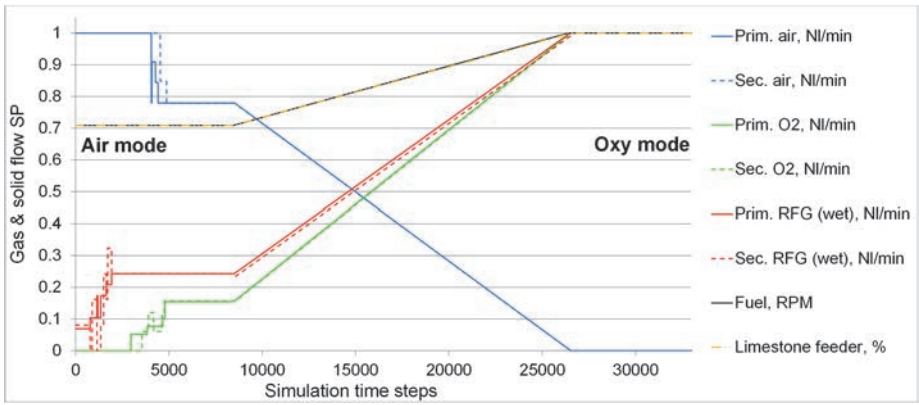

Fig. 14. Direct switching scheme from air to oxy mode (Adapted, with permission, from Publication I © 2013 Elsevier Ltd.).

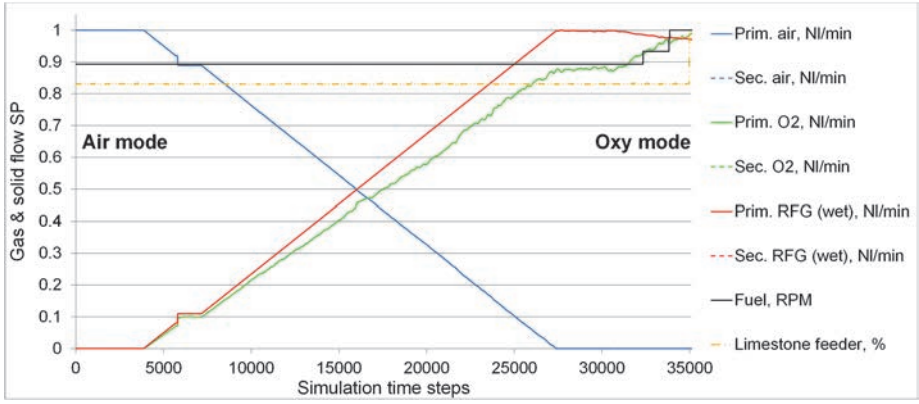

Fig. 15. Sequenced switching scheme from air to oxy mode (Adapted, with permission, from Publication I © 2013 Elsevier Ltd.).

In Table 4 and subsequent sections of the thesis, a "scenario" is defined as a dynamic transition of the CFB process with MV, disturbance, and setpoint changes, simulated for a chosen time range (e.g., a load change ramp). In "air mode" the CFB bed is fluidized by air, whereas in "oxy mode" the air is replaced by a mixture of RFG and pure O_2. A "transition from air to oxy mode" is conducted by ramping down the air flows and ramping up the RFG and pure O_2 flows in a pre-defined manner, while making necessary adjustments to the fuel and limestone feeds.

The simulations in Publication I focused on the transitions between air and oxy mode, as they are relevant especially for early generation dual-fired boilers (cf. Section 2.1). The "direct" (Fig. 14) and "sequenced" (Fig. 15) switching schemes were compared for the air to oxy mode transitions. For the ICPD procedure used in the thesis, the transition simulations enabled a convenient comparison of air and oxy mode in the same flowsheet through a single simulation scenario.

In addition to the scenarios in Table 4, the control solutions derived in Publication I were tested with the same simulator in the supporting publication by Hultgren et al. (2015), using adequately tuned PID controllers. The reported closed-loop simulations included a fuel disturbance (–10%) with flue gas O_2 control, oxidant O_2 percentage setpoint changes with flue gas and oxidant O_2 control, and furnace profile simulations for different primary/secondary oxidant O_2 percentages. In all scenarios of Table 4, the following output variables were monitored:

- Furnace: temperature in elements 1–20, dense bed density (2 elements), freeboard density (2 elements), grid gas velocity, freeboard gas velocity.
- Flue gas/primary oxidant gas/secondary oxidant gas: O_2 vol%, CO_2 vol%, H_2O vol%, temperature, density.

5.3 Simulator-based state estimation

Unscented Kalman filter (UKF) state estimation is used in step 1.2 of the ICPD procedure to refine the analysis results from step 1.1. The main purpose is to adapt the parameters and nominal input signals of the industrial dynamic simulator with experimental data. Bayesian filters, such as the UKF, enable the effective use of uncertain process data for this task, which supports the overall goal of improving the utilization of existing data and models for ICPD. The secondary purpose is to examine discrepancies between measured and simulated data that cannot be linked to reported process states or inputs, i.e., to test hypotheses for observed process behavior. On the whole, both purposes contribute to improved simulator predictions and thus to more informed process design decisions in the ICPD pre-analysis.

The UKF was applied to the oxy-CFB hotloop in Publication II to extend the process analysis from Publication I. A UKF tool was implemented for the hotloop model shown in Subsection 5.1.1, and the tool was used for two case studies to illustrate how the UKF can be utilized in the ICPD procedure. The UKF algorithm is summarized in Subsection 5.3.1 and the case study test matrix in Subsection 5.3.2.

Publication II constitutes the first proper application of the UKF filter for CFB boiler analysis. Previously, Ikonen et al. (2012) and Ikonen, Kovács, and Ritvanen (2013) employed nonlinear particle filter state estimation for the CFB hotloop, including brief considerations about the applicability of the UKF. The linearized extended Kalman filter has been used more frequently for fluidized bed boilers (e.g., Bardelli et al., 1994; Bittanti et al., 1996). For other power plants, the UKF was applied to the commonly used Åström-Bell drum boiler model by Arasu, Prakash, and Prasad (2013), for example. In contrast to this low-dimensional state-space model, a detailed simulator with 855 and 660 states was used in Publication II for the case studies. Only a subset of these states was considered uncertain, however.

5.3.1 Unscented Kalman filter

Bayesian filters form estimates and predictions of evolving states and parameters, given the process dynamics and uncertain data (Särkkä, 2013). The estimation constructs a representation of an unknown vector of random states through its posterior probability density function (pdf) based on measured data. Bayesian filtering consists of the prediction operation, using

$$p(x_k|\mathbf{Y}_{k-1}) = \int p(x_k|x_{k-1})\, p(x_{k-1}|\mathbf{Y}_{k-1}) dx_{k-1}, \tag{13}$$

and the update operation, using equations

$$p(x_k|\mathbf{Y}_k) = p(y_k|x_k) p(x_k|\mathbf{Y}_{k-1}) / p(y_k|\mathbf{Y}_{k-1}) \tag{14}$$

and

$$p(y_k|\mathbf{Y}_{k-1}) = \int p(y_k|x_k)\, p(x_k|\mathbf{Y}_{k-1}) dx_k, \tag{15}$$

where k is the sampling instance, x is the state vector, y is the output vector, $\mathbf{Y}_k$ contains all output measurements up to k, and $p(i|j)$ is the pdf of event i, given j.

The utilized Bayesian algorithm depends on the assumptions made about the system and defines how Eqs. 13–15 can be solved (Daum, 2005). The most common approaches are the linear Kalman filter and the extended Kalman filter. Nonlinear algorithms (Patwardhan, Narasimhan, Jagadeesan, Gopaluni, & Shah, 2012) like the unscented Kalman filter (UKF) and particle filter methods enable the direct use of a nonlinear system model without linearization. In Publication II, the full hotloop simulator could thus be directly implemented with the UKF, while maintaining an acceptable computational load, as the state equation f_{ss} in equations

$$\begin{cases} x(k+1) = f_{ss}(x(k), u(k), c_{ss}(k)) \\ y(k) = w_{ss}\big(x(k), u(k)\big) + d_{ss}(k) \end{cases}, \tag{16}$$

where f_{ss} is the state equation, w_{ss} is the measurement equation, u is the process input vector, c_{ss} is the state noise vector, and d_{ss} is the measurement noise vector.

The UKF algorithm (Julier & Uhlmann, 1997) was described in Publication II, where the scaled UKF formulation was used (van der Merwe, Doucet, de Freitas, & Wan, 2000). In short, the state distribution is approximated with "sigma" points $\mathcal{X}$ by using the unscented transform as

$$\begin{cases} \mathcal{X}_0 = \bar{x} \\ \mathcal{X}_i = \bar{x} + \left(\sqrt{(n_x + \lambda)C_x}\right)_i, i = 1, \ldots, n_x \\ \mathcal{X}_i = \bar{x} - \left(\sqrt{(n_x + \lambda)C_x}\right)_i, i = n_x + 1, \ldots, 2n_x \\ \lambda = \alpha^2(n_x + \kappa) - n_x \end{cases}, \tag{17}$$

where $\mathcal{X}_i$ is the sigma point i, $\bar{x}$ is the state vector mean, C is the covariance of states (x), α and κ are parameters in the scaled unscented transform, and n_x is the state vector dimension. The sigma points are driven through Eq. 16 to obtain $\mathcal{X}_{k+1|k}$ and the transformed measurements $\mathcal{Y}_{k+1}$. The predicted mean and covariance of the states ($\bar{x}_{k+1|k}$ and $C_{k+1|k}$) and the measurements ($\bar{y}_{k+1}$ and C_{yy}) are estimated from $\mathcal{X}_{k+1|k}$ and $\mathcal{Y}_{k+1|k}$. The posterior state mean and covariance are obtained from new measurements y_{k+1} in the measurement update through equations

$$\begin{cases} \bar{x}_{k+1} = \bar{x}_{k+1|k} + K_{k+1}(y_{k+1} - \bar{y}_{k+1}) \\ C_{k+1} = C_{k+1|k} - K_{k+1} C_{yy} K_{k+1}^{\mathrm{T}} \end{cases}, \tag{18}$$

where $\bar{y}$ is the measurement vector mean, C is the covariance of states or measurements (yy), and K is the UKF Kalman gain, calculated from C_{yy} and the x–y cross-correlation matrix.

5.3.2 Target system and test matrix

The UKF tool was used in Publication II to explore potential disturbances and parameter variations related to observed outputs in the oxy-CFB pilot combustor. For scale-up purposes, the tool was also implemented for a medium-scale air-fired CFB power plant, with a similar validated hotloop model from Sumitomo SHI FW. Dynamic measurement data was supplied for both plants by the company, and the data was compared to simulations with similar input flows and operating conditions.

The data for the pilot CFB case study consisted of three oxy-fired load ramp sets (fuel + oxidant flows, ramped at the same speed): slow 15% ramps, fast 15% ramps, and slow 30% ramps. The state estimation was used to investigate whether variations in the reported fuel flows (three fractions) and the hotloop air leakage could have caused the differences observed between the measured and simulated flue gas CO_2 and O_2 percentages, which were used as measurements in Eq. 16.

The industrial CFB case study contained primary air tests (±6% steps) and load change tests (±8% steps). One of the furnace heat transfer coefficients and the fuel moisture content were estimated using the UKF to explain the differences observed between the measured and simulated flue gas O_2 content and furnace temperature values. These process states were used as measurements for the state estimation.

5.4 Degrees of freedom analysis

The degrees of freedom (DOF) analysis (cf. Subsection 4.5.2) is performed in step 1.3 of the ICPD procedure for two purposes. The first is to identify how process structural changes affect the control possibilities. This analysis was performed qualitatively for air- and oxy-firing in Publication I. The structural differences were restricted to the oxidant gas streams, as the work only concerned the CFB hotloop:

- Does splitting the oxidant gas inputs into four components (primary/secondary RFG, primary/secondary pure O_2) require an altered oxidant gas control setup?
- Do the separate oxidant flows generate new possibilities for boiler control?

The second purpose of DOF analysis is to generate data for the control structure selection in step 2, mainly for the selection of MVs and CVs. The control degrees of freedom (CDOF) are evaluated for this purpose using the method of Murthy Konda, Rangaiah, and Krishnaswamy (2006). The CDOF is obtained by comparing the total amount of material/energy streams to the amount of restrained and redundant streams as

$$\mathrm{CDOF} = n_{\mathrm{streams}} - \sum_{\mathrm{units}}(n_{\mathrm{restrained}} + n_{\mathrm{redundant}}), \qquad (19)$$

where n and its subscripts are the stream amounts: total, restrained, and redundant. The restraining number shows how many streams are determined by other streams. Redundancy results from variables that are either self-regulating or sufficiently controlled through the control of other variables.

The CDOF were evaluated in Publication IV for the OTU-CFB simulator (Fig. 12). The combustion and flue gas side CDOF are detailed in Table 5, which also

adds the bed limestone feed and the Intrex air flow to the results of Publication IV. In the analysis shown in Table 5, redundancy resulted from flue gas pressure control and a constant solid material circulation rate. Heat exchangers (HE) were assumed to have a constant inventory, except for the furnace. This analysis is expanded for oxy-combustion in Subsection 6.3.1.

Table 5. Combustion and flue gas path CDOF (Publication IV).

Process section and unit	Process unit type	Streams in + out	Connection streams	Restraining number	Redundant streams
Hotloop		12		2	2
Furnace	Reactor with heat flows	5 + 3	1	0	
Cyclone	Splitter	1 + 2	1	1	
Intrex	HE without inventory	2 + 2	1	1	
Flue gas path		3		3	0
Duct section 1	HE without inventory	1 + 1	1	1	
Duct section 2	HE without inventory	1 + 1	1	1	
Duct section 3	HE without inventory	1 + 1	1	1	
SUM		15		5	2
CDOF	8				

Similarly to the combustion path, the water-steam path CDOF are expanded from Publication IV and shown in Table 6. All of the heat exchangers except for the ECO (liquid phase preheater) were defined as units with pressure changes, with redundancy from main steam and condenser pressure control. The streams and restraining numbers of the combustion side HE units (Table 5) are not repeated in Table 6. The feedwater pump and HP/LP turbine were evaluated without separate input/output energy streams.

The analysis resulted in 11 CDOF, and 9 CDOF remained without the Intrex air and limestone input flows in Table 5. MVs were chosen based on these CDOF in Publication IV: the FW flow, turbine valve position (T.valve), DSH flows 1–3, the reheater bypass valve position (RHvalve), fuel flow, and prim./sec. oxidant flows. Three combined MVs were also formed: “firing power” (fuel + airs), “boiler load” (fuel + airs + FW), and “total DSH flow” (DSH1 + DSH2 + DSH3). Potential CVs were chosen based on Section 2.3: the electrical power, main steam pressure, main steam temperature, EVAP steam temperature, SH2 and SH3 steam temperatures, RH steam temperature, flue gas temperature, and flue gas O_2 content.

Table 6. Water-steam path CDOF (Publication IV).

Process section and unit	Process unit type	Streams in + out	Connection streams	Restraining number	Redundant streams
Feedwater feed		6		4	0
FW pump	Pump	1 + 1	0	1	
EVAP/DSH split	Splitter	1 + 2	1	1	
Main DSH valve	Valve	1 + 1	1	1	
FW valve	Valve	1 + 1	1	1	
Pre-heating		1		1	0
ECO	HE without inventory	1 + 1	1	1	
Evaporation		1		0	0
Evaporator	HE with inventory	1 + 1	1	0	
Superheating		13		7	6
Main DSH split	Splitter	1 + 3	1	1	
DSH1 valve	Valve	1 + 1	1	1	
DSH2 valve	Valve	1 + 1	1	1	
DSH3 valve	Valve	1 + 1	1	1	
Superheater 1	HE with inventory	1 + 1	1	0	
DSH1 spray	Mixer	2 + 1	2	1	
Superheater 2	HE with inventory	1 + 1	1	0	
DSH2 spray	Mixer	2 + 1	2	1	
Superheater 3	HE with inventory	1 + 1	1	0	
DSH3 spray	Mixer	2 + 1	2	1	
Superheater 4	HE with inventory	1 + 1	1	0	
Turbine		3		3	0
Turbine valve	Valve	1 + 1	1	1	
HP turbine	Compressor	1 + 1	1	1	
LP turbine	Compressor	1 + 1	1	1	
Reheating		5		3	2
RH bypass split	Splitter	1 + 2	1	1	
RH bypass valve	Valve	1 + 1	1	1	
Reheater	HE with inventory	1 + 1	1	0	
RH bypass mix	Mixer	2 + 1	2	1	
SUM		29		18	8
CDOF	3				

The third design task in ICPD step 1.3 is to analyze the candidates for throughput manipulator (TPM) variables in the system. The TPM can be defined as the control degree of freedom that is used to regulate the throughput in the primary process path (Price, Lyman, & Georgakis, 1994). In the load-following boiler, throughput is determined by the generated electrical power. Three MVs were identified in

Publication IV as TPM candidates for the OTU-CFB power plant: the turbine valve, the firing power (fuel + air), and the feedwater flow. The open-loop dynamics of these variables were evaluated in the supplementary material of Publication IV based on step responses, cf. Subsection 5.1.2. The responses were quantified for the main steam pressure and temperature, the evaporator temperature, and the electrical power CVs based on properties from Section 4.4:

- *Rise time:* Time between 10% and 90% of the response magnitude.
- *Settling time:* Time to reach ±2% region around the new steady-state.
- *Time delay:* Time after MV step change before the CV changes.

5.5 Control structure selection and interaction analysis

The main purpose of the relative gain analysis in step 2 of the ICPD procedure is to select the control structure between the MVs and CVs from the DOF analysis in step 1.3. This forms the closed-loop process structure for the subsequent ICPD optimization stage. The secondary purpose is to support the qualitative process design in step 1 by evaluating the effect of open-loop parameters on variable interactions and controllability. In this approach, the design ensures that control connections and design parameter changes do not contribute to performance-limiting interactions. For clarity, "control structure" is defined here as a set of MV–CV connections in a decentralized control system. As described in Publication IV, a control structure is commonly annotated in this thesis as a vector of MVs, where the position of the MV in the vector indicates the corresponding controlled CV.

The relative gain analysis approach of the thesis was defined in Publication IV (Fig. 16) and is summarized in Subsection 5.5.1 to facilitate its application to boiler ICPD problems. It expands on the standard literature by considering multiple relative gain methods and control tasks as a stepwise procedure. Control structures are first analyzed at zero frequency through a full partial relative gain (PRG) analysis to establish integral controllability with integrity (ICI, cf. Subsection 4.5.1). Next, ICI structures and non-ICI structures with fast electrical power control (from the TPM analysis in Section 5.4) are studied at higher frequencies to determine how the observed interactions are altered in the dynamic domain. The dynamic analysis was carried out using the dynamic relative gain array (DRGA) in Publications III and IV, while the performance relative gain array (PRGA) and closed-loop disturbance gain (CLDG) were used in Publication V, as they are more relevant for control performance limiting interactions. In the stepwise analysis, MV–CV sets of

increasing size are examined separately with the chosen relative gain methods. The purpose is to highlight interactions associated with specific control tasks.

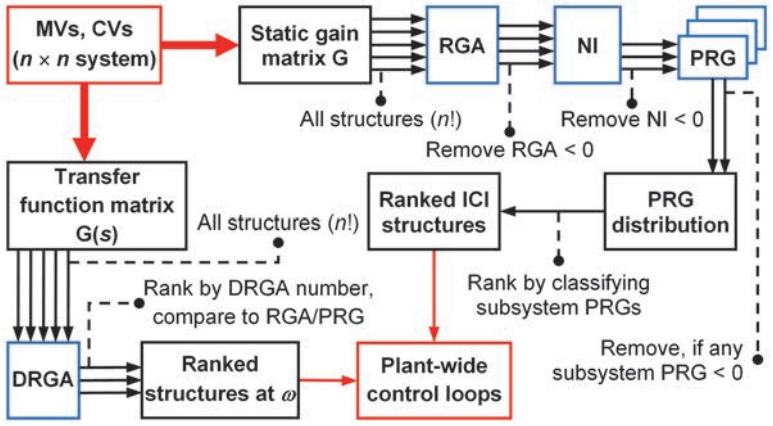

Fig. 16. Relative gain control structure selection and analysis procedure (Adapted, with permission, from Publication IV © 2017 American Chemical Society).

The control structure selection procedure was implemented for the OTU-CFB simulator (Fig. 12) in Publication IV, and dynamic relative gain tools were used for ICPD process design in Publications III and V. These results have been extended for oxy-combustion by Hultgren et al. (2015) and Niva et al. (2017), who performed static ICI PRG analysis on the oxy-CFB hotloop shown in Fig. 11. Detailed relative gain analysis for multiple frequencies and MV–CV systems had not been applied to a plant-wide steam power plant flowsheet prior to Publication IV, where past references on the topic were listed. Additional references include DRGA and NI analysis of a small drum model (Balko & Rosinová, 2015), DRGA analysis of pulverized fuel boiler unit master control (Sun et al., 2017), DRGA analysis of fluidized bed boiler combustion control (Wu et al., 2020), control structure design for individual heat exchanger sections of a steam path based on a non-square RGA formulation (Chandrasekharan, Panda, Swaminathan, & Panda, 2018), and flue gas recirculation setup selection based on the static RGA and the NI (Luo et al., 2015).

5.5.1 Relative gain methods

A full PRG analysis is based on the PRG matrix (Häggblom, 1997a, 1997b). The PRG extends the RGA for partially controlled systems, where specific loops are

closed under integral control. The PRG is evaluated at zero frequency by applying Eq. 9 to the partial subsystem $\bar{\mathbf{G}}_{mn}$ to give

$$\mathrm{PRG}_{mn}(\mathbf{G}) = \mathrm{RGA}(\bar{\mathbf{G}}_{mn}) = \bar{\mathbf{G}}_{mn} \times (\bar{\mathbf{G}}_{mn}^{-1})^{\mathrm{T}}, \tag{20}$$

where $\bar{\mathbf{G}}_{mn}$ can be obtained from $\mathbf{G}$ (Eq. 7) by applying equation

$$\bar{\mathbf{G}}_{mn} = \mathbf{G}(y_{\mathrm{o}}, u_{\mathrm{o}}) - \mathbf{G}(y_{\mathrm{o}}, u_{\mathrm{c}}) \cdot \mathbf{G}(y_{\mathrm{c}}, u_{\mathrm{c}})^{-1} \cdot \mathbf{G}(y_{\mathrm{c}}, u_{\mathrm{o}}) \tag{21}$$

to all closed MV–CV control connections. In Eqs. 20 and 21, $\mathbf{G}$ is the process gain matrix, $\bar{\mathbf{G}}_{mn}$ is the partial subsystem gain matrix with loops y_{c}–u_{c} closed (CV and MV indices "m" and "n"), and "o" denotes open loops.

In the full PRG analysis of the thesis, the PRG is calculated for all possible partial subsystems of a control structure. The analysis reveals whether any of these PRG matrices contain infeasible elements or whether large relative gain changes occur under partial control. In Publication IV, control structures were ranked based on the amount of beneficial and unwanted PRG elements in all subsystems.

As outlined in Publication IV, conditions for ICI controllability can be formed based on the PRG (Häggblom, 1997a, 1997b). $\mathbf{G}$ is ICI controllable if all control connection RGA elements and all control connection PRG elements in all partially controlled subsystems $\bar{\mathbf{G}}_{mn}$ are positive. Checking 2 × 2 subsystems is redundant, if the Niederlinski index (cf. Subsection 4.5.2) of

$$\mathrm{NI} = \det(\mathbf{G})/\det(\hat{\mathbf{G}}) \tag{22}$$

is positive. $\hat{\mathbf{G}}$ is obtained in Eq. 22 by setting to zero all elements of $\mathbf{G}$ that do not correspond to an input–output pairing in a block-decentralized control structure.

The DRGA (Skogestad & Postlethwaite, 2005) is obtained by applying the RGA definition (Eq. 9) to the process transfer matrix $\mathbf{G}(s)$ (Eq. 8) at multiple frequencies. The DRGA was calculated from the system frequency responses in Publications III and IV by using equation

$$\mathrm{DRGA}(\mathbf{G}(s)) = \mathbf{H}(j\omega) \times (\mathbf{H}(j\omega)^{-1})^{\mathrm{T}} = \begin{bmatrix} a_{11} + b_{11}j & \cdots & a_{1n} + b_{1n}j \\ \vdots & \ddots & \vdots \\ a_{m1} + b_{m1}j & \cdots & a_{mn} + b_{mn}j \end{bmatrix}, \tag{23}$$

where $\mathbf{G}(s)$ is the process transfer matrix, $\mathbf{H}(j\omega)$ is the frequency response matrix, and a_{yu} and b_{yu} are the real and complex terms of the DRGA elements between output y and input u, total amounts m and n.

The PRGA extends the DRGA for one-way interactions and control performance (Skogestad & Postlethwaite, 2005). It is evaluated separately for each control structure, where control connections are on the diagonal, and off-diagonal

elements signify performance-limiting interactions, which should be minimized. The PRGA is evaluated as

$$\boldsymbol{\Gamma}(s) = \widehat{\mathbf{G}}(s) \cdot \overline{\mathbf{G}}(s)^{-1} = \begin{bmatrix} \frac{\tilde{y}_1(s)}{\tilde{u}_{c1}(s)} & \cdots & 0 \\ \vdots & \ddots & \vdots \\ 0 & \cdots & \frac{\tilde{y}_m(s)}{\tilde{u}_{cm}(s)} \end{bmatrix} \cdot \begin{bmatrix} \frac{\tilde{y}_1(s)}{\tilde{u}_1(s)} & \cdots & \frac{\tilde{y}_1(s)}{\tilde{u}_n(s)} \\ \vdots & \ddots & \vdots \\ \frac{\tilde{y}_m(s)}{\tilde{u}_1(s)} & \cdots & \frac{\tilde{y}_m(s)}{\tilde{u}_n(s)} \end{bmatrix}^{-1}, \quad (24)$$

where $\boldsymbol{\Gamma}(s)$ is the PRGA, $\overline{\mathbf{G}}(s)$ is the scaled process transfer matrix with scaled inputs $\tilde{u}$ and outputs $\tilde{y}$ (total amounts n and m), and $\widehat{\mathbf{G}}(s)$ is the scaled diagonal transfer matrix of the control connections ($\tilde{u}_{ci}$ is the input for controlling output "i").

DRGA and PRGA elements were presented for multiple frequencies as absolute magnitudes in Publications IV and V. Control structure ranking was simplified by using the RGA number (Eq. 10), which is shown in a frequency-dependent form for the DRGA in equation

$$\text{nDRGA}(\mathbf{H}(j\omega)) = ||\text{DRGA}(\mathbf{H}(j\omega)) - \mathbf{I}||_{\text{N}}, \quad (25)$$

where nDRGA is the dynamic relative gain number and $\mathbf{I}$ is the identity matrix.

The CLDG represents the apparent gains from disturbances to CVs when control loops are closed (Skogestad & Postlethwaite, 2005). It is evaluated separately for each control structure. In order to minimize the effect of disturbances on CVs, the control structure CLDG elements should be small, preferably smaller than the frequency response magnitudes of the corresponding MV–CV connections. The CLDG is evaluated as

$$\widehat{\mathbf{G}}_{\text{d}}(s) = \boldsymbol{\Gamma}(s) \cdot \overline{\mathbf{G}}_{\text{d}}(s), \quad (26)$$

where $\widehat{\mathbf{G}}_{\text{d}}(s)$ is the CLDG and $\overline{\mathbf{G}}_{\text{d}}(s)$ is the scaled disturbance–CV transfer matrix.

PRG, DRGA, and PRGA elements can be classified based on the principles listed in Subsection 4.5.2: values close to 1 are ideal, negative values are infeasible, and small and large values should be avoided. More detailed classes were devised in Publication IV: <0, 0–0.1, 0.1–0.5, 0.5–0.85, 0.85–1.2, 1.2–5, 5–10, and >10. These classes are used in the ICPD procedure.

5.5.2 Target system and test matrix

The control structure was selected for the OTU-CFB in Publication IV based on the procedure illustrated in Fig. 16. The PRG and DRGA were calculated for the MVs

and CVs listed in Section 5.4, using the process static gain and transfer function matrices that were generated in Subsection 5.1.2. Frequency responses were obtained from Matlab for the DRGA evaluation, and the 0–0.5 rad/s range was chosen based on typical load disturbance ramps. Four MV–CV systems were considered in the stepwise analysis, focusing on the main CVs (case 1), steam temperature control (case 2), combustion and steam generation (case 3), and the plant-wide system (case 4). In Chapters 5 and 6, "case" thus refers to a specified system of unconnected MVs and CVs, for which relative gain analysis is performed in order to determine the decentralized MV–CV control structure. The OTU-CFB cases are listed in Table 7.

Table 7. MVs and CVs of Publication IV analysis cases 1–4 (Adapted, with permission, from Publication IV © 2017 American Chemical Society).

Case/Variable	Manipulated input (MV)	Unit	Controlled output (CV)	Unit
Case 1				
1	Turbine valve	%	Main steam pressure	bar
2	Total DSH flow	kg/h	Main steam temperature	°C
3	Boiler load	% of nominal	Output electrical power	MW
Case 2				
1	Turbine valve	%	Main steam pressure	bar
2	DSH1 flow	kg/h	Main steam temperature	°C
3	DSH2 flow	kg/h	Temperature after SH2	°C
4	DSH3 flow	kg/h	Temperature after SH3	°C
5	Boiler load	% of nominal	Output electrical power	MW
Case 3				
1	Turbine valve	%	Main steam pressure	bar
2	Feedwater flow	kg/h	Main steam temperature	°C
3	Fuel flow	kg/h	Temperature after EVAP	°C
4	Primary air flow	kg/h	Flue gas O_2 content	vol%
5	Secondary air flow	kg/h	Flue gas temperature	°C
6	Total DSH flow	kg/h	Output electrical power	MW
Case 4				
1	Turbine valve	%	Main steam pressure	bar
2	Feedwater flow	kg/h	Main steam temperature	°C
3	Secondary air flow	kg/h	Temperature after EVAP	°C
4	DSH1 flow	kg/h	Flue gas O_2 content	vol%
5	DSH2 flow	kg/h	Temperature after SH2	°C
6	DSH3 flow	kg/h	Temperature after SH3	°C
7	RH bypass valve	%	Temperature after RH	°C
8	Firing power	% of nominal	Output electrical power	MW

In the scope of this thesis, replacing the DRGA analysis in Publication IV with the PRGA and CLDG represents the final template for step 2 in the ICPD procedure. Therefore, the unit master control setup was selected in Publication V for the CFB steam path model (Fig. 13) based on the PRGA and the CLDG, as PRG analysis was not necessary for the 2 × 2 system. The PRGA and CLDG were evaluated at 0–0.5 rad/s for Eqs. 11 and 12, and appropriate scaling was applied to the MVs (turbine valve, firing power), CVs (electrical power, steam pressure), and disturbances (DSH flow).

The steam path model was also studied with the DRGA in Publication III. The aim was to discover how the evaporator and superheater steam storage parameters influenced control loop interactions during load changes. Boiler-following PI control was defined for the 2 × 2 MV–CV system, and the DRGA was evaluated at a frequency of 0–0.2 rad/s. Three storage values were tested (nominal, +100% evaporator/+200% superheater, –70% evaporator/–80% superheater), and the resulting changes in the DRGA magnitudes were recorded. These parameter values were then tested for a controlled triangular ±5% electrical power setpoint ramp, and the setpoint tracking performance was compared to the DRGA values.

5.6 Simultaneous ICPD optimization

Dynamic optimization of the closed-loop process is performed in step 3 of the ICPD procedure. The purpose is to find values for the open-loop CFB boiler parameters that were identified in step 1, together with optimal tunings for the controllers in the control structure from step 2. The parameter values are chosen to optimize electrical power tracking for specified load change requirements, while maintaining additional secondary design goals for the process and the control signal.

The ICPD optimization approach was specified in Publication V based on the literature review in Publication III. The approach is briefly described in this section to facilitate the implementation of the ICPD procedure. Subsection 5.6.1 introduces the problem setup, and Subsections 5.6.2 and 5.6.3 elaborate on the optimization objective and algorithm. The optimization was applied to the industrial CFB steam path in Publication V, and this case study is summarized in Subsection 5.6.4.

5.6.1 Problem formulation

The ICPD problem was formulated in Publication V as the fully simultaneous dynamic optimization of continuous process and controller parameters for

simulated closed-loop electrical power setpoint ramps. The load ramp speeds and magnitudes were based on the boiler design criteria, and the simulation time window length was chosen so that the settling of all CV responses was guaranteed. Controllability evaluation was also included in the optimization for the expected MW_e disturbance frequencies to ensure that optimal solutions did not result in uncontrollable systems. In total, the ICPD problem was defined as

$$\min_{X,U} J(y(t), u(t), X, U), \tag{27}$$

with conditions

$$\begin{cases} \xi(x'(t), x(t), u(t), X) = 0 \\ \xi_0(x(0), u(0), X) = 0 \\ \mu\big(y(t), x(t), u(t)\big) = 0 \\ \delta(u'(t), u(t), X, U) \leq 0 \\ \varphi(y(t), u(t), U) = 0 \\ \sigma(y(j\omega), u(j\omega), X) = 0 \\ t \in [0, \Theta] \\ \omega \in [0, \Omega] \end{cases}, \tag{28}$$

where J is the optimization objective, t is time, $[0,\Theta]$ is the simulated time range, ω is frequency, $[0,\Omega]$ is the analyzed frequency range, x are state variables, u are input variables, X are process design parameters, U are controller design parameters, ξ are open-loop process equations with initial conditions ξ_0, δ are process inequality constraints, φ are controller equations, y are output variables, μ are measurement equations for obtaining y, and σ are controllability equations.

The setup in Eqs. 27 and 28 forms the guideline for step 3 of the ICPD procedure. During the optimization, load changes are simulated for the calculation of objective J with the internal model of the algorithm, generated through the connected element approach of Subsection 5.1.2.

5.6.2 Objective function

The optimization objective was constructed in Publication V as a weighted single-objective function based on Section 4.6. This forms the default setup for load-following CFB boiler ICPD problems in this thesis. Function J is set up around the electrical power control performance during the simulated load change, augmented with additional objectives according to equation

$$J = \frac{1}{j_{n1}} j_1 + \frac{1}{j_{n2}} j_2 + \frac{1}{j_{n3}} j_3 + \frac{1}{j_{n4}} j_4 + \frac{1}{j_{n5}} j_5 + \frac{1}{j_{n6}} j_6, \tag{29}$$

where the individual objectives are defined as

$$\begin{cases} j_1 = \int_0^{\Theta} \left(p(t) - z_p(t)\right)^2 dt \\ j_2 = 10 \cdot \int_0^{\Theta} \left(E(t) - z_E(t)\right)^2 dt \\ j_3 = -2 \cdot v(0) \cdot \int_0^{\Theta} v(t)\, dt \\ j_4 = \int_0^{\Theta} |v(t) - \max(v(t), v_{\min})|\, dt + \int_0^{\Theta} |v(t) - \min(v(t), v_{\max})|\, dt \\ j_5 = \int_0^{\Omega} ||\mathbf{\Gamma}(\mathbf{H}(j\omega)) - \mathbf{I}||_{\mathrm{N}}\, d\omega \\ j_6 = 2 \cdot \int_0^{\Omega} \sum \left|\hat{\mathbf{G}}_{\mathrm{d}}(j\omega)\right| d\omega \end{cases} \tag{30}$$

In Eqs. 29 and 30, J is the ICPD objective, j_i is an individual objective i with nominal value j_{ni}, p is pressure, E is electrical power, z_i is the setpoint of output i, $v_{\min}$ and $v_{\max}$ are the minimum and maximum bounds of turbine valve signal v, $\mathbf{\Gamma}$ is the PRGA, $\mathbf{H}$ is the frequency response matrix, $\mathbf{I}$ is the identity matrix, and $\hat{\mathbf{G}}_{\mathrm{d}}$ is the CLDG.

Objectives j_1 and j_2 are the ISE error terms (cf. Section 4.4) for the main steam pressure and electrical power. The electrical power term j_2 has the largest weight as it is the main objective. The weighting of steam pressure objective j_1 depends on the operating mode of the boiler (constant or sliding pressure, cf. Section 2.2).

Objectives j_3 and j_4 are specified for fast turbine valve control action. Since the electrical power output can be altered quickly with the steam control reserve, the capacity to reject unplanned additional $\mathrm{MW_e}$ disturbances during load changes can be maximized by minimizing turbine valve saturation, j_4. However, as constraining the steam flow also contributes to exergy destruction (cf. Section 4.3), turbine valve action should be limited, especially during steady-state operation, resulting in j_3.

Objectives j_5 and j_6 are the objectives for input–output and disturbance controllability, respectively. j_5 is measured as the "PRGA number", obtained by replacing the DRGA with the PRGA, shown in Eq. 24, in the frequency-dependent definition of the relative gain number, shown in Eq. 25. j_6 consists of the integral sum of all terms in the CLDG matrix, Eq. 26. Both terms are integrated over the investigated frequency range.

A single objective was chosen over a multi-objective approach for the ICPD optimization in Publication V to enable a ranking of solutions without additional decision criteria. For this approach, objectives j_1–j_6 were scaled by dividing them by their nominal values j_{n1}–j_{n6}, which were calculated by simulating the target load changes with nominal process parameters and feasible controller tunings. These

nominal values were shown as separate parameters in Eq. 29 for clarity; this differs from the corresponding notation in Publication V, where the terms j_1–j_6 already contained their nominal scaling values. This scaling approach enables a percentage-wise comparison of objectives, where the effect of improved load change performance on other objectives can conveniently be observed. This general approach is proposed for the ICPD procedure in this thesis.

5.6.3 Optimization algorithm

The ICPD optimization was carried out using a hybrid two-level algorithm in Publication V to locate a global optimum for multiple parameters with good computational performance. On the upper level, feasible solution regions were mapped through a global random search with a wide search space and limited iterations. On the lower level, the located regions were refined using a faster local algorithm. Both levels used the same problem formulation (Eqs. 27–30).

The upper-level algorithm was the Matlab 2017 genetic algorithm (Goldberg, 1989). In the algorithm, a population of solutions evolves towards a global optimum, where solutions are either passed on as elites or modified through crossover and mutation operations. In Publication V, the genetic algorithm search consisted of a maximum of 50 rounds and a population of 500 units.

The lower level was a modified version of the Nelder-Mead simplex search (Lagarias, Reeds, Wright, & Wright, 1998) of Matlab 2017. In this approach, a simplex of solution points is modified through reflection, expansion, contraction, or shrink operations during the optimization. The modified algorithm enabled the use of minimum and maximum bounds, as well as periodic simplex reinitialization to avoid local optima.

5.6.4 Target system and test matrix

The ICPD optimization was performed in Publication V for the CFB boiler steam path (Fig. 13). The aim was to optimize the evaporator/superheater mass storage distribution and steam throttling (process targets) together with the boiler unit master controller parameters (control targets) for electrical power setpoint ramps from partial load to full load, where PID controllers had been applied to the control structure from ICPD step 2. The optimized parameters are listed in Table 8. While the combustion side was not included in Publication V, the case study represents a template for simultaneous load-following CFB design. Preliminary tests were also

performed in Publication III, where only the steam pressure tracking was optimized by adjusting the superheater storage and the PID parameters.

Table 8. Process and controller parameters for ICPD design (Adapted, with permission, from Publication V © 2019 Elsevier Ltd.).

Parameter	Name	Min	Max
Total steam storages	τ_{TOT}	0.42	1.69
Evaporator storage percentage of τ_{TOT}	q_E	0.97	1.25
Storage percentage before DSH of SH storage	q_{S1}	0.20	1.80
Turbine valve nominal position	$\bar{v}$	0.73	1.22
Steam *p* gain, P	P_p	0.00	5.20
Steam *p* integrator, I	I_p	0.01	36944.30
Steam *p* derivator, D	D_p	0.00	12.17
Steam *p* derivative filter, N	N_p	0.00	1991.49
Output *E* gain, P	P_E	0.02	114.04
Output *E* integrator, I	I_E	0.00	3873.03

The optimization was conducted separately for four load change scenarios, with the same ramping speed for the electrical power and the steam pressure in sliding-pressure mode (Table 9). The scenarios corresponded to planned load transitions (slow 15% ramps) and unexpected electrical power disturbances (fast 5% ramps). The starting point for the ramps was the 80% load level of the power plant.

Table 9. Load change scenarios optimized through ICPD (Adapted, with permission, from Publication V © 2019 Elsevier Ltd.).

Load change scenario	*E* setpoint (%)	Ramp time (time steps)	Ramp speed (%MW/step)	*p* setpoint (%)
I: Fast constant-pressure	+5	13	0.385	0
II: Slow constant-pressure	+15	210	0.07	0
III: Fast sliding-pressure	+5	13	0.385	+5
IV: Slow sliding-pressure	+15	210	0.07	+15

The time window of one simulation was 3750 time steps after the load ramp, and objectives j_1–j_4 were integrated over this range. Objectives j_5 and j_6 were evaluated for the 0–0.5 rad/s range, using Matlab frequency responses. Suggested solutions were verified through closed-loop simulations with the steam path model and benchmarked against reference simulations, where only the PID parameters had been optimized for load change scenarios I–IV.

6 CFB boiler ICPD design results

This chapter summarizes the main results of Publications I–V and their significance for the CFB boiler ICPD procedure. The results validated the chosen design and analysis methods as being suitable for ICPD. The results also established the methods for the CFB boiler process, as many of them had not been applied to fluidized bed power plants in the existing research literature. As a whole, the results also provided new guidelines for CFB boiler process and control design research.

Section 6.1 discusses the simulation-based design results for the oxy-CFB (Publication I). Section 6.2 shows the hotloop state estimation results (Publication II). Section 6.3 deals with the control degrees of freedom in the CFB (Publications I and IV). Section 6.4 presents the relative gain results for the OTU-CFB control structure selection (Publication IV) and the CFB steam path process design (Publication III). Section 6.5 discusses the simultaneous steam path optimization (Publications III and V). Finally, Section 6.6 presents considerations based on the results for applying the ICPD procedure to generic CFB power plant problems.

6.1 Simulation-based process analysis

The simulations and first-principles analysis in Publication I revealed that oxy-combustion affects dynamics and control in the CFB in three main ways: by altering the combustion atmosphere, through flue gas recirculation dynamics, and by modifying the control degrees of freedom (CDOF). Publication I also listed several additional effects that are not discussed here. Subsection 6.1.1 deals with the first two categories, while the simulations related to the CDOF effects are discussed in Section 6.3. Subsection 6.1.2 discusses the air to oxy switch simulations, with the aim of evaluating how transitions between air and oxy mode should be made.

6.1.1 Combustion atmosphere and recirculation dynamics

In Publication I, it was established how the elevated CO_2 and H_2O content of the oxidant and the flue gas in oxy mode led to elevated gas heat capacities (CO_2, H_2O) and densities (CO_2) compared to air-firing. The specific heat capacity elevation resulted in slower heat flux and temperature responses in oxy mode compared to air mode. This could clearly be seen from the load step simulations in Fig. 17 and can also be derived through first-principles dynamics. The slower response in the heat transfer needs to be considered for process unit sizing and controller tuning in

load-following power plants. For static operating points, the heat capacity contributes to lowered furnace temperatures and shifts in heat exchanger loads.

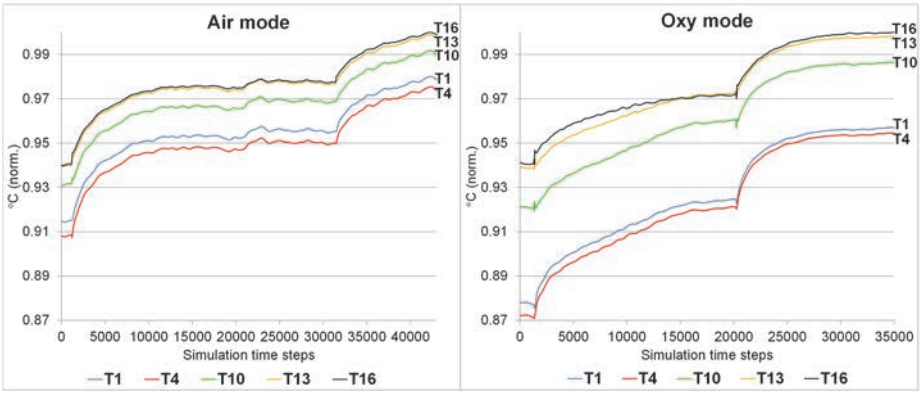

Fig. 17. Normalized furnace temperature responses to two consecutive air and oxy load steps (Adapted, with permission, from Publication I © 2013 Elsevier Ltd.).

Publication I explained how the lower temperature levels can be compensated in oxy mode through oxidant O_2 enrichment, i.e., an oxidant O_2 content higher than that of air. In retrofit and dual-fired boilers, the combustion conditions should be similar to air-firing, which would require an increased oxidant O_2 content and fuel firing power to match the gas specific heat capacity elevation. In oxy greenfield plants, the oxidant O_2 content can be elevated even further, leading to significantly different hotloop and flue gas path designs with higher temperatures and smaller gas flows for added efficiency.

The oxidant and flue gas densities influence the fluidization in the oxy-CFB furnace compared to air-firing. At constant oxidant mass flow, the density increase leads to a reduced volumetric flowrate and thus a decreased fluidization velocity. This was verified from simulations and theory. In Publication I, it was suggested that the density change should be compensated with a constant oxidant volumetric flowrate during air to oxy transitions to maintain the fluidization velocity.

Using RFG as the main oxidant gas component in the oxy-CFB (instead of air) introduces recirculation dynamics for oxidant and flue gas composition responses, unlike air-firing. The effect of the flue gas recirculation rate on the gas composition responses could be seen from the simulations illustrated in Fig. 18. This outcome mainly needs to be considered for the open-loop dynamics and controller design, as the steady-state flue gas composition is largely unaffected by the recycle.

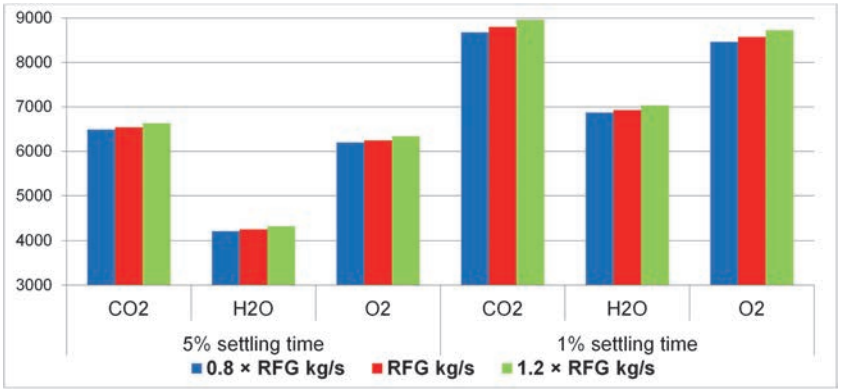

Fig. 18. Flue gas CO_2, H_2O, and O_2 concentration settling times (time steps) for a –10% fuel mass flow disturbance with different RFG rates (Adapted, with permission, from Publication I © 2013 Elsevier Ltd.).

6.1.2 Air to oxy mode switching

The switch simulations showed that feasible air to oxy switches could be made with both the "direct" and the "sequenced" schemes (Figs. 14 and 15). This can be seen from the oxidant and flue gas compositions in Fig. 19, for example.

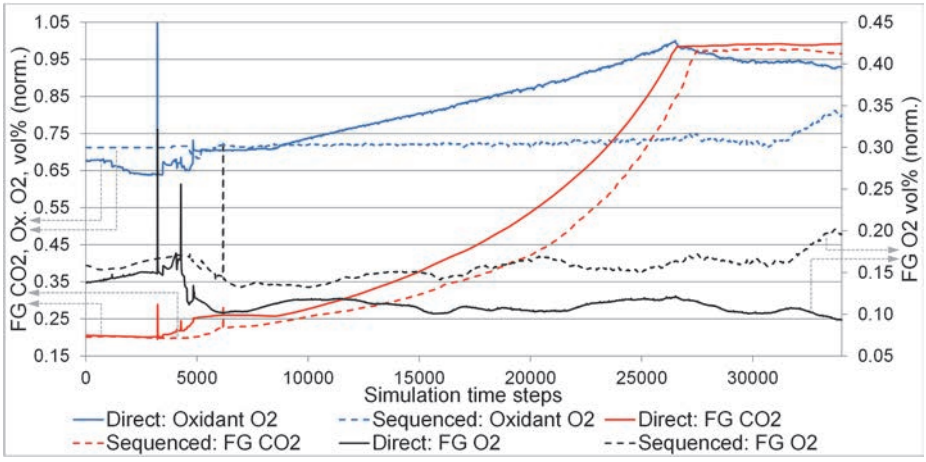

Fig. 19. Normalized primary oxidant (Ox.) O_2, flue gas CO_2, and flue gas O_2 content for the "direct" and "sequenced" switches. Vertical axes of data series are annotated with dashed arrows (Adapted, with permission, from Publication I © 2013 Elsevier Ltd.).

For both switching methods, air-like conditions were maintained throughout the switch transitions (with O_2 enrichment in oxy mode), with no major combustion disturbances based on the flue gas O_2 content. The main differences between the methods were observed in the furnace temperatures (Fig. 20). The "direct" method resulted in a faster and smoother transition than the "sequenced" method, which displayed a decrease both in temperatures and fluidization during the RFG and pure O_2 ramps before the firing power increase at 30000 time steps. This showed how this method was affected more by the oxy-fired gas specific heat capacity elevation than the "direct" method.

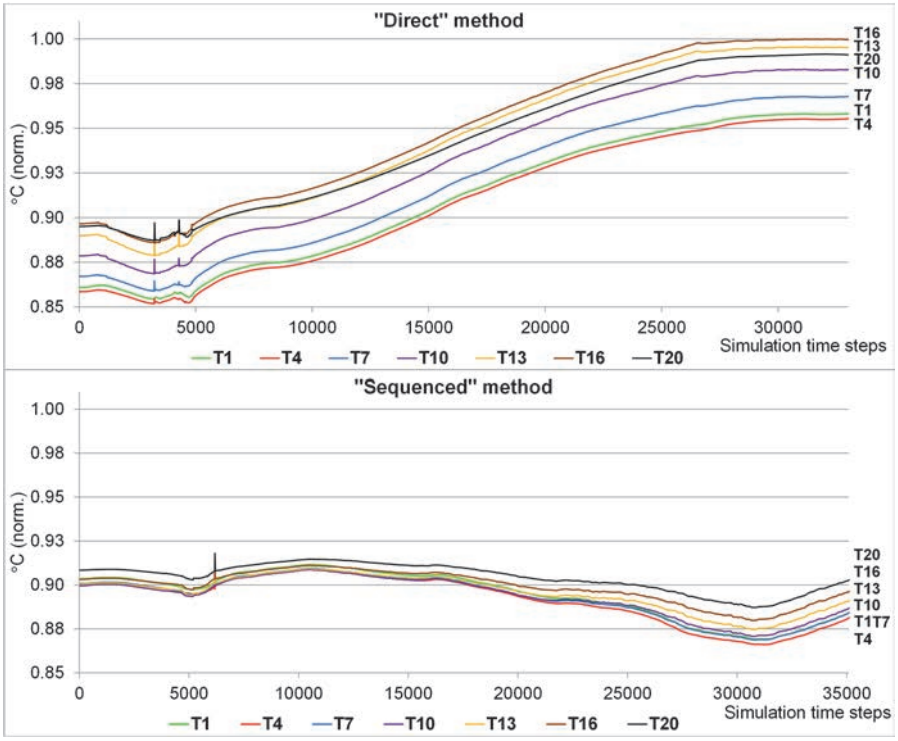

Fig. 20. Normalized temperature responses in furnace elements 1–20 for the "direct" and "sequenced" switches (Adapted, with permission, from Publication I © 2013 Elsevier Ltd.).

Based on the results, it was suggested in Publication I that the "direct" method was preferable for the oxy-CFB hotloop, although modifying all MVs at the same time might be restrictive in practice. For "sequenced" transitions, particular attention

should be paid to the final portions of the gas flow ramps. The switch simulations also verified several of the observations made in Subsection 6.1.1 and Section 6.3.

6.2 CFB hotloop analysis with UKF state estimation

The UKF state estimation tool was implemented successfully for the oxy-CFB pilot combustor and the industrial air-fired boiler, as described in Publication II. The UKF was proven to be applicable to a complex simulator like the hotloop model, and could thus be incorporated into the ICPD procedure. The results showed the benefits of the UKF for the model analysis: good performance, direct use of industrial simulators, and reduced computational load compared to other nonlinear Bayesian algorithms. The estimated fuel mass flow variations and air leakage mass flow for the load ramps in the pilot oxy-CFB case study are illustrated in Fig. 21.

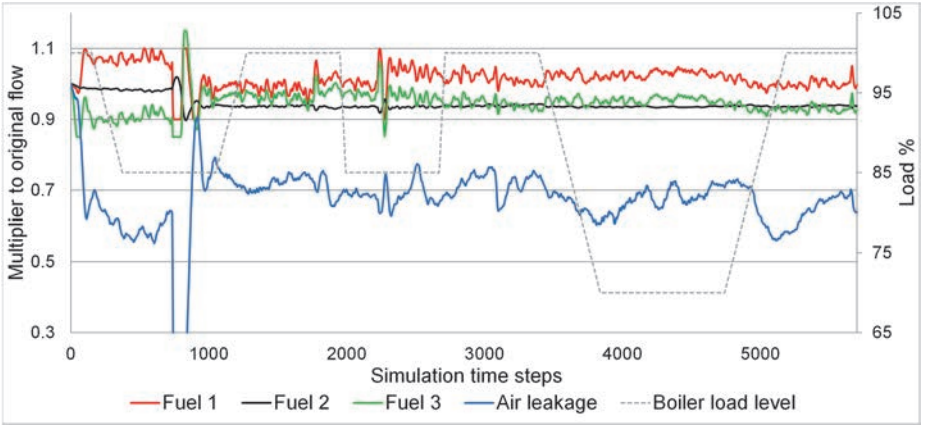

Fig. 21. Estimated fuel flow and air leakage mass flow multipliers during the load ramps in the oxy-CFB (Adapted, with permission, from Publication II © 2014 IEEE).

The corresponding estimated flue gas concentrations are shown in Fig. 22. The estimates shown in Fig. 21 provided a feasible explanation for the observed process behavior and an excellent agreement between the measured and simulated flue gas compositions. The results suggested that a mostly constant level of air leakage had been present during the pilot measurements. This information can be used in oxy-CFB process design, for example for optimizing CO_2 processing costs. The estimated fuel flows contained mostly small oscillations, and these estimates were essential for obtaining accurate input data for the simulator-based ICPD analysis.

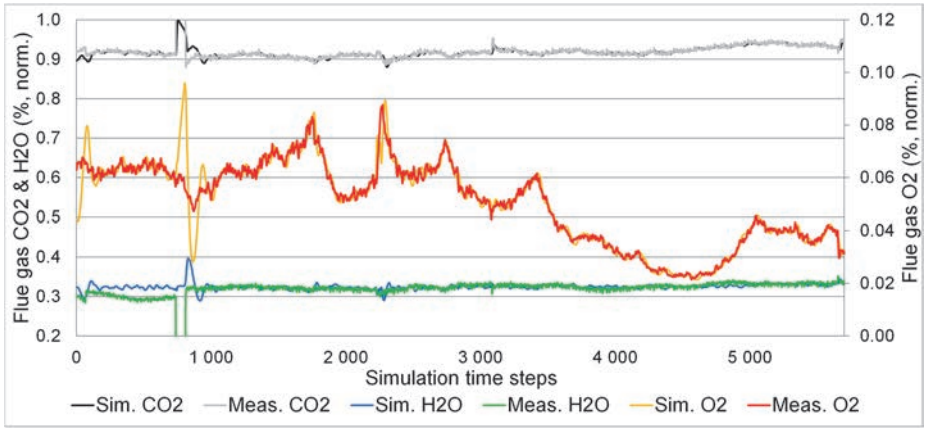

Fig. 22. Measured (Meas.) and estimated (Sim.) flue gas component percentages (normalized) in the oxy-CFB (Adapted, with permission, from Publication II © 2014 IEEE).

The industrial air-fired case study results are provided in Publication II. As in Figs. 21 and 22, the fuel moisture and heat transfer coefficient parameters were adjusted successfully based on the temperature and flue gas O_2 data for all tests described in Subsection 5.3.2, especially for the primary air tests. The estimated fuel moisture variations can be used in ICPD for equipment sizing to reject typical moisture content disturbances, while parameters like the heat transfer coefficient are crucial when adapting the ICPD simulator with noisy dynamic data.

6.3 Degrees of freedom and TPM analysis

The degrees of freedom were analyzed qualitatively based on the CDOF definition for the oxy-CFB in Publication I, and the results supported the simulation-based characterization of the hotloop. Together, these steps provided an overview of how the structure and MVs of the process affected combustion control in the oxy-CFB, as presented in Subsection 6.3.1. Some of the control structures of this subsection were also studied by Hultgren et al. (2015) through closed-loop simulations.

Beside this process characterization, the formal CDOF analysis and dynamic simulations in Publication IV were able to provide the MVs and CVs for the OTU-CFB control design, as well as throughput manipulator (TPM) variable candidates for obtaining fast load changes. While the full CDOF analysis of the plant-wide OTU-CFB flowsheet was already showcased in Section 5.4, the corresponding open-loop TPM variable response analysis is discussed in Subsection 6.3.2.

6.3.1 Oxy-CFB combustion control

The separate RFG and pure O_2 streams in oxy mode led to two additional CDOF compared to air-firing. This is seen in Table 10, which is obtained here by expanding Table 5 to include oxy-firing. How the extra CDOF affected combustion control in the CFB was explored in Publication I. Unlike air-firing, the oxygen supply, furnace cooling, and fluidization become partially decoupled in oxy mode. The oxygen supply to the system is determined by the pure O_2 flow. The RFG flow, in turn, has the largest effect on temperatures (cooling) and fluidization in the furnace. The pure O_2 flow elevates furnace temperatures through combustion while fuel remains; further oxygen can contribute to cooling.

Table 10. Modified CDOF analysis for the oxy-fired CFB boiler combustion side.

Process section and unit	Process unit type	Streams in + out	Connection streams	Restraining number	Redundant streams
Oxidant gas feed		6		4	0
Prim RFG fan	Compressor	1 + 1	1	1	
Sec RFG fan	Compressor	1 + 1	1	1	
Prim O_2/RFG mix	Mixer	2 + 1	1	1	
Sec O_2/RFG mix	Mixer	2 + 1	1	1	
Hotloop		10		2	2
Furnace	Reactor with heat flows	5 + 3	3	0	
Cyclone	Splitter	1 + 2	1	1	
Intrex	HE without inventory	2 + 2	1	1	
Flue gas path		7		5	0
Duct section 1	HE without inventory	1 + 1	1	1	
Duct section 2	HE without inventory	1 + 1	1	1	
Duct section 3	HE without inventory	1 + 1	1	1	
FG recycle point	Splitter	1 + 2	1	1	
Prim/sec RFG split	Splitter	1 + 2	1	1	
SUM		23		11	2
CDOF	10				

The decoupling of the oxidant properties was clearly visible in the RFG step tests of Table 4, where the RFG steps had a significant effect only on the furnace temperature and fluidization (Fig. 23). This decoupling can produce unexpected outcomes during fast load changes. For example, the oxy load ramp simulations described in Publication I revealed that fast ramps for the fuel and oxidant flows

did not necessarily produce fast temperature responses, most probably due to an imbalance between heat generation and furnace cooling during the fast MV changes.

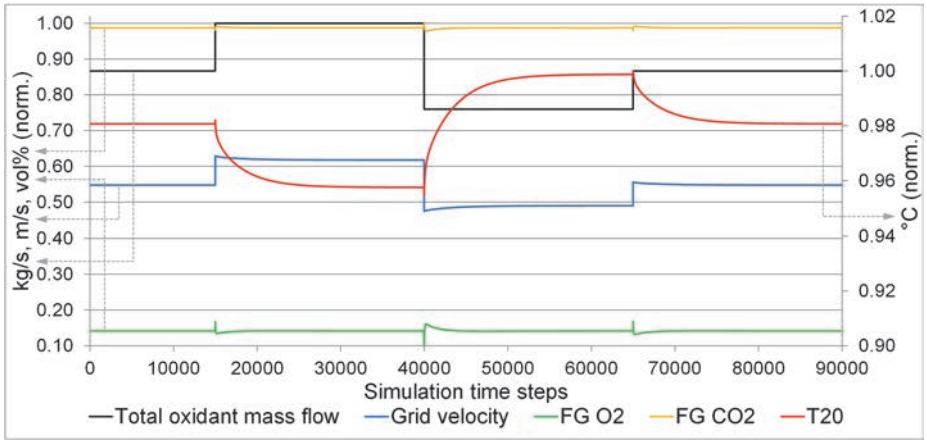

Fig. 23. Normalized gas velocity, furnace temperature, and flue gas O_2 and CO_2 percentage responses to simulated RFG steps in oxy mode with constant firing power. Vertical axes of data series are annotated with dashed arrows (Adapted, with permission, from Publication I © 2013 Elsevier Ltd.).

The control structure in Fig. 24 was proposed for the oxy-CFB in Publication I, based on the decoupling of the oxidant properties. The decoupling calls for oxygen management, and Publication I outlined how the secondary pure O_2 flow or the total secondary oxidant flow could be used for flue gas O_2 control. While the previous option results in smaller fluidization disturbances and a larger flue gas O_2 gain, the oxidant O_2 percentage varies with time. The latter option offers a similar arrangement to air-firing. These findings were confirmed through simulations by Hultgren et al. (2015). The oxidant O_2 content can be controlled with the pure O_2 flow or the RFG flow. Pure O_2 was deemed to be preferable for the primary oxidant, while no preference was found for the secondary oxidant by Hultgren et al. (2015).

Publication I includes an explanation of how the oxy-CFB benefits from oxidant flowrate control, especially for the primary oxidant, to avoid fluidization disturbances. As shown in Fig. 24, the primary RFG is used for this purpose, and the total gas flow setpoint is determined by the boiler firing power. A more extensive option would be to control the bed density or fluidization velocity directly, for example by utilizing a UKF filter as a soft sensor.

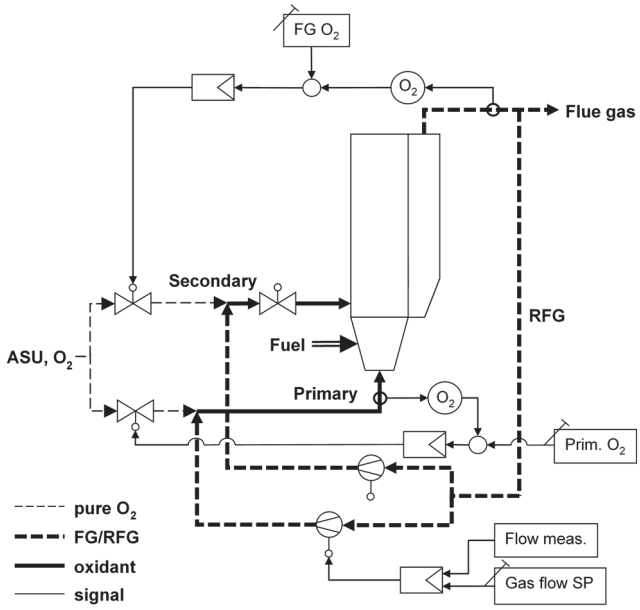

Fig. 24. Proposed oxidant gas control setup in the oxy-CFB (Reprinted, with permission, from Publication I © 2013 Elsevier Ltd.).

The conclusion was drawn in Publication I that the additional CDOF in oxy-firing introduce new control possibilities, but some of these CDOF are consumed by CFB operating constraints. Notably, existing air-fired combustion control structures should not be applied directly to oxy-fired boilers. The decoupled properties of the pure O_2 and RFG flows highlighted that CDOF evaluation should be combined with an analysis of MV–CV dynamics, as was done for the OTU-CFB in Subsection 6.3.2.

6.3.2 Load change TPM variable dynamics

The open-loop dynamics of the TPM variables were analyzed from the OTU-CFB simulator responses in Publication IV according to the principles described in Section 5.4 (Table 11). The turbine valve had the fastest overall response for electrical power and steam pressure, which justifies its use as a TPM for fast load changes. The steam temperature responses were slower due to transient steam flow dynamics. The small static gain between the turbine valve and the electrical power should be noted.

Table 11. Dynamics of load change TPM variables. Results are percentages of the largest value for each CV (Adapted, with permission, from Supporting Material of Publication IV © 2017 American Chemical Society).

TPM property (% of max)	Electrical power	Main steam *p*	Main steam *T*	Evaporator *T*
Turbine valve				
Rise time	0.01	5	100	17
Settling time	33	26	100	60
Time delay	0	0	0	0
Static gain	0.2	–68	–3	–20
Firing power				
Rise time	100	100	74	100
Settling time	100	100	82	100
Time delay	0	67	60	100
Static gain	100	100	100	100
Feedwater flow				
Rise time	0.1	0.4	83	96
Settling time	90	89	94	95
Time delay	0	100	100	50
Static gain	10	18	–98	–72

The firing power predictably had much slower electrical power and steam pressure responses than the turbine valve. However, MV changes also resulted in the largest static gains. Additional testing also revealed that modifying the feedwater and firing power together enabled faster CV responses ("boiler load" MV in Section 5.4).

Feedwater step changes resulted in fast initial responses for steam pressure and electrical power. This was caused by the response shapes, which contained transient overshoots. These observations are potentially useful for obtaining fast load changes in the OTU path, as the output MW_e could in theory be modified using the feedwater flow in turbine-following transitions, and the fast pressure dynamics could be useful in sliding-pressure mode. As a result, the control structure analysis described in Publication IV put special emphasis on the feedwater flow as an MV.

6.4 CFB relative gain analysis

The defined relative gain approach was established as feasible for the CFB control design based on the results in Publications III–V. Plant-wide control structures were successfully defined according to the procedure shown in Fig. 16, and the results illustrated the need for stepwise interaction analysis both at zero frequency and for higher frequencies. The results also demonstrated how the methods could be used

for indicating electrical power control limiting interactions; in Publication III it was shown how this information could be employed in ICPD decision-making. These two aspects are discussed separately in Subsections 6.4.1 and 6.4.2.

6.4.1 Control structure selection

Based on the PRG and DRGA analyses in Publication IV, the suggested control strategy of the OTU-CFB was a combination of turbine-following control (structure I or III) for low-frequency planned disturbances and basic boiler-following control (structure VI) for high-frequency unplanned disturbances. This setup provided ICI controllability with a good PRG distribution at low frequencies, and a low degree of loop interactions at high frequencies, albeit without ICI controllability. The more unconventional structure III employed the feedwater flow to control the electrical power, similar to what was suggested in the TPM analysis of Subsection 6.3.2. Structures I, III, and VI are illustrated in Fig. 25. In the figure, the blue signals correspond to the steam pressure CV, the red signals to the electrical power CV, and the yellow signals to the evaporator temperature CV.

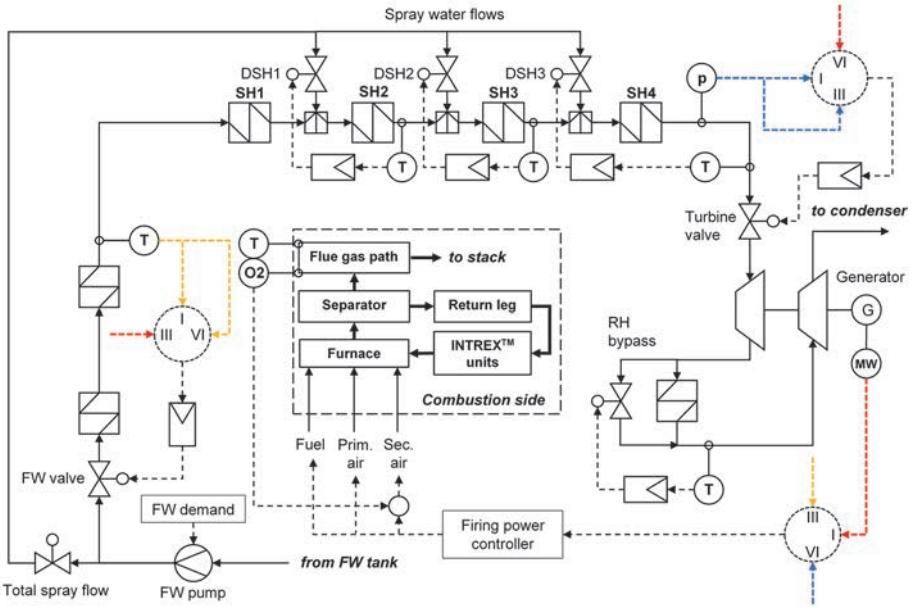

Fig. 25. Control structures I, III, and VI from the stepwise relative gain analysis (Adapted, with permission, from Publication IV © 2017 American Chemical Society).

The corresponding PRG and DRGA analyses of the plant-wide case 4 (cf. Table 7) are illustrated in Table 12 and Fig. 26.

Table 12. PRG distributions and NI values of the ICI control structures of case 4. The control connection notation is given in Fig. 26 (Adapted, with permission, from Publication IV © 2017 American Chemical Society).

Structure	Control connections	NI	Number of PRG elements in range						
			0–0.1	0.1–0.5	0.5–0.85	0.85–1.2	1.2–5	5–10	>10
I	[1 6 2 3 4 5 7 8]	0.321	0	4	7	919	76	2	0
II	[1 6 7 3 4 5 2 8]	0.358	117	47	116	643	85	0	0
III	[1 6 8 3 4 5 7 2]	2.320	122	60	99	632	95	0	0

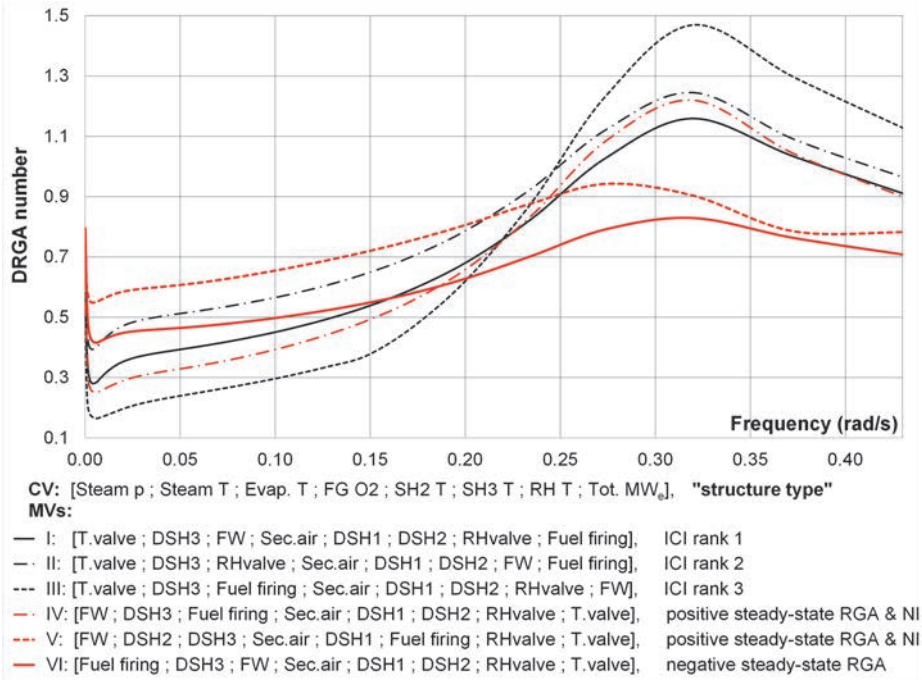

Fig. 26. DRGA numbers for the control structures I–VI in case 4 (Adapted, with permission, from Publication IV © 2017 American Chemical Society).

Three structures were deemed as ICI controllable based on the full PRG analysis (Table 12). Structure II had limited practical significance, although it and other PRG results of case 4 revealed an interaction between the feedwater flow and the

reheater. The basic turbine-following structure I was ranked the highest in terms of its PRG distribution. This outcome was observed for all cases in Table 7, especially case 1. The dominance of turbine-following control was caused by the small static gain between the turbine valve and the electrical power, cf. Subsection 6.3.2.

No conventional boiler-following structures (electrical power–turbine valve, main steam pressure–firing power) were validated as ICI controllable (e.g., structure VI) due to the small negative static RGA element between the firing power and the steam pressure. This result was repeated for the "boiler load" MV in cases 1 and 2. However, positive RGA and NI values were obtained for structures IV and V, which utilized the turbine valve for fast electrical power control. The steam pressure was controlled with the feedwater, which supported the observations of Subsection 6.3.2.

The DRGA ranking in Fig. 26 shows the contrast between preferred control structures at zero and higher frequencies. Structure I was surpassed by structure III even at low frequencies, and structure VI was preferred above 0.2 rad/s. This outcome was even clearer in Publication V: Turbine-following control was only preferable at zero frequency based on the PRGA, and the CLDG indicated that turbine-following electrical power control suffered from DSH spray interactions. Turbine-following control became more feasible at high frequencies in Publication IV when the "boiler load" MV was used in cases 1 and 2.

Combustion control connections were studied in case 3, thus expanding on the results of Sections 6.1 and 6.3 by considering the interactions of variables on the combustion side. The PRG analysis of case 3 is shown in Table 13, resulting in two ICI structures, where only the fuel and feedwater control connections were switched. This emphasizes how these MVs together determine the amount of generated steam, but how the feedwater–electrical power connection leads to reduced ICI controllability. Similar interchangeable MV pairs were observed for the oxy-CFB hotloop in the ICI PRG analysis of Hultgren et al. (2015), for example the primary RFG and pure O_2 flows.

Table 13. PRG distributions and NI values of the ICI control structures in case 3. The control connection notation is given in Fig. 27 (Adapted, with permission, from Publication IV © 2017 American Chemical Society).

Structure	Control connections	NI	Number of PRG elements in range						
			0–0.1	0.1–0.5	0.5–0.85	0.85–1.2	1.2–5	5–10	>10
I	[1 6 2 5 4 3]	0.231	0	0	1	117	62	0	0
II	[1 6 3 5 4 2]	1.600	30	26	21	65	38	0	0

The corresponding DRGA plots of case 3 are shown in Fig. 27. At higher frequencies, nine alternative control structures could be considered based on the DRGA. Similarly to case 4, turbine-following structures were favored below 0.12 rad/s, and boiler-following structures above that. However, the preferred structure varied more at different frequencies than in case 4, with structures I, II, IX, VII, and VI all being preferable in specific ranges. In general, the DRGA favored control setups for high-frequency disturbances that increased the decoupling between the evaporator, the steam flow, and the turbine.

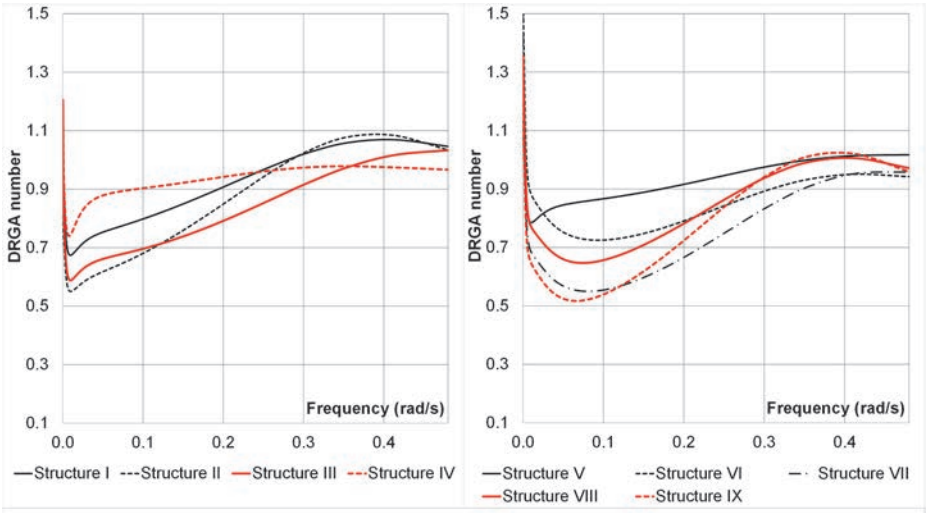

CV:	[Steam p ; Steam T ; Evap. T ; FG O2 ; FG T ; Tot. MW_e],	"structure type"
MVs:		
I:	[T.valve ; DSHtot. ; FW ; Sec.air ; Prim.air ; Fuel],	ICI rank 1
II:	[T.valve ; DSHtot. ; Fuel ; Sec.air ; Prim.air ; FW],	ICI rank 2
III:	[FW ; DSHtot. ; Fuel ; Sec.air ; Prim.air ; T.valve],	positive steady-state RGA & NI
IV:	[Prim.air ; DSHtot. ; FW ; Sec.air ; Fuel ; T.valve],	positive steady-state RGA & NI
V:	[Fuel ; DSHtot. ; FW ; Sec.air ; Prim.air ; T.valve],	negative steady-state RGA
VI:	[Fuel ; DSHtot. ; FW ; Prim.air ; Sec.air ; T.valve],	negative steady-state RGA
VII:	[FW ; DSHtot. ; Fuel ; Prim.air ; Sec.air ; T.valve],	negative steady-state RGA
VIII:	[T.valve ; DSHtot. ; FW ; Prim.air ; Sec.air ; Fuel],	negative steady-state RGA
IX:	[T.valve ; DSHtot. ; Fuel ; Prim.air ; Sec.air ; FW],	negative steady-state RGA

Fig. 27. DRGA numbers for the control structures I–IX in case 3 (Adapted, with permission, from Publication IV © 2017 American Chemical Society).

In general, the chosen relative gain approach was shown to be effective in generating and ranking control structures for the CFB system. The suggested control structures corresponded to industrial practices and thus validated their feasibility. The analysis was also able to highlight unorthodox control connections,

as well as disturbance frequencies that caused controllability issues for specific control setups.

6.4.2 Loop interaction analysis

Several loop interactions were discussed for the OTU-CFB in Publication IV, and the DRGA elements of individual MVs were analyzed in detail, especially for the plant-wide case 4. It could be seen that the interactions caused little change in the preferred control connections for the DSH1, DSH3, and reheater bypass valve MVs in the whole frequency range. The preferred connection was less clear for the other MVs, most importantly the main load change TPM variables: the turbine valve, firing power, and feedwater flow.

The DRGA elements of all MVs in case 4 are shown in Fig. 28. The interaction between electrical power and main steam pressure control was clearly visible from the overall results described in Publication IV, especially for the turbine valve and feedwater flow. Likewise, the PRGA in Publication V showcased a major off-diagonal interaction in the electrical power for both turbine-following and boiler-following control. For the feedwater, the interaction with the firing power in the steam formation was highlighted especially in case 3, and many of the suggested control connections for these variables were interchangeable.

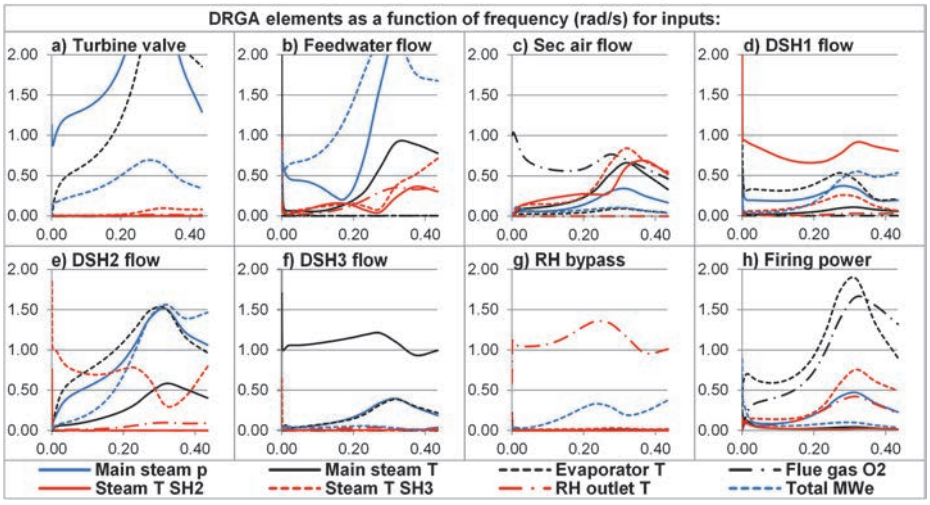

Fig. 28. DRGA element magnitudes for all MV–CV connections in case 4 (Adapted, with permission, from Publication IV © 2017 American Chemical Society).

The ill-conditioning related to steam temperature control was identified as another source of variable interaction. Similar effects of the feedwater and DSH flows on steam temperatures were observed as large PRG elements in cases 2 and 4. The DRGA indicated controllability issues for the middle spray DSH2 (Fig. 28), as well as steam temperature interactions for the feedwater at high frequencies.

On the combustion side, ill-conditioning was observed in case 3 for the primary and secondary oxidant gas flows, as they affect flue gas and furnace properties in a similar way. These findings could be compared to the PRG results of Hultgren et al. (2015) for the oxy-CFB hotloop, where large PRG values and similar effects of gas flow MVs were reported, especially for furnace temperature CVs.

In addition to Publication IV, the DRGA was used for process design in Publication III, by examining how evaporator and superheater steam storage parameters affected loop interactions in the CFB steam path (cf. Subsection 5.5.2). The DRGA plots for the different process parameter levels are shown in Fig. 29. The results illustrated that increasing the superheating mass storage improved controllability by increasing the decoupling between steam generation and the turbine. Increasing the evaporator storage improved controllability in the low-frequency region, but above 0.04 rad/s a small storage was preferable. These findings were directly connected to electrical power setpoint tracking performance through closed-loop simulations, cf. Publication III. The results demonstrated how the DRGA could be used for guiding design decisions in ICPD and thus enabled the use of the PRGA and CLDG as optimization objectives in Publication V.

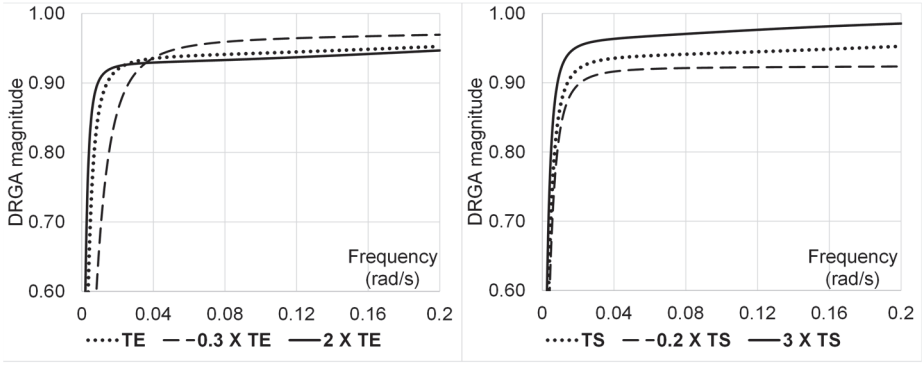

Fig. 29. Effect of lumped evaporator storage (TE) and superheater storage (TS) parameters (change from nominal value) on DRGA element magnitudes (Adapted, with permission, from Publication III © 2017 IFAC).

6.5 CFB steam path ICPD optimization

The ICPD optimization was carried out successfully for the storage distribution, nominal turbine valve position, and unit master PID parameters of the CFB steam path model, as described in Publication V. The optimized load change scenario I is shown in Fig. 30. The results for scenarios II–IV are provided in Publication V.

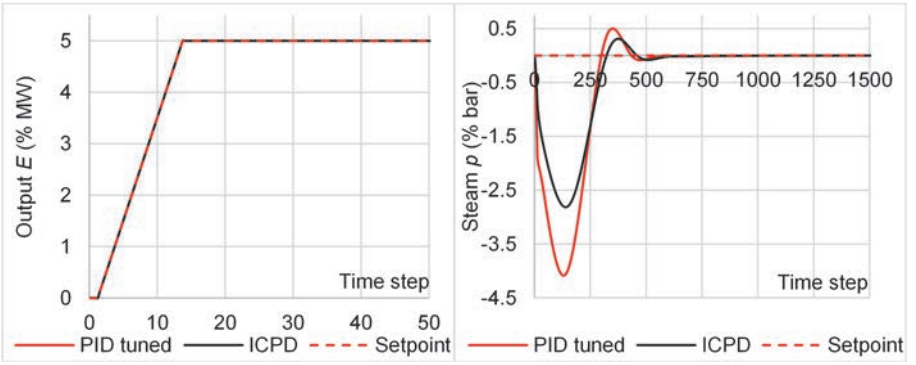

Fig. 30. Scenario I with ICPD optimized and PID optimized parameters (Adapted, with permission, from Publication V © 2019 Elsevier Ltd.).

The optimized process and controller parameters are shown in Table 14. The ICPD optimization maximized the steam storage in the whole steam path for both the constant-pressure and sliding-pressure scenarios. The evaporator storage was minimized, the superheater storage was maximized, and the superheater storage was distributed close to the turbine. The turbine valve opening at 80% load was decreased for the scenarios with the large slow load changes (scenarios II and IV) and increased for the scenarios with the small fast load changes (scenarios I and III).

Table 14. The ICPD optimized process and controller parameters (Table 8) for the scenarios in Table 9. Reported values are multipliers to the nominal starting parameters (Adapted, with permission, from Publication V © 2019 Elsevier Ltd.).

Load change scenario	τ_{TOT}	q_E	q_{S1}	$\bar{v}$	P_p	I_p	D_p	N_p	P_E	I_E
I: Fast constant-pressure	1.69	0.97	0.20	1.08	2.91	2.23	5.09	727.26	2.71	118.88
II: Slow constant-pressure	1.69	0.97	0.20	0.97	1.44	2.48	3.70	55.06	2.31	35.58
III: Fast sliding-pressure	1.69	0.97	0.20	1.08	1.99	0.56	3.78	11.94	2.87	133.01
IV: Slow sliding-pressure	1.69	0.97	0.20	0.97	1.64	0.41	3.33	782.93	1.99	0.08

The ICPD optimization clearly provided better results than the reference simulations, where only the PID controller parameters were optimized. Table 15 shows that the design resulted in a good trade-off between the objectives in Subsection 5.6.2 for all load change scenarios. Accurate electrical power tracking was obtained, steam throttling was minimized, a sufficient steam control reserve was maintained, and no reduction in controllability was observed in terms of the PRGA and CLDG.

Table 15. Objectives j_1–j_6 and total objective J for the ICPD optimized and PID optimized load change scenarios I–IV. Values are % of nominal objective values (Adapted, with permission, from Publication V © 2019 Elsevier Ltd.).

Objective	Scenario I		Scenario II		Scenario III		Scenario IV	
(%)	ICPD	PID	ICPD	PID	ICPD	PID	ICPD	PID
j_1	0.3995	0.7866	0.4686	0.5271	0.8080	0.9536	0.9986	0.8480
j_2	0.0013	0.0000	0.0001	0.3912	0.0012	0.0000	0.0007	0.3865
j_3	1.1563	0.9992	0.9441	0.9956	1.1596	1.0015	0.9602	1.0050
j_4	1.0001	1.0000	0.0005	0.0003	1.0001	1.0000	0.0006	0.0041
j_5	0.9978	1	0.9054	1	0.9980	1	0.9082	1
j_6	0.5662	1	0.5730	1	0.5662	1	0.5728	1
J	0.095	0.215	0.049	0.419	0.125	0.227	0.088	0.439

The results contributed towards setting guidelines for CFB steam path design. For example, it was pointed out in Publication V how the steam storage was maximized even for the sliding-pressure scenarios, although a small storage capacity essentially contributes to fast steam pressure transitions. The outcome could be explained by the chosen optimization objective, as a large steam storage capacity reduces the electrical power disturbances caused by boiler-following turbine valve action. Indeed, the steam path optimization described in Publication III resulted in a small superheater storage capacity in sliding-pressure mode, as only the main steam pressure tracking was optimized.

The results showed how dynamic ICPD optimization inherently contributes to the formation of local optima even for simple process systems. This was mainly attributed to the simultaneous optimization of the process and its controllers, but also to the single-objective formulation and the chosen performance criteria. The challenging nature of the ICPD problem validated the chosen hybrid optimization algorithm, as well as the simplified internal model approach.

6.6 Future directions

In Publications I–V the application of the chosen ICPD design methods was demonstrated for individual CFB boiler design problems, all supporting the overall goal of faster load changes. In addition, several observations were made from these case studies for refining the ICPD procedure for generic load-following CFB power plant design problems. These development suggestions are briefly discussed here.

As a whole, a toolbox of design steps can be assembled from Publications I, II, and IV for qualitative dynamic simulation and control-oriented process design in the CFB. These steps include mapping the effects of altered operating conditions on the open-loop dynamics, mapping the effects of structural changes on the process operation, analyzing the control degrees of freedom (CDOF), evaluating the MV–CV dynamics of TPM variables based on the CDOF, and extending the simulations with measured data through nonlinear state estimation. While the MV–CV analysis and degrees of freedom evaluation were already carried out for the full OTU-CFB flowsheet in Publication IV, the simulator-based analysis from Publications I and II also needs to be expanded to the CFB water-steam cycle. For the state estimation, the main task is to evaluate the feasibility of using the full OTU-CFB simulator in Fig. 12 as the internal model of the UKF tool.

With the PRGA/CLDG modification introduced in Publication V, the relative gain control structure selection procedure of Publication IV is directly applicable to generic CFB problems. Notably, the stepwise relative gain procedure for large MV–CV systems, using multiple methods, is a novel contribution of the thesis. Moreover, the use of relative gain methods as ICPD performance measures should be expanded on, especially for the pre-analysis stage, similarly to Publication III.

The ICPD optimization procedure was validated for the simple CFB steam path model in Publication V. Based on these findings, the next step in CFB boiler ICPD research would be to optimize the plant-wide power plant flowsheet based on the procedure. The main research questions arise from the internal design model type, the controller type, and the objective function formulation.

For the internal model, the main task is to expand the mass storage model described in Publication V with heat exchanger specific mass storages, instead of using lumped storage parameters. Secondly, steam energy content variations should be included by adding heat transfer state equations for the water-steam and combustion/flue gas sides. The water-steam temperature dynamics can be modeled by describing the heat exchanger as an ideal plug flow in a set of pipes, with heat transfer from the pipe wall. The combustion/flue gas side heat storages can be

assumed to be ideally mixed tanks, as they are significantly larger than the water-steam side heat storages.

The closed-loop design model can be obtained for the OTU-CFB flowsheet in Fig. 12 by applying PID controllers to the control structures in Subsection 6.4.1. As stated in Publication V, MPC control should also be investigated for the proposed ICPD procedure in future research efforts. If MIMO controllers are considered, the relative gain control structure selection procedure described in Publications IV and V could readily be modified with the block relative gain (cf. Subsection 4.5.2).

A default ICPD objective function was presented for load-following boilers in Subsection 5.6.2. For a generic CFB problem, objective j_1 should be expanded with an ISE setpoint tracking measure for the main steam temperature, especially if steam temperature controllers or superheater parameters are optimized. Similarly, the exergy penalty associated with evaporative DSH cooling could be considered for efficiency objective j_3. The objective could be employed similarly to the turbine valve, where optimal solutions minimize the use of DSH water during load disturbances, while also minimizing control signal saturation. The sliding-pressure optimization did not consider a separate setpoint trajectory for the steam pressure, the inclusion of which would call for minor integration of process design, control design, and scheduling (cf. Section 3.1). Lastly, an economic constraint should be included in the ICPD optimization, or a separate economic evaluation stage should be added to the results of the ICPD procedure, as suggested in Section 4.1.

7 Conclusions

The increased use of renewable energy in the power grid requires steam power plants to perform fast and frequent load changes, and emission mitigation requires designers to implement process modifications such as carbon capture and storage (CCS) in solid fuel boilers. This thesis presents a systematic study and analysis on how integrated control and process design (ICPD) can contribute to improved load change performance and flexibility regarding process modifications in circulating fluidized bed boiler (CFB) power plants. CFB boilers with increased dynamic performance can be obtained through the ICPD tools and design guidelines that were utilized in this thesis. Therefore, the work enables CFB design to better adjust to the changing demands of modern sustainable power generation, compared to a conventional approach with sequential process and control design steps.

Systematic ICPD was applied to CFB boilers for the first time in this thesis. It was discovered that little ICPD design experience is available for steam power plants in the literature, despite the well-documented benefits of integrating process and control design for various chemical processes. Extreme load change requirements present a major design challenge for solid fuel boilers with slow and interacting dynamics. This challenge has been addressed in the literature through improved control methods (e.g., MPC control) and operating modes (e.g., condensate throttling), but the process and its control system are still largely treated as separate design problems. The thesis concludes that significant potential for increased CFB generation flexibility lies in making control design an intrinsic part of the boiler process design, as the open-loop dynamics determine the upper limit for the load change performance. Another conclusion is that greater effort is needed from the research community to identify industrial case studies, where improved performance could be reached through design integration. ICPD is often considered to be a mature science at this point, even though it has practically never been applied to large-scale load-following combustion power plants prior to this thesis.

A systematic view of the application of ICPD was taken in this thesis. The work provided a novel ICPD characterization focusing on commonly occurring features in ICPD methodologies. The work indicates that this approach helps in the selection of design and analysis methods for a novel application area like the CFB boiler, especially since the scope of current ICPD research is wide and somewhat ill-defined. The characterization places great significance on systematic performance evaluation, which is not commonly emphasized in current ICPD literature. The author would argue that the proper definition and quantification of desirable closed-

loop performance forms the basis for the whole design–control interaction. The suggested performance evaluation approach for the load-following CFB boiler can be labeled as "trajectory design": the electrical power setpoint tracking error is minimized during simulated load ramps together with main steam state variable errors, similar to switchability analysis. This main objective is augmented with additional goals for first-principles efficiency, disturbance rejection capacity, and controllability. The thesis work concludes that this approach is more suitable for load-following problems than, for example, an economic objective, which is commonly used especially in mathematical programming ICPD and has been a defining guideline for boiler process design in the past.

The work carried out during this thesis resulted in a hierarchical ICPD procedure that was shown to be suitable for generating CFB flowsheets with good load-following performance and design flexibility for the oxy-combustion CCS technology. The thesis work concludes that load change performance can be improved most effectively by combining a closed-loop process optimization problem with first-principles knowledge and system analysis. In Publications I–V, it was shown that ICPD methods based on dynamic trajectory optimization, relative gain array tools (partial relative gain, performance relative gain array, closed-loop disturbance gain, Niederlinski index), and first-principles simulation augmented with unscented Kalman filter (UKF) state estimation provided a means for improved control and process design in the CFB boiler. The overall approach can be summarized as simulation-oriented ICPD, as the methods ultimately rely on high-accuracy industrial process simulators. The proposed procedure and its application to the CFB boiler are the novel contributions of the thesis: The chosen design and analysis methods are mostly established in the literature, but many of them were applied here to the CFB boiler for the first time.

In Publication I, it was demonstrated how the chemical, physical, and structural properties of the CFB boiler can be connected to its control performance and how monitoring these properties enables more informed process design decisions for control. The thesis thus emphasizes the importance of first-principles process knowledge and simulation for effective closed-loop design, which somewhat contrasts with the current trend of black-box neural network modeling in process digitalization. The simulation-oriented focus of the thesis is supported by the increasing availability of computing power, which enables the rapid evaluation of complex models in ICPD algorithms. This outlook was reflected in the chosen UKF approach in Publication II: A fully detailed industrial CFB simulator could be used directly for data post-processing, while maintaining acceptable computational

performance. The work also employed Bayesian state estimation unconventionally in ICPD as a model analysis tool rather than for process monitoring and control.

Based on the control structure selection and analysis in Publications III–V, it can be concluded that a comprehensive picture of control interactions in the CFB can only be obtained by investigating different control variable subsystems using multiple relative gain methods. For the same reason, relative gains were examined for the entire load disturbance frequency range instead of analyzing steady-state data or individual frequencies. Furthermore, the thesis demonstrates how relative gain methods can be used as performance measures for interactions and controllability, not just as heuristic pairing rules for manipulated and controlled variables. These findings expand on the typical relative gain analysis literature.

In Publication V, it was outlined that the fully simultaneous optimization of the CFB process and its unit master PID controllers is a feasible, yet challenging task. Most importantly, process parameters and their preferred controller tunings form multiple local optima that call for global optimization approaches. While this aspect will be influenced by the available computing power in the future, the thesis indicates that dynamic response optimization will still require advanced algorithms and simplification in the near future to make the problem practically feasible.

Aside from its contributions to ICPD, the thesis also contributes to increasing CFB boiler design knowledge by providing guidelines for specific process and control design problems. Of these, the most important were how the air-fired CFB should be modified for oxy-firing, how transitions between air and oxy mode should be conducted, how plant-wide OTU-CFB control connections should be selected, which variable interactions have the potential to cause issues for OTU-CFB control performance, and how steam storage capacity should be allocated in the steam path to improve load change performance, ultimately translating into superheater sizing and placement. Notably, these outcomes were specifically enabled by the chosen methods and the overall ICPD approach of the thesis.

This thesis constitutes the first systematic research effort in improving CFB power plant design practices through ICPD. This development should be expanded through additional research. While the present work only concerns the CFB power plant, the outcomes of the thesis are essentially also applicable to other solid fuel power plants to improve their operation for sustainable power generation. The suggested ICPD procedure serves as an improvement over existing CFB design practices. The methods of the procedure were shown to be readily applicable to different industrial CFB boiler problems. In conclusion, the integration of control aspects into process design is both a feasible and a necessary development.

List of references

Alhammadi, H. Y., & Romagnoli, J. A. (2004). Process design and operation: Incorporating environmental, profitability, heat integration and controllability considerations. In P. Seferlis, & M. C. Georgiadis (Eds.), *Computer aided chemical engineering: Vol. 17. The integration of process design and control* (pp. 264–305). Amsterdam: Elsevier. https://doi.org/10.1016/S1570-7946(04)80063-4

Alvarado-Morales, M., Hamid, M. K. A., Sin, G., Gernaey, K. V., Woodley, J. M., & Gani, R. (2010). A model-based methodology for simultaneous design and control of a bioethanol production process. *Computers & Chemical Engineering, 34*(12), 2043–2061. https://doi.org/10.1016/j.compchemeng.2010.07.003

Anthony, E. J., & Hack, H. (2013). Oxy-fired fluidized bed combustion: Technology, prospects and new developments. In F. Scala (Ed.), *Woodhead publishing series in energy: Vol. 59. Fluidized bed technologies for near-zero emission combustion and gasification* (pp. 867–894). Cambridge: Woodhead Publishing. https://doi.org/10.1533/9780857098801.4.867

Arasu, S. K., Prakash, J., & Prasad, V. (2013). Derivative-free estimator based non-linear model predictive control of a boiler-turbine unit. *IFAC Proceedings Volumes, 46*(32), 660–665. https://doi.org/10.3182/20131218-3-IN-2045.00090

Åström, K. J., & Murray, R. M. (2008). *Feedback systems: An introduction for scientists and engineers*. Princeton, NJ: Princeton University Press.

Bahri, P. A., Bandoni, A., & Romagnoli, J. (1996). Operability assessment in chemical plants. *Computers & Chemical Engineering, 20*(Supplement 2), S787–S792. https://doi.org/10.1016/0098-1354(96)00139-1

Balko, P., & Rosinová, D. (2015). Robust decentralized control of nonlinear drum boiler. *IFAC-PapersOnLine, 48*(14), 432–437. https://doi.org/10.1016/j.ifacol.2015.09.495

Bardelli, R., Bittanti, S., Bolzern, P., Campi, M., Carugati, E., De Marco, A., … Prandoni, W. (1994). Application of the extended Kalman filter to the estimation of the char mass in a fluidized bed combustor. *IFAC Proceedings Volumes, 27*(8), 221–226. https://doi.org/10.1016/S1474-6670(17)47719-6

Basu, P. (2006). *Combustion and gasification in fluidized beds*. Boca Raton, FL: Taylor & Francis.

Biegler, L. T. (2018). Advanced optimization strategies for integrated dynamic process operations. *Computers & Chemical Engineering, 114*, 3–13. https://doi.org/10.1016/j.compchemeng.2017.10.016

Bittanti, S., Bolzern, P., Campi, M., De Marco, A., Panseri, R., Poncia, G., & Prandoni, W. (1996). A model of a bubbling fluidized bed combustor for the estimation of the char mass via extended Kalman filter. *IFAC Proceedings Volumes, 29*(1), 6909–6914. https://doi.org/10.1016/S1474-6670(17)58793-5

Bolea, I., Romeo, L. M., & Pallarés, D. (2012). The role of external heat exchangers in oxy-fuel circulating fluidized bed. *Applied Energy, 94*, 215–223. https://doi.org/10.1016/j.apenergy.2012.01.050

Bristol, E. H. (1966). On a new measure of interaction for multivariable process control. *IEEE Transactions on Automatic Control, 11*(1), 133–134. https://doi.org/10.1109/TAC.1966.1098266

Buckley, P. S. (1964). *Techniques of process control*. New York, NY: Wiley.

Burnak, B., Diangelakis, N. A., Katz, J., & Pistikopoulos, E. N. (2019). Integrated process design, scheduling, and control using multiparametric programming. *Computers & Chemical Engineering, 125*, 164–184. https://doi.org/10.1016/j.compchemeng.2019.03.004

Burnak, B., Diangelakis, N. A., & Pistikopoulos, E. N. (2019). Towards the grand unification of process design, scheduling, and control—Utopia or reality? *Processes, 7*(7), 461. https://doi.org/10.3390/pr7070461

Campo, P. J., & Morari, M. (1994). Achievable closed-loop properties of systems under decentralized control: Conditions involving the steady-state gain. *IEEE Transactions on Automatic Control, 39*(5), 932–943. https://doi.org/10.1109/9.284869

Cao, Y., Fuentes-Cortes, L. F., Chen, S., & Zavala, V. M. (2017). Scalable modeling and solution of stochastic multiobjective optimization problems. *Computers & Chemical Engineering, 99*, 185–197. https://doi.org/10.1016/j.compchemeng.2017.01.021

Capra, F., & Martelli, E. (2015). Numerical optimization of combined heat and power Organic Rankine Cycles – Part B: Simultaneous design & part-load optimization. *Energy, 90*(1), 329–343. https://doi.org/10.1016/j.energy.2015.06.113

Chandrasekharan, S., Panda, R. C., Swaminathan, B. N., & Panda, A. (2018). Operational control of an integrated drum boiler of a coal fired thermal power plant. *Energy, 159*, 977–987. https://doi.org/10.1016/j.energy.2018.06.157

Chen, C., & Bollas, G. M. (2017, January). *Semi-batch chemical-looping reactors integrated with combined cycle power plants operating at transient electricity demand*. Paper presented at the FOCAPO / CPC 2017, Foundations of Computer Aided Process Operations / Chemical Process Control Conference, Tucson, AZ, United States.

Chiandussi, G., Codegone, M., Ferrero, S., & Varesio, F. E. (2012). Comparison of multi-objective optimization methodologies for engineering applications. *Computers & Mathematics with Applications, 63*(5), 912–942. https://doi.org/10.1016/j.camwa.2011.11.057

Chiu, M.-S., & Arkun, Y. (1990). Decentralized control structure selection based on integrity considerations. *Industrial & Engineering Chemistry Research, 29*(3), 369–373. https://doi.org/10.1021/ie00099a012

Daoutidis, P., Zachar, M., & Jogwar, S. S. (2016). Sustainability and process control: A survey and perspective. *Journal of Process Control, 44*, 184–206. https://doi.org/10.1016/j.jprocont.2016.06.002

Daum, F. (2005). Nonlinear filters: Beyond the Kalman filter. *IEEE Aerospace and Electronic Systems Magazine, 20*(8), 57–69. https://doi.org/10.1109/MAES.2005.1499276

Diangelakis, N. A., Burnak, B., & Pistikopoulos, E. N. (2017, January). *A multi-parametric programming approach for the simultaneous process scheduling and control – Application to a domestic cogeneration unit*. Paper presented at the FOCAPO / CPC 2017, Foundations of Computer Aided Process Operations / Chemical Process Control Conference, Tucson, AZ, United States.

Diangelakis, N. A., & Pistikopoulos, E. N. (2017a). Modelling, design and control optimization of a residential scale CHP system. In G. M. Kopanos, P. Liu, & M. C. Georgiadis (Eds.), *Advances in energy systems engineering* (pp. 475–506). Cham: Springer. https://doi.org/10.1007/978-3-319-42803-1_16

Diangelakis, N. A., & Pistikopoulos, E. N. (2017b). A multi-scale energy systems engineering approach to residential combined heat and power systems. *Computers & Chemical Engineering, 102*, 128–138. https://doi.org/10.1016/j.compchemeng.2016.10.015

Doležal, R., & Varcop, L. (1970). *Process dynamics: Automatic control of steam generation plant*. Amsterdam: Elsevier.

Engell, S., Trierweiler, J. O., Völker, M., & Pegel, S. (2004). Tools and indices for dynamic I/O-controllability assessment and control structure selection. In P. Seferlis, & M. C. Georgiadis (Eds.), *Computer aided chemical engineering: Vol. 17. The integration of process design and control* (pp. 430–463). Amsterdam: Elsevier. https://doi.org/10.1016/S1570-7946(04)80069-5

Frumkin, J. A., & Doherty, M. F. (2020). A rapid screening methodology for chemical processes. *Computers & Chemical Engineering, 142*, 107039. https://doi.org/10.1016/j.compchemeng.2020.107039

Georgakis, C., Vinson, D. R., Subramanian, S., & Uztürk, D. (2004). A geometric approach for process operability analysis. In P. Seferlis, & M. C. Georgiadis (Eds.), *Computer aided chemical engineering: Vol. 17. The integration of process design and control* (pp. 96–125). Amsterdam: Elsevier. https://doi.org/10.1016/S1570-7946(04)80056-7

Goldberg, D. E. (1989). *Genetic algorithms in search, optimization & machine learning*. Reading, MA: Addison-Wesley.

Gonzalez-Salazar, M. A., Kirsten, T., & Prchlik, L. (2018). Review of the operational flexibility and emissions of gas- and coal-fired power plants in a future with growing renewables. *Renewable and Sustainable Energy Reviews, 82*(1), 1497–1513. https://doi.org/10.1016/j.rser.2017.05.278

Grossmann, I. E., Apap, R. M., Calfa, B. A., García-Herreros, P., & Zhang, Q. (2016). Recent advances in mathematical programming techniques for the optimization of process systems under uncertainty. *Computers & Chemical Engineering, 91*, 3–14. https://doi.org/10.1016/j.compchemeng.2016.03.002

Grossmann, I. E., Calfa, B. A., & Garcia-Herreros, P. (2014). Evolution of concepts and models for quantifying resiliency and flexibility of chemical processes. *Computers & Chemical Engineering, 70*, 22–34. https://doi.org/10.1016/j.compchemeng.2013.12.013

Grossmann, I. E., & Harjunkoski, I. (2019). Process Systems Engineering: Academic and industrial perspectives. *Computers & Chemical Engineering, 126*, 474–484. https://doi.org/10.1016/j.compchemeng.2019.04.028

Gutierrez, G., Ricardez-Sandoval, L. A., Budman, H., & Prada, C. (2014). An MPC-based control structure selection approach for simultaneous process and control design. *Computers & Chemical Engineering, 70,* 11–21. https://doi.org/10.1016/j.compchemeng.2013.08.014

Häggblom, K. E. (1997a). Control structure selection via relative gain analysis of partially controlled systems. In *1997 European Control Conference (ECC)* (pp. 3019–3024). Brussels: Institute of Electrical and Electronics Engineers (IEEE). https://doi.org/10.23919/ECC.1997.7082571

Häggblom, K. E. (1997b, November). *Partial relative gain: A new tool for control structure selection*. Paper presented at the 1997 AIChE Annual Meeting, Los Angeles, CA, United States. Retrieved from http://users.abo.fi/khaggblo/RS/aic971.pdf

Hamid, M. K. A., Sin, G., & Gani, R. (2010). Integration of process design and controller design for chemical processes using model-based methodology. *Computers & Chemical Engineering, 34*(5), 683–699. https://doi.org/10.1016/j.compchemeng.2010.01.016

Hänninen, M., & Ylijoki, J. (2008). *VTT tiedotteita – Research notes: Vol. 2443. The one-dimensional separate two-phase flow model of APROS*. Espoo: VTT Technical Research Centre of Finland. Retrieved from https://www.vttresearch.com/sites/default/files/pdf/tiedotteet/2008/T2443.pdf

He, M.-J., Cai, W.-J., Ni, W., & Xie, L.-H. (2009). RNGA based control system configuration for multivariable processes. *Journal of Process Control, 19*(6), 1036–1042. https://doi.org/10.1016/j.jprocont.2009.01.004

Hernjak, N., Doyle, F. J., III., Ogunnaike, B. A., & Pearson, R. K. (2004). Chemical process characterization for control design. In P. Seferlis, & M. C. Georgiadis (Eds.), *Computer aided chemical engineering: Vol. 17. The integration of process design and control* (pp. 42–75). Amsterdam: Elsevier. https://doi.org/10.1016/S1570-7946(04)80054-3

Hovd, M., Ma, D. L., & Braatz, R. D. (2003). On the computation of disturbance rejection measures. *Industrial & Engineering Chemistry Research, 42*(10), 2183–2188. https://doi.org/10.1021/ie010533w

Hultgren, M., Kovács, J., & Ikonen, E. (2015). Combustion control in oxy-fired circulating fluidized bed combustion. In D. Bankiewicz, M. Mäkinen, & P. Yrjas (Eds.), *Proceedings of the 22nd International Conference on Fluidized Bed Conversion: Vol. 2* (pp. 1195–1205). Turku: Åbo Akademi.

Huusom, J. K. (2015). Challenges and opportunities in integration of design and control. *Computers & Chemical Engineering, 81*, 138–146. https://doi.org/10.1016/j.compchemeng.2015.03.019

Ikonen, E., Kovacs, J., Aaltonen, H., Ritvanen, J., Selek, I., & Kettunen, A. (2012). Analysis and tuning of a CFB model using particle filtering. *IFAC Proceedings Volumes, 45*(21), 711–716. https://doi.org/10.3182/20120902-4-FR-2032.00124

Ikonen, E., Kovács, J., & Ritvanen, J. (2013). Circulating fluidized bed hot-loop analysis, tuning, and state-estimation using particle filtering. *International Journal of Innovative Computing, Information and Control, 9*(8), 3357–3376. Retrieved from http://www.ijicic.org/ijicic-12-06061.pdf

International Energy Agency. (2011). *Harnessing variable renewables: A guide to the balancing challenge*. Paris: OECD Publishing. https://doi.org/10.1787/9789264111394-en

Jacobsen, E. W., & Skogestad, S. (1991). Design modifications for improved controllability of distillation columns. In L. Puigjaner, & A. Espuña (Eds.), *Computer-Oriented Process Engineering: Proceedings of COPE-91* (pp. 123–128). Amsterdam: Elsevier. Retrieved from https://folk.ntnu.no/skoge/publications/1991/cope91_Design/cope91_Design.pdf

Jain, A., & Babu, B. V. (2015). Relative response array: A new tool for control configuration selection. *International Journal of Chemical Engineering and Applications, 6*(5), 356–362. https://doi.org/10.7763/IJCEA.2015.V6.509

Jelali, M. (2006). An overview of control performance assessment technology and industrial applications. *Control Engineering Practice, 14*(5), 441–466. https://doi.org/10.1016/j.conengprac.2005.11.005

Jin, B., Zhao, H., & Zheng, C. (2016). Dynamic exergy method and its application for CO_2 compression and purification unit in oxy-combustion power plants. *Chemical Engineering Science, 144*, 336–345. https://doi.org/10.1016/j.ces.2016.01.044

Jørgensen, S. B., Gani, R., & Andersen, T. R. (1999, June). *Towards integration of controllability into plant design*. Paper presented at the 7th IEEE Mediterranean Conference on Control and Automation (MED '99), Haifa, Israel. Retrieved from http://www.med-control.org/main/conferences

Joronen, T., Kovács, J., & Majanne, Y. (Eds.). (2007). *SAS julkaisusarja: Vol. 33. Voimalaitosautomaatio*. Helsinki: Suomen Automaatioseura ry (SAS).

Julier, S. J., & Uhlmann, J. K. (1997). New extension of the Kalman filter to nonlinear systems. In I. Kadar (Ed.), *AeroSense '97, Proceedings of SPIE: Vol. 3068. Signal Processing, Sensor Fusion, and Target Recognition VI* (pp. 182–193). Orlando, FL: The International Society for Optical Engineering (SPIE). https://doi.org/10.1117/12.280797

Kalman, R. E. (1960). On the general theory of control systems. *IFAC Proceedings Volumes, 1*(1), 491–502. https://doi.org/10.1016/S1474-6670(17)70094-8

Kariwala, V., Skogestad, S., & Forbes, J. F. (2006). Relative gain array for norm-bounded uncertain systems. *Industrial & Engineering Chemistry Research, 45*(5), 1751–1757. https://doi.org/10.1021/ie050790r

Kaushik, S. C., Reddy, V. S., & Tyagi, S. K. (2011). Energy and exergy analyses of thermal power plants: A review. *Renewable and Sustainable Energy Reviews, 15*(4), 1857–1872. https://doi.org/10.1016/j.rser.2010.12.007

Klefenz, G. (1986). *Automatic control of steam power plants* (3rd rev. ed.). Mannheim: B.I.-Wissenschaftsverlag.

Klöpffer, W., & Grahl, B. (2014). *Life cycle assessment (LCA): A guide to best practic*e. Weinheim: Wiley.

Koller, R. W., & Ricardez-Sandoval, L. A. (2017). A dynamic optimization framework for integration of design, control and scheduling of multi-product chemical processes under disturbance and uncertainty. *Computers & Chemical Engineering, 106*, 147–159. https://doi.org/10.1016/j.compchemeng.2017.05.007

Kookos, I. K., & Perkins, J. D. (2004). The back-off approach to simultaneous design and control. In P. Seferlis, & M. C. Georgiadis (Eds.), *Computer aided chemical engineering: Vol. 17. The integration of process design and control* (pp. 216–238). Amsterdam: Elsevier. https://doi.org/10.1016/S1570-7946(04)80061-0

Kovács, J., Kettunen, A., Ikonen, E., Hultgren, M., & Niva, L. (2015). Addressing the challenge of fast load change requirements. In D. Bankiewicz, M. Mäkinen, & P. Yrjas (Eds.), *Proceedings of the 22nd International Conference on Fluidized Bed Conversion: Vol. 1* (pp. 253– 262). Turku: Åbo Akademi.

Kovács, J., Kettunen, A., & Ojala, J. (2012). Modelling and control design of once-through boilers. *IFAC Proceedings Volumes, 45*(21), 196–200. https://doi.org/10.3182/20120902-4-FR-2032.00036

Kragelund, M., Wisniewski, R., Mølbak, T., Nielsen, R. J., & Edlund, K. (2008). On propagating requirements and selecting fuels for a Benson boiler. *IFAC Proceedings Volumes, 41*(2), 347–352. https://doi.org/10.3182/20080706-5-KR-1001.00059

Lagarias, J. C., Reeds, J. A., Wright, M. H., & Wright, P. E. (1998). Convergence properties of the Nelder-Mead simplex method in low dimensions. *SIAM Journal on Optimization, 9*(1), 112–147. https://doi.org/10.1137/S1052623496303470

Lappalainen, J., Tourunen, A., Mikkonen, H., Hänninen, M., & Kovács, J. (2014). Modelling and dynamic simulation of a supercritical, oxy combustion circulating fluidized bed power plant concept—Firing mode switching case. *International Journal of Greenhouse Gas Control, 28*, 11–24. https://doi.org/10.1016/j.ijggc.2014.06.015

Larsson, T., & Skogestad, S. (2000). Plantwide control—A review and a new design procedure. *Modeling, Identification and Control, 21*(4), 209–240. https://doi.org/10.4173/mic.2000.4.2

Leckner, B., & Gómez-Barea, A. (2014). Oxy-fuel combustion in circulating fluidized bed boilers. *Applied Energy, 125*, 308–318. https://doi.org/10.1016/j.apenergy.2014.03.050

Lee, H. H., Koppel, L. B., & Lim, H. C. (1972). Integrated approach to design and control of a class of countercurrent processes. *Industrial & Engineering Chemistry Process Design and Development, 11*(3), 376–382. https://doi.org/10.1021/i260043a009

Lewin, D. R., Seider, W. D., & Seader, J. D. (2002). Integrated process design instruction. *Computers & Chemical Engineering, 26*(2), 295–306. https://doi.org/10.1016/S0098-1354(01)00747-5

Liu, P., Georgiadis, M. C., & Pistikopoulos, E. N. (2011). Advances in energy systems engineering. *Industrial & Engineering Chemistry Research, 50*(9), 4915–4926. https://doi.org/10.1021/ie101383h

Liu, Q., Li, X., Liu, H., & Guo, Z. (2020). Multi-objective metaheuristics for discrete optimization problems: A review of the state-of-the-art. *Applied Soft Computing, 93*, 106382. https://doi.org/10.1016/j.asoc.2020.106382

Liu, Q., Shi, Y., Zhong, W., & Yu, A. (2019). Co-firing of coal and biomass in oxy-fuel fluidized bed for CO_2 capture: A review of recent advances. *Chinese Journal of Chemical Engineering, 27*(10), 2261–2272. https://doi.org/10.1016/j.cjche.2019.07.013

Luo, X., Cao, P., & Xu, F. (2016). Dynamic interaction analysis and pairing evaluation in control configuration design. *Chinese Journal of Chemical Engineering, 24*(7), 861–868. https://doi.org/10.1016/j.cjche.2016.04.016

Luo, W., Wang, Q., Guo, J., Liu, Z., & Zheng, C. (2015). Exergy-based control strategy selection for flue gas recycle in oxy-fuel combustion plant. *Fuel, 161*, 87–96. https://doi.org/10.1016/j.fuel.2015.08.036

Luyben, W. L. (1996). Design and control degrees of freedom. *Industrial & Engineering Chemistry Research, 35*(7), 2204−2214. https://doi.org/10.1021/ie960038d

Luyben, W. L. (2004). The need for simultaneous design education. In P. Seferlis, & M. C. Georgiadis (Eds.), *Computer aided chemical engineering: Vol. 17. The integration of process design and control* (pp. 10–41). Amsterdam: Elsevier. https://doi.org/10.1016/S1570-7946(04)80053-1

Luyben, W. L., Tyréus, B. D., & Luyben, M. L. (1999). *Plantwide process control*. New York, NY: McGraw-Hill.

Lyman, P. R., & Luyben, W. L. (1994). A method for assessing the effects of design parameters on controllability. *IFAC Proceedings Volumes, 27*(7), 85–91. https://doi.org/10.1016/S1474-6670(17)47969-9

Majanne, Y., & Maasalo, M. (2009). Dynamic simulation assisted design of industrial power plant process and control. *IFAC Proceedings Volumes, 42*(9), 326–331. https://doi.org/10.3182/20090705-4-SF-2005.00058

Manousiouthakis, V., Savage, R., & Arkun, Y. (1986). Synthesis of decentralized process control structures using the concept of block relative gain. *AIChE Journal, 32*(6), 991–1003. https://doi.org/10.1002/aic.690320609

Martín, M., & Adams, T. A., II. (2019). Challenges and future directions for process and product synthesis and design. *Computers & Chemical Engineering, 128*, 421–436. https://doi.org/10.1016/j.compchemeng.2019.06.022

Mehta, S., & Ricardez-Sandoval, L. A. (2016). Integration of design and control of dynamic systems under uncertainty: A new back-off approach. *Industrial & Engineering Chemistry Research, 55*(2), 485–498. https://doi.org/10.1021/acs.iecr.5b03522

Mencarelli, L., Chen, Q., Pagot, A., & Grossmann, I. E. (2020). A review on superstructure optimization approaches in process system engineering. *Computers & Chemical Engineering, 136*, 106808. https://doi.org/10.1016/j.compchemeng.2020.106808

Mertens, N., Alobaid, F., Starkloff, R., Epple, B., & Kim, H.-G. (2015). Comparative investigation of drum-type and once-through heat recovery steam generator during start-up. *Applied Energy, 144*, 250–260. https://doi.org/10.1016/j.apenergy.2015.01.065

Mitsos, A., Asprion, N., Floudas, C. A., Bortz, M., Baldea, M., Bonvin, D., … Schäfer, P. (2018). Challenges in process optimization for new feedstocks and energy sources. *Computers & Chemical Engineering, 113*, 209–221. https://doi.org/10.1016/j.compchemeng.2018.03.013

Mohideen, M. J., Perkins, J. D., & Pistikopoulos, E. N. (1996). Optimal synthesis and design of dynamic systems under uncertainty. *Computers & Chemical Engineering, 20*(Supplement 2), S895–S900. https://doi.org/10.1016/0098-1354(96)00157-3

Montelongo-Luna, J. M., Svrcek, W. Y., & Young, B. R. (2011). The relative exergy array—A new measure for interactions in process design and control. *The Canadian Journal of Chemical Engineering, 89*(3), 545–549. https://doi.org/10.1002/cjce.20422

Morari, M. (1992). Effect of design on the controllability of chemical plants. *IFAC Proceedings Volumes, 25*(24), 3–16. https://doi.org/10.1016/S1474-6670(17)54006-9

Munir, M. T., Yu, W., & Young, B. R. (2013). The relative exergy-destroyed array: A new tool for control structure design. *The Canadian Journal of Chemical Engineering, 91*(10), 1686–1694. https://doi.org/10.1002/cjce.21797

Muñoz, D. A., Gerhard, J., & Marquardt, W. (2012). A normal vector approach for integrated process and control design with uncertain model parameters and disturbances. *Computers & Chemical Engineering, 40*, 202–212. https://doi.org/10.1016/j.compchemeng.2012.01.016

Murthy Konda, N. V. S. N., Rangaiah, G. P., & Krishnaswamy, P. R. (2006). A simple and effective procedure for control degrees of freedom. *Chemical Engineering Science, 61*(4), 1184–1194. https://doi.org/10.1016/j.ces.2005.08.026

Narraway, L. T., Perkins, J. D., & Barton, G. W. (1991). Interaction between process design and process control: Economic analysis of process dynamics. *Journal of Process Control, 1*(5), 243–250. https://doi.org/10.1016/0959-1524(91)85015-B

Nikačević, N. M., Huesman, A. E. M., Van den Hof, P. M. J., & Stankiewicz, A. I. (2012). Opportunities and challenges for process control in process intensification. *Chemical Engineering and Processing: Process Intensification, 52*, 1–15. https://doi.org/10.1016/j.cep.2011.11.006

Niva, L., Hultgren, M., Ikonen, E., & Kovács, J. (2017). Control structure design for oxy-fired circulating fluidized bed boilers using self-optimizing control and partial relative gain analyses. *IFAC-PapersOnLine, 50*(1), 2023–2030. https://doi.org/10.1016/j.ifacol.2017.08.199

Ogata, K. (2010). *Modern control engineering* (5th ed.). New Jersey, NJ: Prentice Hall.

Ogunnaike, B. A., & Ray, W. H. (1994). *Process dynamics, modeling, and control*. New York, NY: Oxford University Press.

Oyama, H., & Durand, H. (2020). Interactions between control and process design under economic model predictive control. *Journal of Process Control, 92*, 1–18. https://doi.org/10.1016/j.jprocont.2020.05.009

Patwardhan, S. C., Narasimhan, S., Jagadeesan, P., Gopaluni, B., & Shah, S. L. (2012). Nonlinear Bayesian state estimation: A review of recent developments. *Control Engineering Practice, 20*(10), 933–953. https://doi.org/10.1016/j.conengprac.2012.04.003

Perkins, J. D. (1989). Interactions between process design and process control. *IFAC Proceedings Volumes, 22*(8), 195–203. https://doi.org/10.1016/S1474-6670(17)53357-1

Perkins, J. D., & Walsh, S. P. K. (1996). Optimization as a tool for design/control integration. *Computers & Chemical Engineering, 20*(4), 315–323. https://doi.org/10.1016/0098-1354(95)00022-4

Pistikopoulos, E. N., & Diangelakis, N. A. (2016). Towards the integration of process design, control and scheduling: Are we getting closer? *Computers & Chemical Engineering, 91*, 85–92. https://doi.org/10.1016/j.compchemeng.2015.11.002

Pistikopoulos, E. N., Diangelakis, N. A., Oberdieck, R., Papathanasiou, M. M., Nascu, I., & Sun, M. (2015). PAROC—An integrated framework and software platform for the optimisation and advanced model-based control of process systems. *Chemical Engineering Science, 136*, 115–138. https://doi.org/10.1016/j.ces.2015.02.030

Powell, K. M., Hedengren, J. D., & Edgar, T. F. (2014). Dynamic optimization of a hybrid solar thermal and fossil fuel system. *Solar Energy, 108*, 210–218. https://doi.org/10.1016/j.solener.2014.07.004

Price, R. M., Lyman, P. R., & Georgakis, C. (1994). Throughput manipulation in plantwide control structures. *Industrial & Engineering Chemistry Research, 33*(5), 1197–1207. https://doi.org/10.1021/ie00029a016

Rafiei, M., & Ricardez-Sandoval, L. A. (2020a). Integration of design and control for industrial-scale applications under uncertainty: A trust region approach. *Computers & Chemical Engineering, 141*, 107006. https://doi.org/10.1016/j.compchemeng.2020.107006

Rafiei, M., & Ricardez-Sandoval, L. A. (2020b). New frontiers, challenges, and opportunities in integration of design and control for enterprise-wide sustainability. *Computers & Chemical Engineering, 132*, 106610. https://doi.org/10.1016/j.compchemeng.2019.106610

Ricardez-Sandoval, L. A., Budman, H. M., & Douglas, P. L. (2009). Integration of design and control for chemical processes: A review of the literature and some recent results. *Annual Reviews in Control, 33*(2), 158–171. https://doi.org/10.1016/j.arcontrol.2009.06.001

Ritvanen, J., Kovacs, J., Salo, M., Hultgren, M., Tourunen, A., & Hyppänen, T. (2012). 1-D dynamic simulation study of oxygen fired coal combustion in pilot and large scale CFB boilers. In *Proceedings of the 21st International Conference on Fluidized Bed Combustion: Vol. 1* (pp. 72–79). Naples: EnzoAlbanoEditore.

Rosenbrock, H. H. (1970). *State-space and multivariable theory*. London: Nelson.

Sakizlis, V., Perkins, J. D., & Pistikopoulos, E. N. (2004). Recent advances in optimization-based simultaneous process and control design. *Computers & Chemical Engineering, 28*(10), 2069–2086. https://doi.org/10.1016/j.compchemeng.2004.03.018

Sargent, R. W. H. (1967). Integrated design and optimization of processes. *Chemical Engineering Progress, 63*(9), 71–78.

Sarkar, D. K. (2015). *Thermal power plant: Design and operation*. Amsterdam: Elsevier. https://doi.org/10.1016/C2014-0-00536-9

Särkkä, S. (2013). *Institute of Mathematical Statistics textbooks: Vol. 3. Bayesian filtering and smoothing*. Cambridge: Cambridge University Press. https://doi.org/10.1017/CBO9781139344203

Schweickhardt, T., & Allgöwer, F. (2004). Quantitative nonlinearity assessment – An introduction to nonlinearity measures. In P. Seferlis, & M. C. Georgiadis (Eds.), *Computer aided chemical engineering: Vol. 17. The integration of process design and control* (pp. 76–95). Amsterdam: Elsevier. https://doi.org/10.1016/S1570-7946(04)80055-5

Schweiger, C. A., & Floudas, C. A. (1998). Interaction of design and control: Optimization with dynamic models. In W. H. Hager, & P. M. Pardalos (Eds.), *Applied Optimization: Vol. 15. Optimal control: Theory, algorithms, and applications* (pp. 388–435). Dordrecht: Springer. https://doi.org/10.1007/978-1-4757-6095-8_19

Seddighi, S. (2017). Design of large scale oxy-fuel fluidized bed boilers: Constant thermal power and constant furnace size scenarios. *Energy, 118*, 1286–1294. https://doi.org/10.1016/j.energy.2016.11.004

Seddighi, S., Clough, P. T., Anthony, E. J., Hughes, R. W., & Lu, P. (2018). Scale-up challenges and opportunities for carbon capture by oxy-fuel circulating fluidized beds. *Applied Energy, 232*, 527–542. https://doi.org/10.1016/j.apenergy.2018.09.167

Seddighi, S., Pallarès, D., Normann, F., & Johnsson, F. (2015). Heat extraction from a utility-scale oxy-fuel-fired CFB boiler. *Chemical Engineering Science, 130*, 144–150. https://doi.org/10.1016/j.ces.2015.03.015

Sharifzadeh, M. (2013). Integration of process design and control: A review. *Chemical Engineering Research and Design, 91*(12), 2515–2549. https://doi.org/10.1016/j.cherd.2013.05.007

Sharifzadeh, M., Bumb, P., & Shah, N. (2016). Carbon capture from pulverized coal power plant (PCPP): Solvent performance comparison at an industrial scale. *Applied Energy, 163*, 423–435. https://doi.org/10.1016/j.apenergy.2015.11.017

Sharifzadeh, M., & Shah, N. (2019). MEA-based CO_2 capture integrated with natural gas combined cycle or pulverized coal power plants: Operability and controllability through integrated design and control. *Journal of Cleaner Production, 207*, 271–283. https://doi.org/10.1016/j.jclepro.2018.09.115

Shields, R. W., & Pearson, J. B. (1976). Structural controllability of multiinput linear systems. *IEEE Transactions on Automatic Control, 21*(2), 203–212. https://doi.org/10.1109/TAC.1976.1101198

Siirola, J. J., & Edgar, T. F. (2012). Process energy systems: Control, economic, and sustainability objectives. *Computers & Chemical Engineering, 47*, 134–144. https://doi.org/10.1016/j.compchemeng.2012.06.019

Singh, R. I., & Kumar, R. (2016). Current status and experimental investigation of oxy-fired fluidized bed. *Renewable and Sustainable Energy Reviews, 61*, 398–420. https://doi.org/10.1016/j.rser.2016.04.021

Skogestad, S. (1994). A procedure for SISO controllability analysis - With application to design of pH processes. *IFAC Proceedings Volumes, 27*(7), 25–30. https://doi.org/10.1016/S1474-6670(17)47959-6

Skogestad, S. (2004). Control structure design for complete chemical plants. *Computers & Chemical Engineering, 28*(1–2), 219–234. https://doi.org/10.1016/j.compchemeng.2003.08.002

Skogestad, S., & Postlethwaite, I. (2005). *Multivariable feedback control: Analysis and design* (2nd ed.). Chichester: Wiley.

Smith, R. (2005). *Chemical process design and integration* (2nd ed.). Chichester: Wiley.

Stanger, R., Wall, T., Spörl, R., Paneru, M., Grathwohl, S., Weidmann, M., … Santos, S. (2015). Oxyfuel combustion for CO_2 capture in power plants. *International Journal of Greenhouse Gas Control, 40*, 55–125. https://doi.org/10.1016/j.ijggc.2015.06.010

Stephanopoulos, G., & Ng, C. (2000). Perspectives on the synthesis of plant-wide control structures. *Journal of Process Control, 10*(2–3), 97–111. https://doi.org/10.1016/S0959-1524(99)00023-2

Sun, L., Hua, Q., Li, D., Pan, L., Xue, Y., & Lee, K. Y. (2017). Direct energy balance based active disturbance rejection control for coal-fired power plant. *ISA Transactions, 70*, 486–493. https://doi.org/10.1016/j.isatra.2017.06.003

Swartz, C. L. E., & Kawajiri, Y. (2019) Design for dynamic operation - A review and new perspectives for an increasingly dynamic plant operating environment. *Computers & Chemical Engineering, 128*, 329–339. https://doi.org/10.1016/j.compchemeng.2019.06.002

Szargut, J. (2005). *Developments in heat transfer: Vol. 18. Exergy method: Technical and ecological applications*. Southampton: WIT Press.

Teichgraeber, H., Brodrick, P. G., & Brandt, A. R. (2017). Optimal design and operations of a flexible oxyfuel natural gas plant. *Energy, 141*, 506–518. https://doi.org/10.1016/j.energy.2017.09.087

Ulbig, A., & Andersson, G. (2015). Analyzing operational flexibility of electric power systems. *International Journal of Electrical Power & Energy Systems, 72*, 155–164. https://doi.org/10.1016/j.ijepes.2015.02.028

van der Merwe, R., Doucet, A., de Freitas, N., & Wan, E. (2000). *The unscented particle filter, Technical report CUED/F-INFENG/TR 380*. Cambridge: Cambridge University Engineering Department.

van de Wal, M., & de Jager, B. (2001). A review of methods for input/output selection. *Automatica, 37*(4), 487–510. https://doi.org/10.1016/S0005-1098(00)00181-3

Vasbinder, E. M., Hoo, K. A., & Mann, U. (2004). Synthesis of plantwide control structures using a decision-based methodology. In P. Seferlis, & M. C. Georgiadis (Eds.), *Computer aided chemical engineering: Vol. 17. The integration of process design and control* (pp. 375–400). Amsterdam: Elsevier. https://doi.org/10.1016/S1570-7946(04)80067-1

Vega, P., Lamanna de Rocco, R., Revollar, S., & Francisco, M. (2014). Integrated design and control of chemical processes – Part I: Revision and classification. *Computers & Chemical Engineering, 71*, 602–617. https://doi.org/10.1016/j.compchemeng.2014.05.010

Vu, T. T. L., Bahri, P. A., & Romagnoli, J. A. (1997). Operability considerations in chemical processes: A switchability analysis. *Computers & Chemical Engineering, 21*(Supplement), S143–S148. https://doi.org/10.1016/S0098-1354(97)87493-5

Weitz, O., & Lewin, D. R. (1996). Dynamic controllability and resiliency diagnosis using steady state process flowsheet data. *Computers & Chemical Engineering, 20*(4), 325–335. https://doi.org/10.1016/0098-1354(95)00023-2

White, V., Perkins, J. D., & Espie, D. M. (1996). Switchability analysis. *Computers & Chemical Engineering, 20*(4), 469–474. https://doi.org/10.1016/0098-1354(95)00037-2

Wu, Z., Li, D., Xue, Y., Sun, L., He, T., & Zheng, S. (2020). Modified active disturbance rejection control for fluidized bed combustor. *ISA Transactions, 102*, 135–153. https://doi.org/10.1016/j.isatra.2020.03.003

Xiong, Q., Cai, W.-J., & He, M.-J. (2005). A practical loop pairing criterion for multivariable processes. *Journal of Process Control, 15*(7), 741–747. https://doi.org/10.1016/j.jprocont.2005.03.008

Yuan, Z., Chen, B., Sin, G., & Gani, R. (2012). State-of-the-art and progress in the optimization-based simultaneous design and control for chemical processes. *AIChE Journal, 58*(6), 1640–1659. https://doi.org/10.1002/aic.13786

Zhang, H., Gao, M., Hong, F., Liu, J., & Wang, X. (2019). Control-oriented modelling and investigation on quick load change control of subcritical circulating fluidized bed unit. *Applied Thermal Engineering, 163*, 114420. https://doi.org/10.1016/j.applthermaleng.2019.114420

Zhao, Y., Liu, M., Wang, C., Li, X., Chong, D., & Yan, J. (2018). Increasing operational flexibility of supercritical coal-fired power plants by regulating thermal system configuration during transient processes. *Applied Energy, 228*, 2375–2386. https://doi.org/10.1016/j.apenergy.2018.07.070

Zhao, Y., Wang, C., Liu, M., Chong, D., & Yan, J. (2018). Improving operational flexibility by regulating extraction steam of high-pressure heaters on a 660 MW supercritical coal-fired power plant: A dynamic simulation. *Applied Energy, 212*, 1295–1309. https://doi.org/10.1016/j.apenergy.2018.01.017

Ziegler, J. G., & Nichols, N. B. (1943). Process lags in automatic-control circuits. *Transactions of the A.S.M.E., 65*, 433–444.

Zimmerman, N., Kyprianidis, K., & Lindberg, C.-F. (2018). Waste fuel combustion: Dynamic modeling and control. *Processes, 6*(11), 222. https://doi.org/10.3390/pr6110222

Zotică, C., Nord, L. O., Kovács, J., & Skogestad, S. (2020). Optimal operation and control of heat to power cycles: A new perspective from a systematic plantwide control approach. *Computers & Chemical Engineering, 141*, 106995. https://doi.org/10.1016/j.compchemeng.2020.106995

Original publications

I Hultgren, M., Ikonen, E., & Kovács, J. (2014). Oxidant control and air-oxy switching concepts for CFB furnace operation. *Computers & Chemical Engineering, 61*, 203–219. https://doi.org/10.1016/j.compchemeng.2013.10.018

II Hultgren, M., Ikonen, E., & Kovács, J. (2014). Circulating fluidized bed boiler state estimation with an unscented Kalman filter tool. In *2014 IEEE Conference on Control Applications (CCA)* (pp. 310–315). Antibes: Institute of Electrical and Electronics Engineers (IEEE). https://doi.org/10.1109/CCA.2014.6981364

III Hultgren, M., Ikonen, E., & Kovács, J. (2017). Integrated control and process design in CFB boiler design and control – Application possibilities. *IFAC-PapersOnLine, 50*(1), 1997–2004. https://doi.org/10.1016/j.ifacol.2017.08.180

IV Hultgren, M., Ikonen, E., & Kovács, J. (2017). Once-through circulating fluidized bed boiler control design with the dynamic relative gain array and partial relative gain. *Industrial & Engineering Chemistry Research, 56*(48), 14290–14303. https://doi.org/10.1021/acs.iecr.7b03259

V Hultgren, M., Ikonen, E., & Kovács, J. (2019). Integrated control and process design for improved load changes in fluidized bed boiler steam path. *Chemical Engineering Science, 199*, 164–178. https://doi.org/10.1016/j.ces.2019.01.025

Reprinted with permission from Elsevier (Publications I and V © 2013, 2019 Elsevier Ltd.), IEEE (Publication II © 2014 IEEE), IFAC (Publication III © 2017 IFAC), and American Chemical Society (Publication IV © 2017 American Chemical Society).

Original publications are not included in the electronic version of the dissertation.

797. Kilpijärvi, Joni (2021) RF-microwave sensor development for cell and human in vitro and ex vivo monitoring

798. Huikari, Jaakko (2021) 2D CMOS SPAD array techniques in 1D pulsed TOF distance measurement applications

799. Peyvasteh, Motahareh (2021) Polarimetric and spectral imaging approaches for quantitative characterization of inhomogeneous scattering media including biotissues

800. Shehab, Mohammad (2021) Energy efficient QoS provisioning and resource allocation for machine type communication

801. Jounila, Henri (2021) Integroidulla HSEQ-johtamisella kokonaisvaltaista yritysvastuullisuutta : tapaustutkimuksia yritysten työturvallisuuden ja HSEQ:n kehittämisestä

802. Nellattukuzhi Sreenivasan, Harisankar (2021) Synthesis and alkali activation of Magnesium-rich aluminosilicates

803. Kallio, Johanna (2021) Unobtrusive stress assessment in knowledge work using real-life environmental sensor data

804. Meriö, Leo-Juhani (2021) Observations and analysis of snow cover and runoff in boreal catchments

805. Lovén, Lauri (2021) Spatial dependency in Edge-native Artificial Intelligence

806. Törmänen, Matti (2021) Improved analysis of tube flow fractionation data for measurements in the pulp and paper industry

807. Rusanen, Annu (2021) Catalytic conversion of sawdust-based sugars into 5-hydroxymethylfurfural and furfural

808. Yaraghi, Navid (2021) Analyzing human impacts on the quality and quantity of river water

809. Tarakanchikova, Yana (2021) Multilayered polyelectrolyte assemblies as delivery system for biomedical applications

810. Shaheen, Rana Azhar (2021) Design aspects of millimeter wave multiband front-ends

811. Kodukula, Suresh (2021) Ridging in stabilized ferritic stainless steels : The effects of casting and hot-rolling parameters

812. Hietaharju, Petri (2021) Predictive optimization of heat demand utilizing heat storage capacity of buildings

Book orders:
Virtual book store
http://verkkokauppa.juvenesprint.fi

UNIVERSITY OF OULU P.O. Box 8000 FI-90014 UNIVERSITY OF OULU FINLAND

ACTA UNIVERSITATIS OULUENSIS

SERIES EDITORS

A
SCIENTIAE RERUM NATURALIUM
University Lecturer Tuomo Glumoff

B
HUMANIORA
University Lecturer Santeri Palviainen

C
TECHNICA
Postdoctoral researcher Jani Peräntie

D
MEDICA
University Lecturer Anne Tuomisto

E
SCIENTIAE RERUM SOCIALIUM
University Lecturer Veli-Matti Ulvinen

F
SCRIPTA ACADEMICA
Planning Director Pertti Tikkanen

G
OECONOMICA
Professor Jari Juga

H
ARCHITECTONICA
Associate Professor (tenure) Anu Soikkeli

EDITOR IN CHIEF
University Lecturer Santeri Palviainen

PUBLICATIONS EDITOR
Publications Editor Kirsti Nurkkala

ISBN 978-952-62-3136-5 (Paperback)
ISBN 978-952-62-3137-2 (PDF)
ISSN 0355-3213 (Print)
ISSN 1796-2226 (Online)

UNIVERSITY OF OULU